Molecular, genetic and developmental aspects of flower evolution

Marie Monniaux

HABILITATION A DIRIGER DES RECHERCHES

Présentée devant
l'Université Claude Bernard Lyon 1

Aspects moléculaires, génétiques et développementaux de l'évolution de la fleur

Molecular, genetic and developmental aspects of flower evolution

Marie MONNIAUX
Chargée de recherche CNRS

Soutenance prévue le 5 avril 2023 devant le jury composé de:

Sandra CORTIJO, Chargée de recherche CNRS, Rapportrice
Patrick LAUFS, Directeur de recherche INRAe, Rapporteur
Catherine DAMERVAL, Directrice de recherche CNRS, Rapportrice
Christophe TREHIN, Maître de Conférence UCBL, Examinateur
Marie DELATTRE, Directrice de recherche CNRS, Examinatrice

OUTLINE

1. Sayou C, Monniaux M, Nanao MH, Moyroud E et al., A Promiscuous Intermediate Underlies the Evolution of LEAFY DNA Binding Specificity. 2014. Science.

2. Monniaux M, Pieper B et al., The role of APETALA1 in petal number robustness. 2018. Elife.

3. Chopy M et al., Cell layer-specific expression of the B-class MADS-box gene *PhDEF* drives petal tube or limb development in petunia flowers. 2021. bioRxiv.

Marie MONNIAUX

Curriculum vitae

Date of birth: 22/10/1986 (36 years old)
Nationality: French
2 children (4yo and 1yo)
Researcher unique identifier: ORCID: 0000-0001-6847-3902

CURRENT POSITION

2017–today Permanent CNRS researcher (chargée de recherche classe normale), Laboratory for Plant Reproduction and Development (RDP), ENS de Lyon, France.

PREVIOUS POSITIONS

2013–2017 Post-doctoral fellow with Dr. Angela Hay (hay@mpipz.mpg.de), Max Planck Institute for Plant Breeding Research (MPIPZ), Department of Comparative Development and Genetics, Cologne, Germany. **Genetic and developmental basis of petal number variation.**

2011–2012 Temporary lecturer position (Attaché Temporaire d'Enseignement et de Recherche) as a fourth year of thesis (LPCV, Grenoble).

EDUCATION

2012 PhD in plant biology, Laboratory for Plant and Cell Physiology (LPCV), CEA Grenoble, Université Grenoble Alpes, France. **Evolution of the floral regulatory LEAFY in the green lineage,** supervised by Dr. François Parcy (francois.parcy@cea.fr).

2009 Master's degree in Biosciences, Ecole Normale Supérieure de Lyon (ENS de Lyon), France – obtained with distinction.

2008 "Agrégation" – French competitive exam for biology and geology secondary level teaching – obtained with rank 9/87.

2006 Bachelor's degree (Licence) in Cell and Molecular Biology, ENS de Lyon, France – obtained with distinction.

2005 Admission to the ENS de Lyon (competitive exam).

FUNDING AND GRANT APPLICATIONS

2021 Interviewed for an ERC Starting Grant application, LS3 panel. Ranked B after the interview step.

2021 EMBO short-term fellowship, **13 k€**, to support my visit to the group of Prof. Cris Kuhlemeier, University of Bern, Switzerland (May–July 2021).

2020–2024 ANR JCJC (French Research agency, young investigator program) **260 k€** – RDP.

2019–2021 Elan ERC grant, University of Lyon, **50 k€** – RDP.

2017 Seal of excellence (score > 85%) for a non-funded application to a Marie Curie post-doctoral fellowship to join the RDP lab.

2014–2016 EMBO post-doctoral fellowship, **70 k€** – MPIPZ.

TUTORING AND TEACHING

Tutoring

2022 Lou Quadrio (**Licence 3 student** from Université Catholique de Lyon) for 2 months at the RDP lab, 100% tutoring.

2020–2023 Quentin Cavallini–Speisser (**PhD student** from UCB Lyon1) for 3 years at the RDP lab, recruited under my ANR–JCJC funding, 100% tutoring with accreditation from UCB Lyon1.

2020–2021 Jordan Brun (**Assistant Engineer**) for 6 months at the RDP lab, recruited under my ELAN–ERC funding, 50% management shared with Michiel Vandenbussche.

2020 Quentin Cavallini–Speisser (**Master 2 student** from UCB Lyon1) for 6 months at the RDP lab, 100 % tutoring (2 months in the lab, 4 months online tutoring during lockdown).

2019 Rémy Belois (**Master 1 student** from Université Clermont–Ferrand) for 4 months at the RDP lab, 100 % tutoring.

2018 Caroline Chevallier (**Licence 3 student** from UCB Lyon 1) for 4 months at the RDP lab, 100 % tutoring.

2013–2017 Evangelos Kouklas (**PhD student** from Universitat zu Köln) for 3 years at the MPIPZ, 25 % tutoring shared with Angela Hay.

2014 Léa Rambaud (**Master 1 student** from ENS de Lyon) for 4 months at the MPIPZ, 50 % tutoring shared with Angela Hay.

Teaching and science popularization

2022 Lecture and research conference (2h) for the UE Europe "Stem cells and Development", Master 2 Biology ENS de Lyon

2021–2022 Conferences for the public on "Darwin's abominable mystery" (2h) and on "Land plant evolution" (2h), Université Ouverte Lyon 1

2019 Introduction to research to high school students, event "Declics"

2009–today Regular lab tours for high–school students, Participation to the French science popularisation event "Fête de la Science"

2009–2013 260 h teaching activity at the University Grenoble–Alpes during my PhD and ATER position:

– Licence 1, Practical Training of **Organismal Biology**, 147 h.

– Licence 1, Lectures of **Discovery of Biology**, 28,5 h.

– Licence 2, Exercises of **Ecology**, 16,5 h.

– Licence 2, Practical Training of **Plant Physiology**, 24 h.

– Licence 3, Lectures (4,5 h) and Exercises (26 h) of **Plant Genetics and Development**.

– Master 1, Practical Training of **Plant Physiology**, 16h.

ADMINISTRATIVE DUTIES

PhD juries and advisory committees

2022 PhD jury member for Antonin Galien (LPCV, Grenoble).

2021 PhD jury member for Pierre Galipot (MNHN, Paris), Nathalie Bouré (IJPB, Université Paris Saclay) and Jeanne Loue-Manifel (RDP).

2020-today Member of the PhD advisory committees of Philippe Rieu (LPCV, Grenoble), Nicolas Dalle (RDP) and Joris Macquet (LIPM).

2018 PhD jury member for Léa Rambaud (RDP).

Conference organization

2021 Member of the scientific committee for the meeting EvoLyon, gathering scientists around Lyon working on evolutionary biology.

Panel and reviewing activities

2021 Nominated jury member for the CNRS selection of researchers, section 23 (Integrative Plant Biology).

2020 Panel member for the DFG research unit ICIPS (Innovation and Coevolution in Plant Sexual Reproduction) and reviewing of a grant application for the French research agency (ANR).

2014-today Review editor for Frontiers in Plant Science, section Plant Development and EvoDevo.

2014-today Regular review for various journals upon request (Frontiers in Plant Science, Trends in Plant Science, Journal of Experimental Botany) – Publons

Other lab duties

2021 Elected member of the RDP lab council.

2018-today CNRS "correspondante égalité" for gender equality.

2017-today In charge of ordering *in vitro* culture products for the RDP lab.

2015-2017 Member of the Post-doc Initiative (MPIPZ), organization of seminars, trainings and a post-doc retreat.

COLLABORATIONS

Present

- Ben Rimon (Institute of Plant Sciences, Israel) for the link between petal identity and maturation traits.

- Chloé Zubieta (LPCV, Grenoble) for biochemical assays on floral transcription factors.

- Francesca Quattrocchio (University of Amsterdam, Netherlands) for the link between petal identity and pigmentation.

- Cris Kuhlemeier (University of Bern, Switzerland) for the evolution of petunia floral morphology.

Past (PhD)

- Fabien Nogué (IJPB, Versailles) to develop *Physcomitrella patens* culture in the laboratory. Collaboration still ongoing in my PhD lab.

- Stefan Rensing (University of Marburg, Germany) to investigate the function of LFY in *Physcomitrella patens*. Collaboration still ongoing in my PhD lab.

ORAL COMMUNICATIONS AND POSTERS

– (invited) **Mechano-Morpho-Evo-Devo symposium,** Insitut Pasteur, Paris, France (12–13 December 2022).

– **17th World Petunia Days,** Milan, Italy (4–7 July 2019). "Dissecting petunia petal development".

– (poster) **Workshop on Molecular mechanisms controlling flower development,** Giens, France (18–21 June 2019). "Contribution of cell layers to petunia petal development".

– (invited) **SFR Biosciences Days,** Sainte-Foy-lès-Lyon, France (19 june 2018). "Genetic basis of petal number robustness".

– (poster) **Evo-devo summer school,** Venise, Italy (18–21 September 2017). "Evolution of floral morphologies".

– **EMBO Fellows Meeting,** EMBL Heidelberg, Germany (13–16 June 2017). "Petal number variation in *Cardamine hirsuta*".

– **Euro Evo Devo 2016,** Uppsala, Sweden (26–29 July 2016). "Genetic basis of petal number variation in *Cardamine hirsuta*".

– **New model systems for linking evolution and ecology,** EMBL Heidelberg, Germany (8–11 May 2016). "Petal number variation in *Cardamine hirsuta*".

– **Euro Evo Devo 2014,** Vienna, Austria (22–25 July 2014). "Evolution of the floral regulator LEAFY in the green lineage".

– **Workshop on Molecular mechanisms controlling flower development,** Giens, France (8–12 June 2013). "800 million years of LEAFY evolution".

– (poster) **Workshop on Molecular mechanisms controlling flower development,** Maratea, Italy (14–17 June 2011). "Evolution of the floral regulatory LEAFY in land plants and prediction of its target genes".

PUBLICATIONS

(* shared authorship, #corresponding author, names are underlined if they are students that I tutored)

– (in prep) **Monniaux M#.** Unusual suspects in flower evolution. 2023. Science (perspective).

– Cavallini-Speisser Q, Morel P, **Monniaux M#.** Petal cellular identities. 2021. Frontiers in Plant Science. 12:2430. *doi: 10.3389/fpls.2021.745507*

– (preprint) Chopy M, Cavallini-Speisser Q, Chambrier P, Morel P, Just J, Hugouvieux V, Rodrigues Bento S, Zubieta C, Vandenbussche M#, **Monniaux M#.** Cell layer-specific expression of the B-class MADS-box gene *PhDEF* drives petal tube or limb development in petunia flowers. 2021. bioRxiv. *doi: 10.1101/2021.04.03.438311*

– Morel P, Chambrier P, Boltz V, Chamot S, Rozier F, Rodrigues Bento S, Trehin C, **Monniaux M,** Zethof J, Vandenbussche M. Divergent Functional Diversification Patterns in the SEP/AGL6/AP1 MADS-Box Transcription Factor Superclade. 2019. The Plant Cell. 31(12):3033-3056. *doi: 10.1105/tpc.19.00162*

– **Monniaux M#,** Vandenbussche M. How to Evolve a Perianth: A Review of Cadastral Mechanisms for Perianth Identity. 2018. Frontiers in Plant Science. 29;9:1573. *doi: 10.3389/fpls.2018.01573*

– **Monniaux M*,** Pieper B*, McKim SM, Routier-Kierzkowska AL, Kierzkowski D, Smith RS, Hay A. The role of *APETALA1* in petal number robustness. 2018. Elife. 18;7. *doi: 10.7554/eLife.39399*

– McKim SM, Routier-Kierzkowska AL, **Monniaux M**, Kierzkowski D, Pieper B, Smith RS, Tsiantis M, Hay A. Seasonal Regulation of Petal Number. 2017. Plant Physiology. 175(2):886–903. *doi: 10.1104/pp.17.00563*

– Moyroud E, **Monniaux M**, Thévenon E, Dumas R, Scutt CP, Frohlich MW, Parcy F. A link between LEAFY and B-gene homologues in *Welwitschia mirabilis* sheds light on ancestral mechanisms prefiguring floral development. 2017. New Phytologist. 216(2):469–481. *doi: 10.1111/nph.14483*

– **Monniaux M**, McKim SM, Cartolano M, Thévenon E, Parcy F, Tsiantis M, Hay A. Conservation vs divergence in *LEAFY* and *APETALA1* functions between *Arabidopsis thaliana* and *Cardamine hirsuta*. 2017. New Phytologist. 216(2):469–481. *doi: 10.1111/nph.14483*

– **Monniaux M**, Hay A. Cells, walls, and endless forms. 2016. Current Opinion in Plant Biology. 34:114–121. *doi: 10.1016/j.pbi.2016.10.010*

– **Monniaux M***, Pieper B*, Hay A. Stochastic variation in *Cardamine hirsuta* petal number. 2016. Annals of Botany. 117(5):881–7. *doi: 10.1093/aob/mcv131*

– Pieper B, **Monniaux M**, Hay A. The genetic architecture of petal number in *Cardamine hirsuta*. 2016. New Phytologist 209(1):395–406. *doi: 10.1111/nph.13586*

– Sayou C*, **Monniaux M***, Nanao MH*, Moyroud E*, Brockington SF, Thévenon E, Chahtane H, Warthmann N, Melkonian M, Zhang Y, Wong GK, Weigel D, Parcy F, Dumas R. A Promiscuous Intermediate Underlies the Evolution of LEAFY DNA Binding Specificity. 2014. Science. 343(6171):645–8. *doi: 10.1126/science.1248229*

– Chahtane H, Vachon G, Le Masson M, Thévenon E, Périgon S, Mihajlovic N, Kalinina A, Michard R, Moyroud E, **Monniaux M**, Sayou C, Grbic V, Parcy F, Tichtinsky G. A variant of LEAFY reveals its capacity to stimulate meristem development by inducing RAX1. 2013. The Plant Journal. 74(4):678–89. *doi: 10.1111/tpj.12156*

– Moyroud E, Minguet EG, Ott F, Yant L, Posé D, **Monniaux M**, Blanchet S, Bastien O, Thévenon E, Weigel D, Schmid M, Parcy F. Prediction of regulatory interactions from genome sequences using a biophysical model for the Arabidopsis LEAFY transcription factor. 2011. The Plant Cell. 23(4):1293–306. *doi: 10.1105/tpc.111.083329*

– Winter CM, Austin RS, Blanvillain-Baufumé S, Reback MA, **Monniaux M**, Wu MF, Sang Y, Yamaguchi A, Yamaguchi N, Parker JE, Parcy F, Jensen ST, Li H, Wagner D. LEAFY target genes reveal floral regulatory logic, cis motifs, and a link to biotic stimulus response. 2011. Developmental Cell. 20(4):430–43. *doi: 10.1016/j.devcel.2011.03.019*

– Moyroud E, Kusters E, **Monniaux M**, Koes R, Parcy F. LEAFY blossoms. 2010. Trends in Plant Science. 15(6):346–52. *doi: 10.1016/j.tplants.2010.03.007*

SOFT SKILLS TRAININGS

– **Several trainings on gender equality**, sexist and sexual violence, listening to victims of sexist and sexual violence, organized by the CNRS for equality referents (2018–today).

– **EMBO "Leadership" workshop**, EMBL Heidelberg, Germany (10–13 June 2017).

CAREER BREAKS

October 2018–January 2019	Maternity leave (4 months)
April 2022–August 2022	Maternity leave (5 months)

General Introduction:

Flower development and evolution

Flowers have fascinated scientists for centuries, with their wonderful diversity of shapes, colours and structures coming in all sizes. The first flower arose around 250 million years ago in a clade that subsequently witnessed very rapid radiation, which generated the 370,000 species that are found today on Earth (Sauquet et al., 2022; Lughadha et al., 2016). In this introduction, I will first present a brief summary of the position of flowering plants in the phylogeny, what is known about their emergence and the possible reasons for their rapid radiation. Then, I will introduce the current knowledge about how to build a flower: from the formation of the flower meristem, to the specification of floral organ identity and the construction of floral organs with specific mature traits.

The green lineage: from green algae to flowering plants

The green lineage (Viridiplantae, Fig. 0-1) comprises a group of oxygenic photosynthetic organisms containing chloroplasts, originating more than 500 million years ago and comprising about 500,000 species (One Thousand Plant Transcriptomes Initiative, 2019).

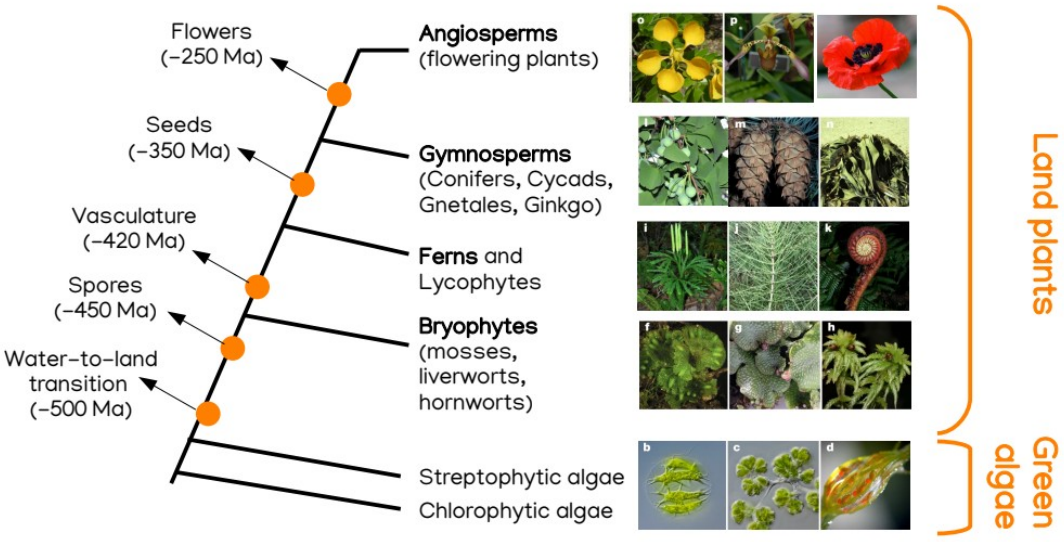

Figure 0-1: Simplified phylogeny from the green lineage (phylogeny and pictures modified from (One Thousand Plant Transcriptomes Initiative, 2019)). This phylogeny displays the major clades and the key innovations witnessed during evolution with their rough estimated age.

All land plants stem from green algae that went through the water-to-land transition, with all the morphological and physiological changes implied (de Vries and Archibald, 2018). The first spores appeared short before the divergence of Bryophytes from the stem group, true vasculature is found in Tracheophytes (i.e. vascular plants: ferns, lycophytes, Gymnosperms and Angiosperms,) while seeds are found in Spermatophytes (i.e. seed plants: Gymnosperms and Angiosperms). The first flower then appeared some 250 million years ago in the proximal ancestor of Angiosperms (flowering plants).

The « abominable mystery » of flower evolution

Flowering plants comprise about 370,000 species, an astonishingly high number in comparison to their sister group the Gymnosperms, that comprises about 1,000 species (Lughadha et al., 2016). The structure of the flower is very different to the one of reproductive cones from gymnosperms (Fig. 0-2). The flower is generally considered to display several key evolutionary innovations: male and female organs are grouped together in a single structure with a compressed axis, reproductive organs are protected by the perianth (sepals and petals in eudicots in particular), the double fertilization leads to the simultaneous formation of the embryo and a nutritious tissue that surrounds it, the ovule and seed have a double integument, and the ovule is enclosed within a carpel that will produce a fruit after fertilization. These innovations have probably played major roles in the evolution of the reproductive strategy of angiosperms: the bisexuality of flowers grants the possibility for efficient self-pollination; the perianth has evolved attractive features for pollinators, thereby allowing cross-fertilization and the avoidance of inbreeding depression; the seed has abundant reserves and can withstand harsh conditions before germination; and the fruit often plays a role in seed dispersal and colonization of new environments. Key innovations are generally defined as novel phenotypic traits that result in evolutionary radiations (Soltis and Soltis, 2016). Indeed, extant angiosperms are the result of an intense radiation that took place in a relatively short time, but the role of each of the key innovations cited earlier in this radiation process, if they had any, is unclear.

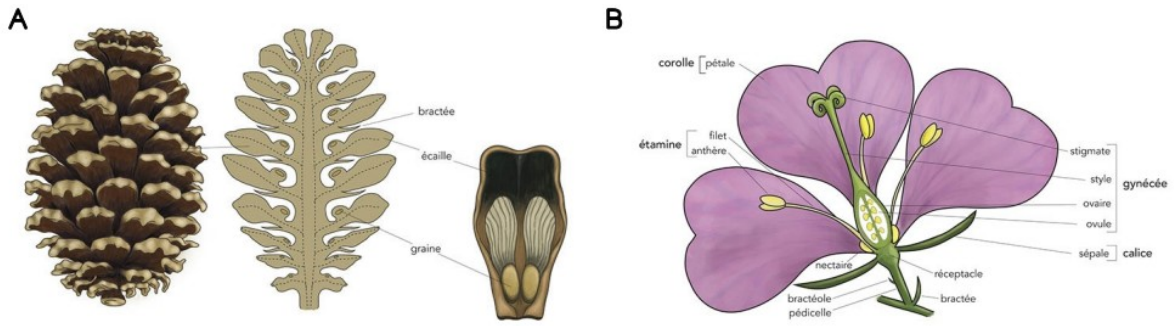

Figure 0-2: Female gymnosperm cone and angiosperm flower. A: The female gymnosperm cone is composed of several scales that subtend naked ovules (and later seeds). **B:** The flower is a bisexual compressed axis surrounded by the perianth (sepals and petals in eudicots). Ovules are enclosed in an ovary that will later develop as a fruit after fertilization. Pictures from © Presses de l'Université Laval.

The famous biologist Charles Darwin wrote in 1879 a letter to a friend and colleague, Joseph Hooker, stating that « *The rapid development as far as we can judge of all the higher plants within recent geological times is an abominable mystery » (Friedman, 2009)*. Indeed, on top of the several key innovations found in the flower and the extreme radiation of flowering plants, no clear fossil intermediate between angiosperm and gymnosperm reproductive structures could be found in the fossil record. Although Darwin had produced the ground-breaking theory of evolution by natural selection, he saw evolution as a slow and gradual process and was quite reluctant to contemplate that evolution sometimes does make leaps (saltationism or theory of punctuated equilibrium) (Eldredge and Gould, 1971; Friedman, 2009). The « abominable mystery » encompasses multiple different questions about flower evolution (Sauquet and Magallón, 2018), of which two are central to me:

1) How did the first flower appear so suddenly during evolution? In particular, in which order did each key innovation arise, and what did the proximal ancestor of flowering plants (i.e. the ancestral flower) look like?
2) How did flowering plants radiate so rapidly?

Since Darwin, much progress has been made on these two questions and the origin of the flower is not such an abominable mystery after all, especially if one believes in rapid evolution. New fossils with intermediate features between angiosperms and gymnosperms are regularly found, and although their interpretation can be dubious and it is not always clear where they stand in the phylogenetic tree of seed plants, flowers' key innovations likely did not appear all at once (Bateman, 2020). Large phylogenetic reconstructions have allowed to propose a picture for the ancestral flower, with a whole set of traits considered to be the ancestral one, before the large radiation of flowering plants started (Sauquet et al., 2017). Finally, several mechanisms have been proposed to explain the rapid radiation of angiosperms, and in particular the co-evolution with pollinators is often cited as a key mechanism, but it is likely the result of a combination of multiple factors (Sauquet and Magallón, 2018). Still, because of their astonishing morphological diversity, flowers remain a fascinating system to decipher the complex mechanisms of morphological evolution.

Building a flower

In order to understand how flowers evolve, one must understand how they are built. Flowers initiate from the shoot apical meristem (SAM), the reservoir of stem cells that divides and generates lateral organs. In the vegetative state, the SAM produces leaves. Then comes the floral transition, whose timing is determined by a combination of endogenous (age, hormones...) and exogenous (photoperiod, vernalization...) cues (Pajoro et al., 2014), which turns the vegetative SAM into an inflorescence meristem. Briefly, these signals are integrated by a handful of so-called floral integrators, among which FT (FLOWERING LOCUS T) and LEAFY (LFY) (Blázquez and Weigel, 2000). In particular, FT moves from the leaf (where light signals are perceived) to the SAM where it activates the expression of the floral meristem identity genes *AP1* (*APETALA1*) and *LFY* (Corbesier et al., 2007). The expression of *AP1* and *LFY* in a lateral primordia identifies it as a floral one.

AP1 and LFY then activate the expression of floral organ identity genes. The classical « ABC model » proposes that the combinatorial expression of A-, B- and C-class genes defines the identity of sepals, petals, stamens and carpels (Fig. 0-3) (Coen and Meyerowitz, 1991; Schwarz-Sommer et al., 1990). In *Arabidopsis thaliana*, *AP1* and *AP2* are classically viewed as A-class genes, *AP3* and *PI* (*PISTILLATA*) are B-class genes and *AGAMOUS* (*AG*) is a C-class gene. This model was later extended to include a D-function for ovule identity (Colombo et al., 1995) and an E-function for all floral organ identity, carried by the *SEPALLATA* (*SEP*) genes (Pelaz et al., 2000, 2001). The existence of the A function has been largely debated (Causier et al., 2010; Litt and Kramer, 2010), and it appears that A-class genes rather have a cadastral function in repressing the expansion of B- and C-class genes to the outer floral whorls, rather than in defining floral organ identity per se (Morel et al., 2017; Monniaux and Vandenbussche, 2018). In *Petunia hybrida*, B and C functions are largely conserved as compared to *A. thaliana* (although gene duplications have resulted in subfunctionnalization of all players) but the A function is split between several B- and C-class gene repressors from different gene families (Morel et al., 2017; Vandenbussche et al., 2004; Heijmans et al., 2012). Overall, the role of LFY in activating the expression of the ABC genes is key to define floral organ identity, and more details about LFY are given in the chapter of my PhD work.

Most of the ABC players are MADS-box transcription factors, and they have been proposed to act as tetramers on DNA to regulate target gene expression (Fig. 0-3). This "quartet model" gives a molecular

explanation for the combinatorial gene activity evidenced from genetic experiments (Theissen and Saedler, 2001; Theissen et al., 2016). B-class proteins group in two paralogous clades: the AP3/DEF clade and the PI/GLO clade, and members from the two clades form obligate heterodimers in order to bind their DNA targets (Riechmann et al., 1996b, 1996a). For instance in petunia, which is the model species that I am currently using to explore petal development, there are two AP3/DEF-type proteins and two PI/GLO-type proteins, and due to their particular expression patterns and dimerization preferences, there are three possible heterodimers that can be formed in petals and stamens and that might activate sligthly different target genes according to the individual DNA-binding specificity of each protein (Fig. 0-3) (Vandenbussche et al., 2004).

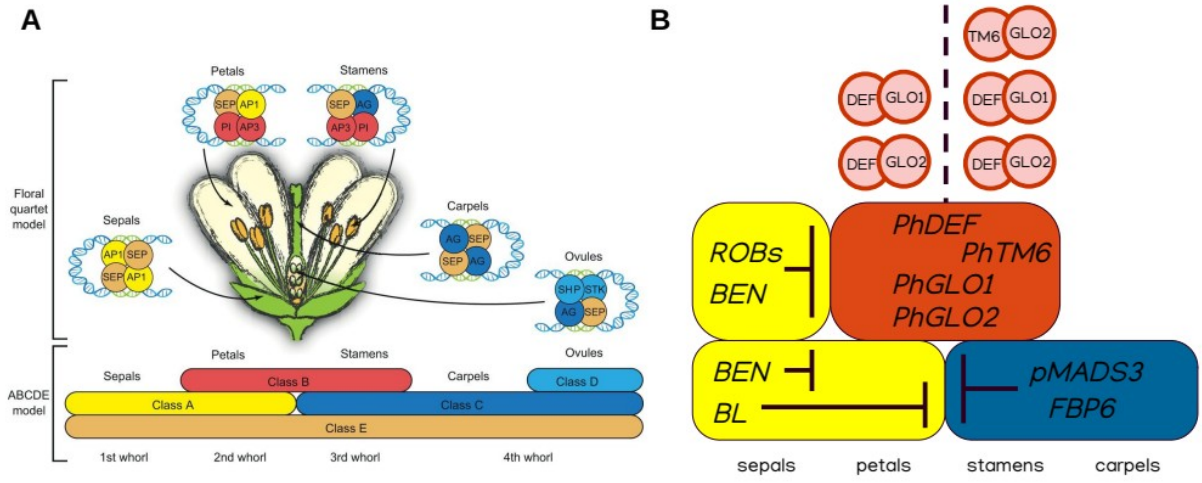

Figure 0-3: The ABC model of floral organ development. A: ABCDE model and floral quartet model proposed for *A. thaliana*, from (Theissen et al., 2016). **B:** ABC model in petunia, modified from (Morel et al., 2017). The A function is split between the *AP2-like* genes *ROB1-3* and *BEN* and the *miRNA169*-family gene *BLIND* (Cartolano et al., 2007). The B function is fulfilled by *PhDEF, PhTM6, PhGLO1* and *PhGLO2*. Putative protein complexes are shown above and differ in the petal and stamen region, since *PhTM6* is not expressed in petals (Vandenbussche et al., 2004; Rijpkema et al., 2006). The C function is redundantly fulfilled by *pMADS3* and *FBP6* (Heijmans et al., 2012).

Changes in flower morphology during evolution can be due to changes in floral organ identity, i.e. homeotic changes. For instance, double flowers in Rose result from the homeotic conversion of stamens into petals, which is due to a restriction of *AG* expression towards the inner whorls of the flower, itself caused by the extended expression in the outer whorls of an *AP2-like* gene that represses *AG* expression (Dubois et al., 2010; François et al., 2018). However, most morphological changes observed in angiosperms are not caused by homeotic changes, but rather by changes in floral organ colour, shape or size (Moyroud and Glover, 2017). Therefore, understanding what happens downstream of the specification of floral organ identity is also crucial to understand flower morphological evolution.

An ID is not enough: from organ identity to organ maturation

Specifying floral organ identity is the first step in building floral organs; however it is not necessarily sufficient to trigger the aquisition of all mature traits. For instance, a petal needs to form conical cells with a particular cuticle structure, to produce pigmentation, volatiles... while aquiring the correct shape and size, and this whole process can take several days. Indeed, floral homeotic genes are expressed at high levels throughout organ development, and pulsed perturbation of *AP3* gene activity (with an inducible miRNA) results in different degrees of homeotic perturbation in *A. thaliana* flowers, depending on the stage at which

the knock-down is performed (Wuest et al., 2012). Therefore, homeotic gene expression needs to be maintained until floral organs are almost fully developed, otherwise they show defects in the differentiation of some of their traits. Today, the direct target genes of LFY and most of the ABC players have been identified by ChIP-Seq mainly in young flowers (Chen et al., 2018), however how MADS-box TFs direct the entire formation of floral organs, with all their different cell types and complex traits, is mostly unknown and requires the determination of target genes in a cell-specific manner and with a precise temporal resolution (Heisler et al., 2022; Dornelas et al., 2011a).

Most changes in floral morphology that happened during evolution affect these mature traits of floral organs. Petals are particularly labile and their size, shape and colour has witnessed extensive change during evolution. For instance, several eudicot species develop spurs, which are extensions of a floral organ that contains nectar. The columbine flowers (*Aquilegia*) can form extremely long spurs from their petals, up to 15 cm long in *A. longissima*. Differential spur growth between species depends on differences in cell elongation only, controlled by hormones (brassinosteroids and auxin) and transcription factors (from the TCP family in particular) (Puzey et al., 2012; Yant et al., 2015; Zhang et al., 2020). In contrast, the emergence of spurs from a non-spurred individual only depends on cell division (controlled by the POPOVICH transcription factor) (Ballerini et al., 2020). Evolution has thus been tinkering with the shape (curved vs. straight) and size of spurs in the *Aquilegia* genus by affecting either cell division or cell elongation, through various pathways (auxin, brassinosteroids, different regulators of cell division or elongation...). All players of the petal developmental process, whether they are regulatory or effectors genes, are potential targets for evolution to modify floral organ shape, making the identification of the key players in morphological evolution a very uncertain and tedious process. And some very unusual suspects (i.e. genes unknown for the floral developmental pathway) are sometimes found to impact floral morphological evolution (Monniaux 2023, in prep).

My research career has been revolving around questions of flower development and evolution. During my PhD, I investigated the evolution of the DNA-binding specificity of LFY in the green lineage. During my post-doc, I studied how petal number can shift from robust to variable, and I investigated the genetic and developmental basis of petal initiation. Currently, I study petal development in petunia, and in particular the contribution of the different cell layers of the petal to its final morphology, and how mature traits are specified in the different cell types of the petal from a handful of homeotic genes. Therefore, I have studied flower evo-devo in different model systems and at many different scales.

PhD work (2009-2013):

Evolution of the floral regulator LEAFY in the green lineage

Laboratory for Plant and Cell Physiology (LPCV), Grenoble

Thesis advisor: **François Parcy**

Overview LEAFY (LFY) is a major floral regulator in angiosperms, in which it specifies the identity of the floral meristems and activates the ABC genes that determine floral organ identity. As such, LFY has indispensable roles in the construction of a flower and it does so by recognizing a 19-bp specific palindromic motif on DNA, thereby regulating its target genes. However, LFY is also present in other land plants (mosses, ferns, gymnosperms) and even in some green algae, all of these groups being flower-less. Moreover, *LFY* did not form a gene family and remained essentially as a single-copy gene during land plant evolution, preventing it from evolving new roles by sub- or neo-functionalization after duplication. LFY represents then a case study to understand the evolution of a major regulator and its target genes without having duplicates and problems of redundancy. During my PhD, I have found both changes in *trans* (LFY DNA-binding specificity) and in *cis* (LFY target genes) in this network. LFY has been able to change its DNA-binding specificity by transiently adopting a relaxed specificity, which likely allowed a smooth change in the downstream regulatory network. But even in species with similar LFY DNA-binding specificities, the LFY regulatory network evolved in *cis* and target genes were kept, lost or gained.

1. Evolution of LFY DNA-binding specificity in the green lineage

In the model plant *Arabidopsis thaliana*, LFY has characteristics of a pioneer transcription factor (TF), able to bind to closed chromatin regions and open them to launch the floral gene expression programme (Lai et al., 2021). LFY forms a dimer to bind DNA and recognizes a 19-bp palindromic site (Hames et al., 2008), that we later named a ‘‘type I’’ motif (Fig. 1-1). It then regulates a large set of genes by activating or repressing their expression, and in particular MADS-box genes that are key regulators of reproductive development (Parcy et al., 1998; Moyroud et al., 2011; Winter et al., 2011). Being unable to influence transcription on its own, the LFY protein does so by interacting with co-regulators such as UNUSUAL FLORAL ORGANS (UFO), WUSCHEL (WUS) or SEPALLATA3 (SEP3) (Parcy et al., 1998; Gallois et al., 2004; Chae et al., 2008; Liu et al., 2009). The spatio-temporal expression pattern of these co-regulators will result in the activation of LFY target genes in specific domains, and in particular the ABC-class genes that specify the identity of the different floral organs in their right location (Parcy et al., 1998; Moyroud et al., 2010). Thus in Arabidopsis, we have a good understanding of the molecular mode of action of LFY in specifying a flower.

However, the *LFY* gene is also found in non-flowering plants from the green lineage (see Fig. 0-1) (Wilhelmsson et al., 2017). When I started my PhD, it was already suspected that LFY from the moss *Physcomitrium patens* (PpLFY1 and PpLFY2 proteins) had a different DNA-binding specificity than angiosperm LFY proteins (Maizel et al., 2005). However, the extent of this possible change in specificity, and if PpLFY1/2 proteins were a particular case or not, was unknown. Strikingly, *LFY* did not evolve as part of a gene family, and remained as a single-copy gene in most plants species, for over 800 million years (Wilhelmsson et al., 2017; Gao et al., 2019). This is quite unusual as compared to most regulatory genes that tend to duplicate in order to evolve, such as the MADS-box genes that gather over 100 paralogs in *A. thaliana (Airoldi and Davies, 2012)*. Genes largely evolve by duplication, since it allows one of the copy to evolve freely while a back-up paralog still retains the ancestral, and sometimes indispensable, function

(Ohno, 1970). It therefore raised the following question: can an essential regulatory gene evolve as a single copy? And from what was known at the time of my PhD, LFY indeed had an essential role in *P. patens*, allowing the first cell division in the zygote to occur (Tanahashi et al., 2005).

Most of the work of my PhD consisted in characterizing LFY DNA-binding specificity from a wide range of plant species, from the green algae to the angiosperms, by purifying recombinant proteins produced in *Escherichia coli* and performing SELEX (Systematic Evolution of Ligands by EXponential enrichment) assays (Tuerk and Gold, 1990; Djordjevic, 2007). For our SELEX assay, a random 30-bp DNA library is mixed with the LFY protein, and protein-DNA complexes are isolated with magnetic beads (covered with nickel, bound by the 6xHis tag used to purify the recombinant protein). The library is amplified by PCR and the whole procedure is repeated until the library is enriched in oligonucleotides specifically bound by the protein, which is tested at each cycle by gel shift assays. This library is then sequenced and the alignment of these sequences yields a logo that represents the DNA binding preferences of the TF in a quantitative manner (Schneider and Stephens, 1990; Bailey and Elkan, 1995). Our SELEX assays revealed that LFY had adopted three kinds of DNA binding specificities across the green lineage (Fig. 1-1) (Sayou et al., 2014) (key publication 1, p.46). The most common specificity is shared by LFY proteins from vascular plants and liverworts; we named it “type I”. In the group of mosses, represented by *P. patens*, LFY adopts a different specificity that we named “type II”. It differs from “type I” by mainly 2 nucleotides on each half-site (where each LFY monomer binds), whereas the general organization of the motif is similar to “type I”. To understand the molecular determinants of these preferences, another PhD student from the lab (Camille Sayou) crystallized PpLFY1 in contact with DNA. This revealed that only 2 amino acids determine the “type I” vs “type II” specificity. Finally, “type III” specificity was adopted by LFY proteins from green algae and hornworts. This specificity was highly similar to “type II”, except that the 3 central nucleotides that separate half-binding sites were absent. Using the crystal structure of PpLFY1, we predicted that removing these central 3 nucleotides would affect the dimerisation mode of LFY, with monomers not being side-by-side on DNA but rather facing each other (schematized on Fig. 1-1), which is also supported by different lines of biochemical evidence. Therefore, LFY proteins changed of DNA binding specificity through two mechanisms: a likely change in the dimerisation mode, and a change in the binding specificity of each monomer.

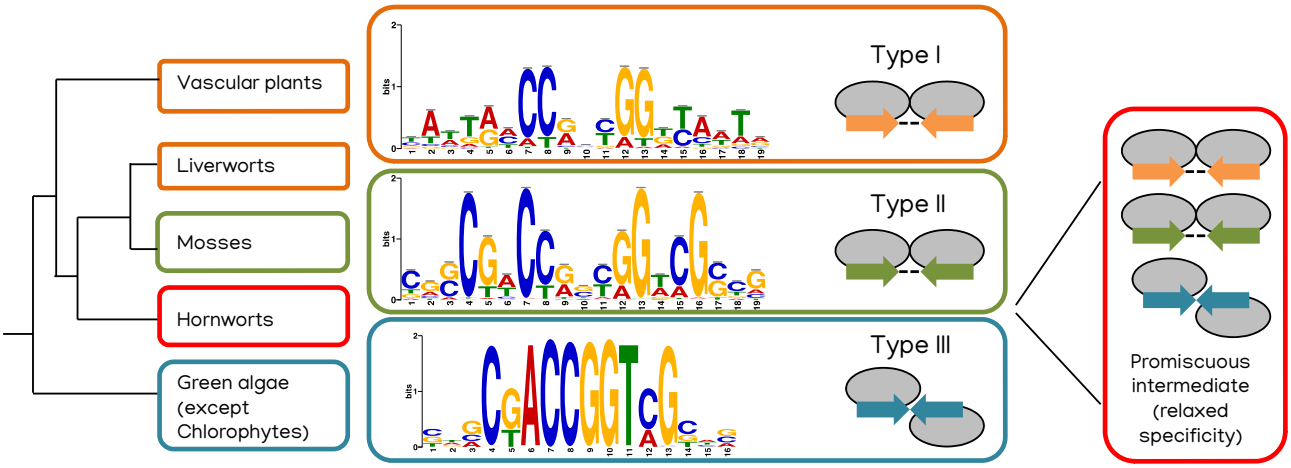

Figure 1-1. Model for the evolution of LFY DNA-binding specificity in the green lineage.
Half LFY-binding sites, bound by one LFY monomer, are represented by arrows and the color represents the different DNA-binding specificities of LFY monomers. In green algae, LFY binds DNA with a “type III specificity” where the two LFY monomers bind on each side of the DNA without direct contact between them. In mosses, liverworts and vascular plants, the two LFY monomers bind side-by-side on DNA with a direct dimerization surface, but the DNA-binding specificity of monomers is different between “type I” (vascular plants and liverworts) and “type II” (mosses). In hornworts, LFY proteins bind all three types of motifs with a similar affinity.

The question remained as to how these different specificities could have appeared during evolution without dramatic consequences. The answer came from one instance of a LFY protein that is able to recognize all three types of motifs with a similar affinity (Sayou et al., 2014). We have found this promiscuous form in *Nothoceros aenigmaticus*, a member of the hornworts. In our final model (Fig. 1-1), we propose that the ancestral LFY protein could recognize "type III" sequences only. Next, it acquired a novel dimerisation mode, and became at that point able to recognize all three types of binding sites with a relaxed specificity (for unknown molecular reasons). Later on, specific amino acid changes restricted the specificity of the protein to either "type I" or "type II". Thus, it is possible for a TF to evolve different DNA-binding specificites without resorting to gene duplication but thanks to the transient acquisition of a relaxed specificity instead.

The effects of these smooth changes in LFY DNA binding specificity on the regulation of its target genes are unknown so far. In our study, we found a minor enrichment in "type II" binding motifs in MADS-box genes in the *P. patens* genome. This suggests that in *P. patens* and *A. thaliana*, LFY might regulate the expression of a common set of MADS-box genes through the binding to "type II" or "type I" motifs respectively, which is in favor of the co-evolution of LFY DNA-binding specificity and its *cis* elements. This phenomenon of compensation between *cis* and *trans* mutations has been already evidenced in several living organisms (Fisher et al., 2006; Kuo et al., 2010; Barrière et al., 2012; Paris et al., 2013), and it might be an important mechanism to temper the deleterious effect of mutations. An extensive genome-wide characterization of *cis* elements and target gene expression is now needed to understand the evolution of LFY and its targets throughout plant evolution.

Since the end of PhD, new evidence came to support or temper what we proposed in (Sayou et al., 2014). First, the crystal structure of LFY from *Nothoceros aenigmaticus* (our hornwort species with a promiscuous form of LFY) was solved on "type III" DNA, which confirmed the face-to-face binding mode that we infered by modeling before (F. Parcy, personal communication, confidential). Second, in a recent study Gao and colleagues mined the 1KP and Phytozome transcriptome databases for all available *LFY* sequences (which we did at the time of my PhD, but of course many more sequences were deposited since then) (Gao et al., 2019). They have found two cases of fern species with each two copies of LFY: a promiscuous form and a "type I" form. They built LFY phylogenies and found that the fern promiscuous LFY clustered together with the other promiscuous LFYs from hornworts (while the "type I" LFY clustered with other fern species "type I" LFYs, as expected). This discrepancy between the LFY phylogeny and the species phylogeny supports the hypothesis of an ancestral duplication of LFY in its promiscuous form, after the divergence of hornworts with the rest of land plant species (Fig 1-2). Later on, in these two particular fern species, one copy of LFY remained promiscuous while the other one evolved towards a "type I" specificity. In other land plant species, one of the two copies was systematically lost and the other one evolved either a "type I" or a "type II" specificity. Thus, in contrast to what we proposed, LFY did duplicate during its evolution, and it is possible that this duplication helped LFY to specialize into "type I" or "type II", even though it already had a relaxed specificity at that time. These new findings temper our initial conclusions that LFY evolved without duplicating, but the presence of a promiscuous form that served as a platform for LFY evolution is also confirmed by the study of Gao et al., and this transition form likely played an important role for LFY evolution.

2. Changes in the floral LFY network

In angiosperms, the DNA-binding specificity of LFY is essentially the same in all species that we assessed. However, this does not necesarily mean that the regulatory network controlled by LFY is exactly the same, and I have studied in detail two cases where it has been modified. This work relies on the previous

development, in my PhD group, of a biophysical model to predict the presence of LFY DNA-binding sites on a genomic sequence with high accuracy (Moyroud et al., 2011).

(1) The first example is in roses, and this unpublished study was done in collaboration with the group of Mohammed Bendahmane at the RDP laboratory. In Arabidopsis, LFY regulates the expression of *AG*, a C-class gene determining stamen and carpel identity, but not the one of *SHATTERPROOF* (*SHP*), a paralogous gene controlling gynoecium and fruit development (Liljegren et al., 2000; Favaro et al., 2003; Pinyopich et al., 2003). In contrast in Antirrhinum, the ortholog of *SHP* is the gene fulfilling the C-function and regulated by the LFY ortholog, whereas the *AG* ortholog has little role in floral organ identity (Causier et al., 2005). In roses, some evidence suggested that both the *AG* and *SHP* orthologs could mediate the C function and we wanted to test this hypothesis. In situ hybridizations performed in the group of M. Bendahmane showed that *AG* and *SHP* in Rosa gallica were both expressed in stamens and carpels in a partially overlapping pattern. Then, we reasoned that the presence of LFY binding sites in *AG* and *SHP* would support their early role in floral organ identity determination, i.e. in the C function. I analyzed the intronic sequences of *AG* and *SHP* genes from several Rosa species (Fig. 1-2). In each of them, I have found a good predicted binding site that we named *LFY-bs1* and I validated these sites in vitro by gel shift assays against the *Rosa chinensis* LFY protein, suggesting that LFY can bind (and therefore might regulate the expression of) both *AG* and *SHP* genes in roses. Finally, in vivo experiments are still missing to provide definitive evidence that LFY can activate both *AG* and *SHP* in roses, and rose petal agro-infiltration with an activated form of LFY (LFY-VP16) were considered but never performed. Still, it is likely that in roses, both *AG* and *SHP* participate to the C function and are activated by LFY. From this study and others from the literature (Kater et al., 1998; Nitasaka, 2003; Causier et al., 2005), it appears that the functions of *AG* and *SHP* orthologs have been very labile during evolution, with different patterns of sub- and neo-functionnalization to fulfill the complex C-function (which entails stamen and carpel identity, initiation, development and maturation). Therefore, this represents a case of high plasticity for a small regulatory network controlling a major reproductive function.

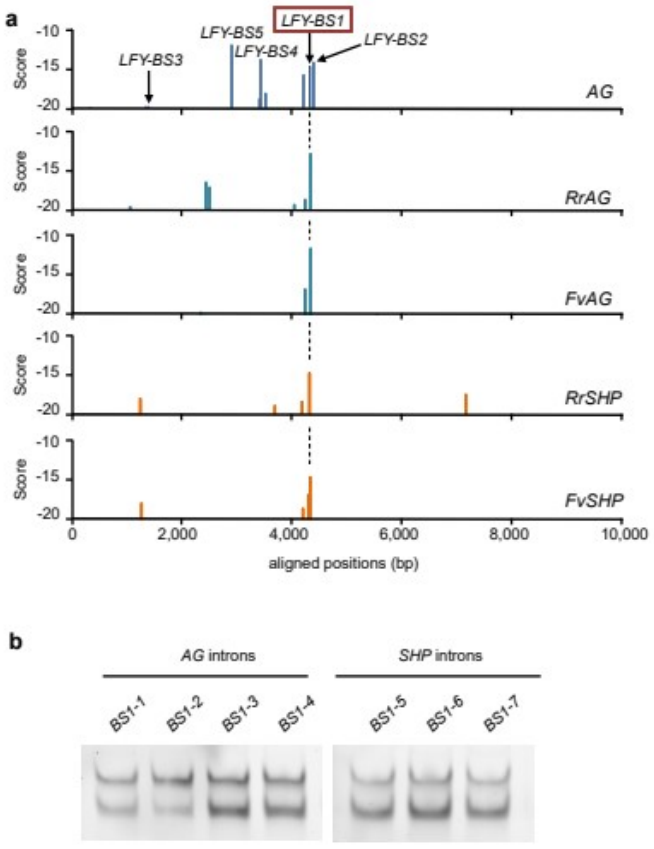

Figure 1-2. Prediction and in vitro validation of LFY binding sites in intronic sequences of *AG* and *SHP*.

(a) Predicted binding score for *Rosa chinensis* LFY on aligned intronic sequences of *AG* (Arabidopsis), *AG* and *SHP* from *Rosa rugosa* (Rr) and *Fragaria vesca* (Fv).

(b) Gel shift assays of LFY-BS1 sites from *AG* and *SHP* introns from various rose species, tested with the *Rosa chinensis* LFY protein. Only the shift in migration is shown here, the lower and higher bands represent the monomeric and dimeric binding states of LFY respectively.

(2) The second example is in Cardamine, and this study was performed while I was a post-doc in Angela Hay's group (Monniaux et al., 2017). In Arabidopsis, LFY directly activates the expression of *APETALA1* (*AP1*), which specifies floral meristem identity. *AP1* is also activated by other floral regulators (among which the FT/FD complex) later in the development of the inflorescence (Wigge et al., 2005). As a result, even in full *lfy* mutants, the leafy shoots that are produced show floral features, such as whorled phyllotaxis, sepals and central carpels, particularly at late floral nodes. These floral features are completely lost in *lfy ap1* double mutants that produce leafy shoots. In Cardamine, we have found that *lfy* mutants directly produce leafy shoots without any signs of floral identity. Consistently, *AP1* expression was completely absent in these mutants. This shows that in Cardamine, *AP1* expression has become entirely dependent on LFY, whereas it also depends on FT/FD in Arabidopsis. Current work by Michiel Vandenbussche indicates that, on the opposite, in petunia AP1 expression is no longer regulated by the LFY ortholog and has become fully dependent on FT-like genes (unpublished work, confidential), and other studies have shown that the regulation of *AP1* by LFY or FT/FD is evolutionary very labile (Monniaux et al., 2017). Therefore, here again there has been extensive rewiring of the small network that specifies floral meristem identity during flowering plant evolution.

The gene regulatory network controlled by LFY, although crucial for reproductive development, has witnessed extensive rewiring during angiosperm evolution. It is difficult to assess if this has had any strong functional and ecological consequences on the development of the plant. Most likely not, but this rather exemplifies the intense and random molecular tinkering that takes place during evolution.

3. Glimpses of the pre-floral LFY network

At the time of my PhD, the function of LFY in non-flowering plants was elusive. It was known that B- and C-class genes, which are crucial for reproductive development in angiosperms, were also expressed in gymnosperm reproductive structures. However, whether the expression of these genes was also controlled by LFY, and hence whether a sort of pre-floral network existed, was unknown. I participated in a study on the gymnosperm species *Welwitschia mirabilis* (Moyroud et al., 2017) in which we showed that *LFY* indeed was expressed in male cones, just preceding B-class gene expression. By several lines of biochemical evidence including gel shift assays, we found that Welwitschia LFY is able to bind to cis-regulatory elements in the promoter of B-class genes, and therefore that it likely regulates their expression. This is the first evidence that the control of B-class genes by LFY could have predated the appearance of the flower. The origin of the flower is often referred to as « an abominable mystery » based on a quote by Charles Darwin (see introduction), but it looks like several of the molecular determinants of the flower and their relationship with each other were already present in a non-flowering ancestor. This mirrors many other examples where a functional trait evolved after the apparition of its components (Blount et al., 2012), as has been found for the origin of symbiotic relationships between plants and fungi for instance, for which algae are already pre-adapted but miss some parts of the pathway to form a functional symbiosis (Delaux et al., 2015). The common ancestor between gymnosperms and angiosperms already had a functional LFY/B-genes regulation, but it took extra unknown steps for the first flower to emerge.

Outside of seed plants, it was known at the start of my PhD that PpLFY1/2 controlled the first zygotic division in *P. patens* (Tanahashi et al., 2005) and, together with findings in *A. thaliana* that supported a role for LFY in establishing floral meristematic activity (Chahtane et al., 2013), we proposed that the ancestral role of LFY was to regulate meristematic activity (either in vegetative or reproductive contexts) (Moyroud et al., 2010). Since then, additional evidence came from the fern *Ceratopteris richardii* in which

LFY maintains apical cell activity, necessary for the proper development of aerial organs (Plackett et al., 2018). Plackett et al. have thus proposed that LFY regulated cell proliferation in the common ancestor of land plants, and that this function was later co-opted in different shoot developmental contexts to regulate meristematic activity in vegetative or reproductive phases (Plackett et al., 2018). Identifying the LFY target genes regulating these ancestral functions is now at the center of the funded ANR project BEFLORE, involving my former PhD supervisor François Parcy and Yoan Coudert, a researcher at the RDP lab; therefore I am still remotely involved in this project through informal discussions.

The role of LFY in green algae is completely unkown so far, and we can only speculate that it regulates cell division in these species. Emerging model species in streptophytic algae whose genomes are sequenced and that are becoming amenable to genetic transformation (Zhou and von Schwartzenberg, 2020) will surely help resolve the question of the ancestral role and of the origin of LFY.

Post-doc work (2013-2017):

Genetic and developmental basis of petal number variation

Max Planck Institute for Plant Breeding Research, Cologne, Germany

Group leader: **Angela Hay**

Overview In spite of their enormous inter-specific diversity, flowers are remarkably stable structures within a species and their bauplan is generally robust to genetic, environment or stochastic perturbations. However, in the crucifer *Cardamine hirsuta*, flowers initiate a variable number of petals. Comparing variable petal initiation in *C. hirsuta* to robust petal initiation in the related species *Arabidopsis thaliana*, we found that cis-regulatory divergence in the A-class gene *APETALA1* (*AP1*) underlaid this morphological difference. Introducing the *A. thaliana AP1* gene in *C. hirsuta* was sufficient to restore stable petal number, while introducing the *C. hirsuta AP1* gene in *A. thaliana* caused petal number to vary. We also mapped the QTL underlying petal number variation within *C. hirsuta* and did not find *AP1* in these loci, showing that inter- and intra-specific variation in petal number have different genetic determinants. Finally, we showed that petal number variation is likely a trait under selection and we propose that it might cause variation in outcrossing frequency, which could be a selective advantage in fluctuating environments.

1. Genetic basis of inter- and intra-specific difference in petal number

The floral bauplan, i.e. the identity, number and position of floral organs is generally stable within a species. Flower architecture is therefore considered as a canalized trait, since it does not change in response to genetic, environment or stochastic perturbations, in contrast to leaf shape that is a highly plastic trait (Givnish, 2002). However, *Cardamine hirsuta* is an exception to this observation as its flowers display a variable loss of petals, as compared to its relative *Arabidopsis thaliana* that stably initiates 4 petals (Fig. 2-1). *C. hirsuta* petal number is a plastic trait that varies in response to genetic (between *C. hirsuta* accessions), environment (temperature, light quality, day length...) and stochastic perturbations (Monniaux et al., 2016; McKim et al., 2017; Monniaux et al., 2018). This decanalization is a recent event since most other *Cardamine* species have a robust number of petals.

Figure 2-1. Stable petal number in *A. thaliana* vs. variable petal number in *C. hirsuta*.
Flowers with 0, 1, 2, 3 or 4 petals can be found on a single *C. hirsuta* plant.

Before I joined the lab as a post-doc, it had been found by chance that the *APETALA1* (*AP1*) locus was sufficient to cause stable or variable petal number, depending on its species of origin (Monniaux et al., 2018) (key publication 2, p. 50). Indeed, adding the *A. thaliana AP1* (*AtAP1*) genomic construct into *C. hirsuta* was sufficient to canalize petal number to 4 (whereas adding an extra copy of the *C. hirsuta AP1* (*ChAP1*) locus did not alter petal number much). Conversely, variable petal number could be obtained in *A. thaliana* by inserting the *ChAP1* locus into an *ap1* mutant background. This shows that variability in petal number is a cryptic trait in *A. thaliana*, that is normally canalized by the presence of the *AtAP1* locus, but that can be revealed when this locus is absent (Fig. 2-2).

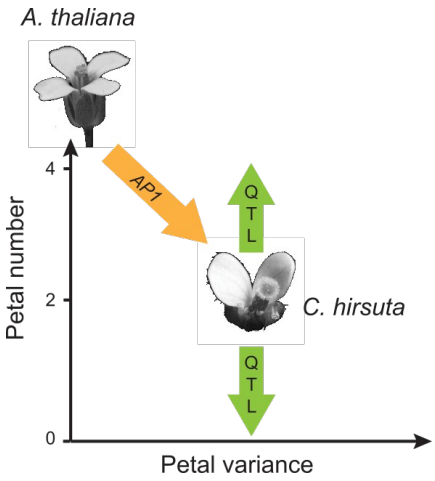

Figure 2-2. Decanalization of petal number in *C. hirsuta*.
In *A. thaliana*, petal number equals 4 and petal variance is null. Change in *AP1* expression (pattern and dose) in *C. hirsuta* caused petal number to vary with an average petal number close to 2. Other loci than *AP1*, mapped as QTL, influence average petal number in different *C. hirsuta* accessions.

Petal number is always variable in *C. hirsuta* natural accessions, but average petal number is different between accessions. Therefore, we wondered if genetic variation in *AP1* could also explain this difference in average petal number observed in natural populations. Quantitative Trait Loci (QTL) mapping in several F2 populations generated from different *C. hirsuta* accessions revealed 9 QTL, but none of them contained the *AP1* locus (Monniaux et al., 2018). The genetic basis for inter- and intra-specific variation in petal number is therefore different. These loci have not been fine-mapped yet but two of them contain *YABBY* genes which are known regulators of the adaxial/abaxial polarity of lateral organs (Angela Hay, personal communication, confidential). Indeed, petals in *C. hirsuta* tend to initiate slightly more frequently on the abaxial side of the flower, where there is simply more space for them on the meristem to initiate. Therefore, natural variation in *YABBY* genes might slightly affect the abaxial-adaxial patterning of the flower, which could influence petal initiation between *C. hirsuta* accessions, in a context where robustness of petal initiation has been lost. However, the effect of those genes is fully masked when *AtAP1* is present in *C. hirsuta* and no variation in petal number can be detected any longer. Therefore, we were able to identify genetic variation that influences petal number both in *C. hirsuta* and *A. thaliana*, but this variation is entirely cryptic in wild-type *A. thaliana* because the *AtAP1* locus masks its effects by epistasis (Fig. 2-2).

2. From genetics to development: *AP1* expression and petal initiation

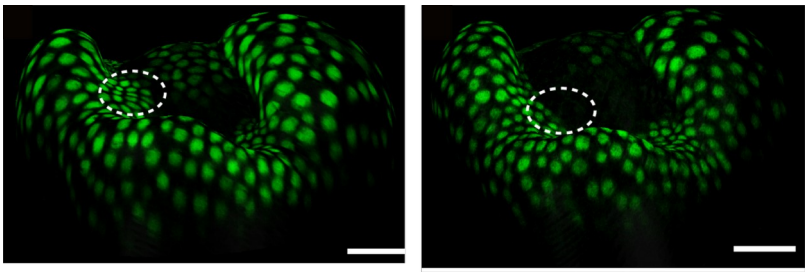

Figure 2-3. Expression pattern of *AtAP1* and *ChAP1* in *C. hirsuta* flowers.
Side views of young *C. hirsuta* flowers expressing *gAtAP1:GFP* (left) or *gChAP1:GFP* (right), i.e. transcriptional GFP fusions of the genomic *AtAP1* or *ChAP1* locus. The dotted circle indicates the petal initiation domain. Scale bar: 20 µm.

Since we identified *AP1* as the causal locus in petal number decanalization, we tested whether this was due to changes in protein function or in regulatory elements. We found that promoter regions of *AtAP1* and *ChAP1* were recapitulating most of the effects of the full genes on petal number variation, while coding sequences had no influence. We therefore looked at the *AtAP1* and *ChAP1* spatio-temporal expression pattern in *C. hirsuta*, using GFP transcriptional fusions with a full *AP1* genomic locus from each species. We

found that *AtAP1* expression extended more in the petal initiation domain than *ChAP1*, whose expression tended to remain more restricted to the sepal whorl (Fig. 2-3) (Monniaux et al., 2018).

What could be the link between *AP1* expression and petal initiation? *AP1* has been historically described as an A-class gene in the ABC model for floral organ identity (Coen and Meyerowitz, 1991; Schwarz-Sommer et al., 1990), ie. a gene necessary to specify sepal and petal identity, but not their initiation. However, several studies have now nuanced this homeotic role for *AP1* and questioned the existence of the A function itself (Causier et al., 2010; Morel et al., 2017). Indeed in *A. thaliana*, the *ap1* mutants do not really show defects in petal identity but rather in their initiation, and double *ap1 agl24* mutants initiate normal petals (Yu et al., 2004), showing that petal identity can be specified even in the absence of *AP1*. The current view in the literature is that *AP1* and other genes from the A-function are rather floral meristem patterning genes, that repress the expansion of B- and C-class genes to the outer whorls of the flower, rather than actively specifying an organ identity per se (Monniaux and Vandenbussche, 2018).

PETAL LOSS (*PTL*) and *RABBIT EARS* (*RBE*) are two genes that were identified to play a specific role in petal initiation, and a general framework for petal initiation has been proposed (Fig. 2-4). *PTL* is expressed in the boundary domain between sepals (i.e. in the first floral whorl, but importantly not in the second whorl where petals do initiate), where it represses growth (Lampugnani et al., 2012). This growth repression follows the establishment of a boundary domain between sepals, where *CUP SHAPED COTYLEDON* (*CUC*) genes are expressed (Lampugnani et al., 2012; Aida et al., 1997). Establishment of this boundary domain is indirectly necessary for petals to initiate in the adjacent domain. Indeed, *cuc1/2* double mutants display fused sepals and defects in petal initiation, both in *A. thaliana* and *C. hirsuta*, while the triple *cuc1/2 ptl* mutant has an even more decreased petal number than *cuc1/2* or *ptl* mutants (Lampugnani et al., 2012; Aida et al., 1997). Therefore, a current view of petal initiation is that both *PTL* and *CUC* genes act to repress growth of the inter-sepal domain (although their action is partly independent and they repress growth in different directions), thereby indirectly granting more space for petals to initiate in the adjacent domain in the second whorl (Lampugnani et al., 2012). PTL also acts non-cell-autonomously, likely by regulating the transcription of several genes among which *UNUSUAL FLORAL ORGANS* (*UFO*), to influence petal initiation in the adjacent whorl, where *RBE* is expressed (Takeda et al., 2022). RBE represses the expression of several genes to allow petal outgrowth (Huang et al., 2012; Krizek et al., 2006; Li et al., 2016). Petal initiation can be visualized by the presence of auxin peaks (visible with the DR5 reporter for auxin signaling) in whorl 2 (Lampugnani et al., 2013), and these peaks are slightly displaced in the *ptl* mutant as they tend to overlap with the inter-sepal domain (Lampugnani et al., 2012). *PTL* therefore ensures the correct auxin dynamics necessary for robust petal initiation (Lampugnani et al., 2013).

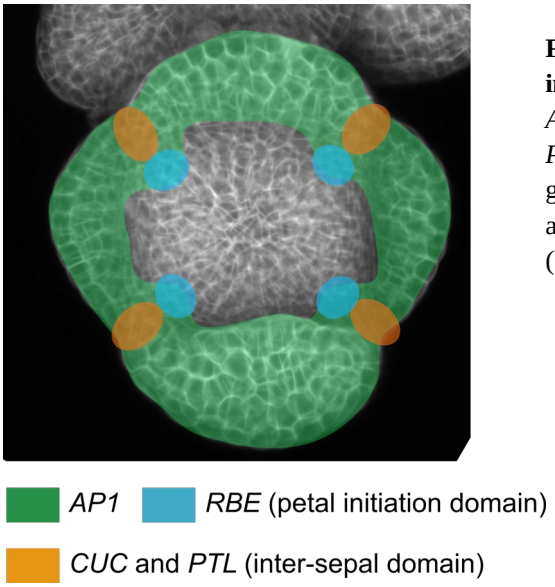

Figure 2-4. Spatio-temporal expression pattern of some genes involved in petal initiation.
AP1 (green) is expressed in whorls 1 and 2, while *CUC* genes and *PTL* (orange) are expressed in the inter-sepal domain. They repress growth of this domain and *PTL* induces gene expression non-autonomously in the petal initiation domain where *RBE* is expressed (blue) and where auxin peaks are also found.

In *C. hirsuta*, auxin peaks are broader than in *A. thaliana* and sometimes clearly displaced in the inter-sepal domain (Monniaux et al., 2018). However, this is not due to defects in *PTL* function since *PTL* is correctly expressed in the inter-sepal domain in *C. hirsuta*, and introducing the genomic *PTL* locus from *A. thaliana* into *C. hirsuta* fails to complement the variable petal phenotype (Monniaux et al., 2018). *RBE* is also correctly and robustly expressed in *C. hirsuta* (personal data, unpublished). Recent results from Léa Rambaud, a post-doc who took over this project, indicate that the boundary genes *CUC* are correctly expressed in *C. hirsuta*, but their expression domain is broader and less focused than what is observed in *A. thaliana*, similarly to what I observed for auxin peaks. This unprecise definition of the boundary domain between sepals might be responsible for the uncorrect placement of auxin peaks and the subsequent variable initiation of petals. However, it remains for the moment unclear how this relates to the shift in *AP1* expression that broke the robustness of the system and caused the emergence of the variable phenotype.

3. Petal number variation: a trait under positive selection?

The recent decanalization of petal number in *C. hirsuta* prompted us to ask this intriguing question: is variable petal number under positive selection and could it entail any possible benefit in the reproductive strategy of this species? *C. hirsuta* is mostly a selfing species (Hay et al., 2014), and transition to selfing is generally associated with a reduction in floral display: attracting pollinators is not needed anymore and attractive floral traits tend to be lost by drift. In particular, reduction in floral size and petal loss have been documented (Sicard and Lenhard, 2011; Bowman et al., 1999). In this context, petal loss is generally viewed as a secondary consequence of the transition to selfing, but not as a driver for this process.

In order to explore whether petal number variation evolved under positive selection or by genetic drift, we first had to determine if petal number and its variation indeed had a genetic basis, or if these traits were mostly influenced by the environment. This can be addressed by creating experimental populations for QTL mapping, which was mostly done by Bjorn Pieper, another post-doc in the lab at that time. He found that petal number in *C. hirsuta* has a strong genetic basis, with a broad-sense heritability at 0.86-0.9, and 15 QTL were identified to influence average petal number with small to medium effects (Pieper et al., 2016). Petal number variation also has a rather strong genetic basis, with a broad-sense heritability of 0.58 and 4 QTL that were found to influence this trait (Monniaux et al., 2016). Importantly, these variation QTL also influence average petal number, showing that average petal number and its variation are inherently linked traits, both having a strong genetic constituant. The rather high heritability of these two traits suggests that they have the potential to evolve relatively fast under balancing selection.

We observed that it was relatively easy to obtain individuals with an average number of petals close to 4 in experimental populations (crossing two accessions together and looking at the segregating F2 progeny), whereas such individuals were almost never observed in the wild (Fig. 2-5) (Monniaux et al., 2018). This suggested that standing genetic variation was sufficient to create these individuals in the wild, but that they were counter-selected. The exact reason for this possible counter-selection is unknown so far. However, we have found that average petal number influences outcrossing frequency in controlled field experiments. Indeed, we grew together wild-type plants and an EMS mutagenesis mutant called *four petals 2* (*fp2*) that has a high average petal number, in a controlled field environment. We genotyped the progeny of each plant for a marker discriminating between the wt and mutant alleles close to the *FP2* locus, and found that *fp2* plants tended to outcross slightly more frequently than wt plants (Monniaux et al., 2018). Therefore, higher petal number is associated with a higher outcrossing rate. This might be due to physical reasons (petals help open the flower, whose reproductive organs are then exposed to pollinators) and/or to the fact that flowers with more petals better attract pollinators.

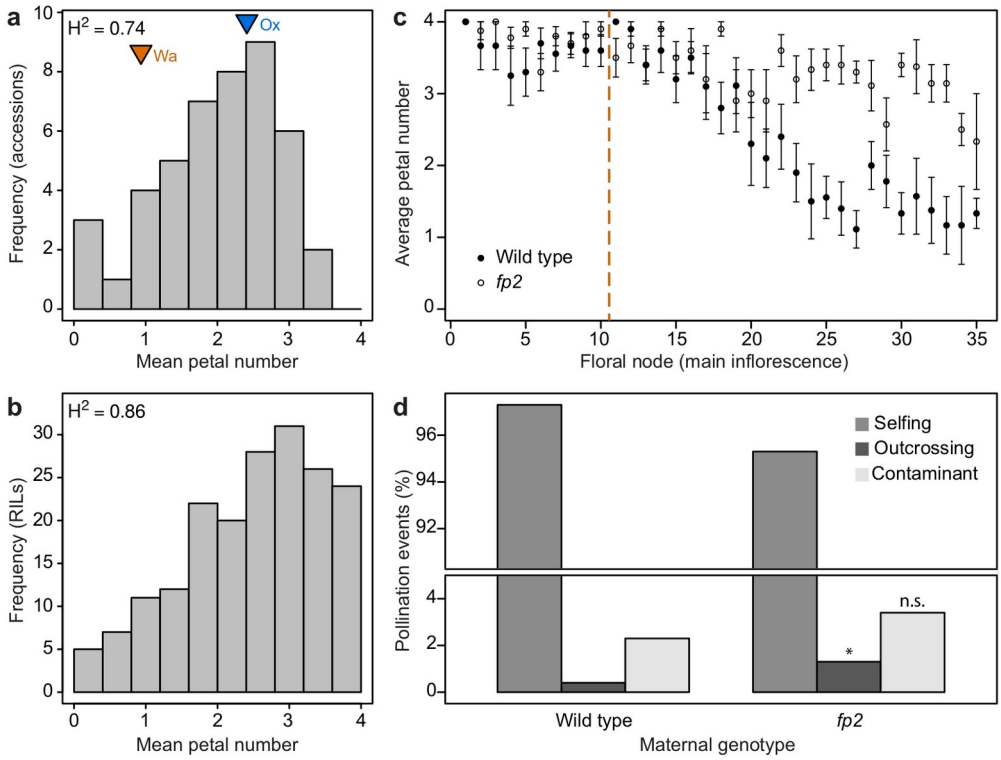

Figure 2-5. Petal number in natural and experimental populations, and link with outcrossing rate.
(a-b) Distributions of C. hirsuta petal number in 45 natural accessions (a) and a population of RIL derived from Ox and Wa accessions (b). (c) Average petal number at every floral node in homozygous wild-type and *fp2* plants in field conditions. (d) Progeny of 10 wild-type and 10 *fp*2 mothers were genotyped for a marker close to the *FP2* locus to determine their paternity (« selfing » if genotype of the progeny corresponds to the maternal genotype, « outcrossing » if heterozygous, « contaminant » if the other genotype).

The question remains as to why individuals with higher petal number would be counter-selected in nature then? *C. hirsuta* is mostly a selfing species, therefore having a slightly higher outcrossing rate as found in the *fp2* mutant should be beneficial for the plant, by maintaing higher genetic diversity in the population and limiting the inbreeding depression associated with selfing. From there, we can only speculate that petal number variation itself, and not its average, might be under selection. Petal number varies largely in response to environmental conditions, and it might be advantageous to the plant to vary its outcrossing rates depending on external conditions that could influence the frequency of pollinators visits. Plasticity of the trait itself might be a selective advantage granting more resilience and more evolvability to the plant than a fixed petal number, and therefore a fixed outcrossing rate, would.

Current work and perspectives (from 2017 onwards):

The contribution of cell layers to petunia petal development and evolution

Laboratory for Plant Reproduction and Development, ENS de Lyon, France

Overview Since 2017, I have joined the group « Evo-devo of the flower », led by Michiel Vandenbussche, in the RDP lab in Lyon. I have switched model systems and started using petunia (Petunia x hybrida mostly) to unravel mechanisms controlling petal development. In particular, we have identified mutants affecting the identity of either one layer of the petal or the other (the epidermis or the mesophyll), which results in drastically different petal morphologies. I have been using this system to investigate how cell layers contribute to petunia petal development, and in particular how they acquire their distinct identities during the course of development. This project uses a strictly delimited system of a few mutants, yet it has developed into broad questions of fundamental importance. Most of this work is still ongoing and all questions are basically unanswered, and I have decided to focus my attention on characterizing the gene regulatory network in the different layers of the petal (part 2 of this chapter). However, here I will also present all the potential outcomes of the project for possible future research (parts 3 and 4).

Flowering plants' aerial organs are structured in cell layers that do not mix during development, and that originate from the L1, L2 and L3 layers from the shoot apical meristem. Since plant cells cannot relocate, the layered structure is maintained during organ emergence and growth through oriented cell divisions only, with cell invasion events between layers being very rare (Satina et al., 1940; Meyerowitz, 1997; Stewart and Burk, 1970; Scheres, 2001). Therefore layers are considered to be clonally-independent, which raises the following question: how do cell layers coordinate their development and manage to grow at the same pace to generate organs with a robust morphology?

In the plant field, it is usually acknowledged that the epidermis controls organ growth, by being under tension and restricting growth of the underlying inner tissues that tend to expand (Kutschera et al., 1987). This "epidermal-growth-control theory" has been proposed based on physical experiments on stems (cutting or separating layers) and is compatible with the mode of action of auxin, a plant hormone that is a major contributor to growth and that mostly acts in the epidermis (Kutschera and Niklas, 2007; Kierzkowski et al., 2013). Manipulating gene expression in distinct layers has led to somehow different conclusions: epidermal expression of the *BRI1* gene, involved in perception of the brassinosteroid hormone, is sufficient to restore *bri1* dwarf mutant phenotypes, showing that the epidermis can be a driver for organ growth (Savaldi-Goldstein et al., 2007; Savaldi-Goldstein and Chory, 2008). However, expressing *BRI1* in the vasculature (protophloem) is also sufficient to restore plant dwarfism (Kang et al., 2017; Graeff et al., 2020), suggesting that this effect is rather due to BRI1-specific properties than to layer-specific properties. Therefore, genetical and physical experiments are not strictly comparable, and the question of which layer is in control of organ growth is more complex than it seems.

We have found in petunia layer-specific mutants for a major petal identity regulator, showing that different cell layers drive development of subdomains of the petal. I will below describe this system in more details, and how I am using it to tackle the role of cell layers during petunia petal development and evolution.

1. Distinct cell layers drive development of the petunia petal tube and limbs

Petunia (*Petunia x hybrida*) petals are mostly derived from L1 and L2 layers (Satina and Blakeslee, 1941), forming the epidermis and the mesophyll respectively. Five petals initiate and fuse to form the mature corolla, organized in a tube opening on wide and pigmented limbs (Fig. 3-1, A). In petunia, petal development is partly governed by the petal identity transcription factor PhDEF (Vandenbussche et al., 2004), belonging to the large MADS-box protein family and orthologous to Arabidopsis APETALA3 (both are B-class regulators from the ABC model of floral organ identity (Coen and Meyerowitz, 1991; Schwarz-Sommer et al., 1990)). The *phdef* homozygous mutant forms sepals instead of petals (Fig. 3-1, A), showing that *PhDEF* expression is necessary to trigger the whole petal developmental program in a floral context (Vandenbussche et al., 2004). However, the PhDEF protein is not the only contributor to petal identity and its paralogs PhGLO1 and PhGLO2, with whom PhDEF forms obligate heterodimers, also contribute to the determination of petal identity (Vandenbussche et al., 2004). This obligate heterodimerization is the reason why the single *phdef* mutant, as well as the double *phglo1 phglo2* mutant, loose entirely their petal identity. *PhDEF* is also expressed in stamens but redundancy with its paralog *PhTM6* masks this effect in the single *phdef* mutant (Rijpkema et al., 2006). Therefore, *PhDEF* is a major contributor to petal identity and development in petunia.

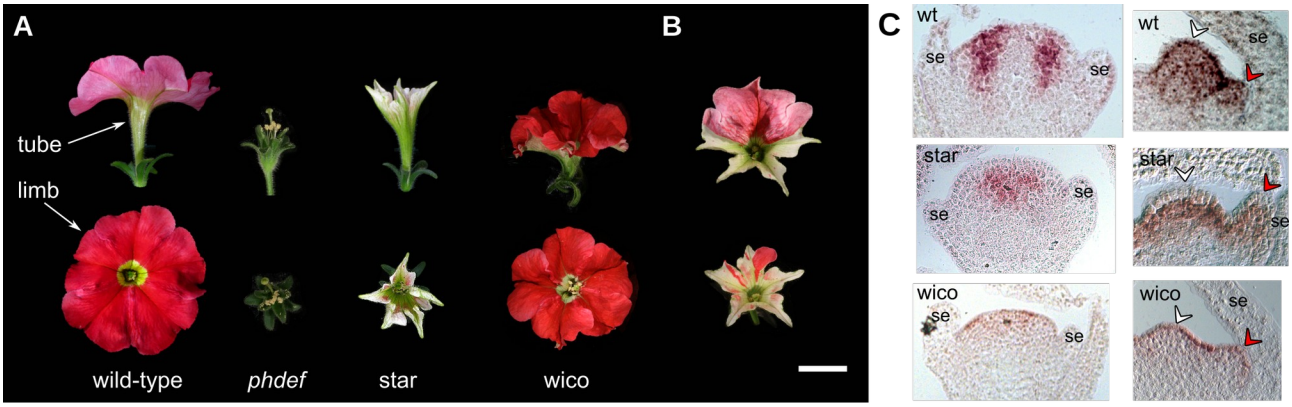

Figure 3-1. The star and wico flowers derive from the *phdef* mutant. A: Top and side views of a wild-type, a *phdef*, a star and a wico flower. Scale bar = 1 cm. **B:** Star flowers with 2 petals (up) or small petal sectors (down) showing additional transposon excision in the epidermis. **C:** *In situ* hybridization of *PhDEF* transcript in wild-type, star and wico flowers (longitudinal sections). Left: young flower initiating its sepals (se); right: flower initiating its petals (red arrow) and stamens (white arrow).

We obtained layer-specific *phdef* mutant flowers with striking phenotypes (Chopy et al., 2021) (key publication 3, p. 72) (Fig. 3-1). These flowers spontaneously appeared on *phdef-151* plants, a transposon insertion allele causing a knock-out of the *PhDEF* gene (Fig. 3-2, A). The transposon actively excises in the petunia line that we are using, which generally restores a wild-type phenotype in revertant flowers (Gerats et al., 1990). However, in the case of this particular mutation, revertant flowers showed two contrasting phenotypes where only a subdomain of the petal, *i.e.* the tube or the limbs, develops properly (Fig. 3-1, A). Star flowers develop a normal tube but their limbs are small, star-shaped and unpigmented. On the contrary, wico flowers develop normally-shaped and pigmented limbs while the tube hardly develops. An early excision event cause an entire branch or flower to display the phenotype, whereas late excisions result in single revertant petals or sectors (Fig. 3-1, B). We have quantified and characterized these phenotypes in depth, and we have found that cell elongation is strongly reduced in the wico tube, while cell division is mostly defective in the star limbs (Chopy et al., 2021).

By examining the descendency of these flowers (since gametes are strictly L2-derived) and performing *in situ* hybridization for *PhDEF* (Fig. 3-1, C), we found that these flower phenotypes are caused by the layer-specific excision of the transposon, restoring a wild-type *PhDEF* allele in one layer of the flower only (Fig. 3-2). The wico and star flowers thus carry a wild-type *PhDEF* allele in their epidermis or mesophyll respectively, while the other layer is still mutant for *phdef*. **Hence, the petunia petal has a modular structure, with the development of each module being driven by distinct cell layers.**

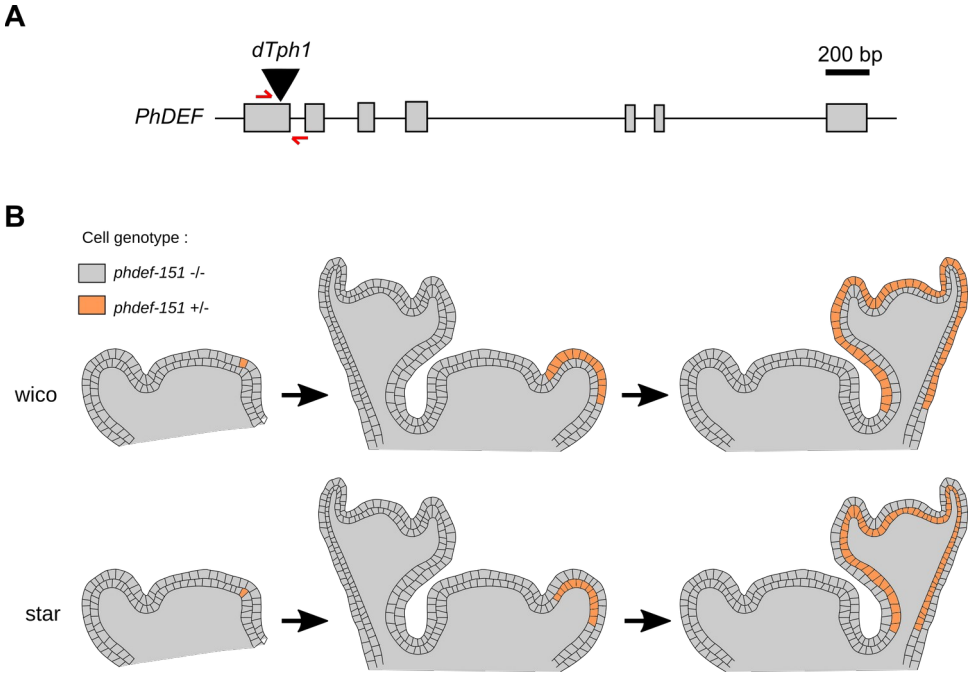

Figure 3-2: Layer-specific excision of the *dTph1* transposon inserted into *PhDEF* causes the star and wico phenotypes. A: *PhDEF* gene model (exons in grey boxes, regulatory regions and introns in black line) showing the position of insertion of the *dTph1* transposon causing the *phdef-151* knock-out mutation. The transposon contains stop codons in both orientations and all possible frames, which leads to the production of a truncated protein. **B:** Schematic view of a longitudinal section of the shoot apical meristem of a *phdef-151* homozygous mutant, with one cell in the L1 (wico) or in the L2 (star) layer reverting to a heterozygous *phdef-151 +/-* genotype, due to the excision of the *dTph1* transposon from the *PhDEF* gene. As a result of several rounds of anticlinal divisions, branches or flowers generated will be periclinal chimeras, i.e. organs with layers of different genotypes for *PhDEF*. The *phdef-151* allele is fully recessive, and *phdef-151 +/-* plants are indistinguishable from wild-type.

We also examined how cell identity is affected in the different layers of these chimeric flowers. This has revealed that in layers devoid of *PhDEF* expression (i.e. the star epidermis or the wico mesophyll), cells display intermediate features between petal and sepal cells (Fig. 3-3). Indeed, star epidermal cells are domed, which is in between the clear conical cells of wild-type petals and the flat puzzle cells of sepals. Similarly, wico mesophyll cells are green and photosynthetic like sepal mesophyll cells, but display a petal-like tissue organization (Chopy et al., 2021). This shows that non-autonomous effects influence cell identity across layers.

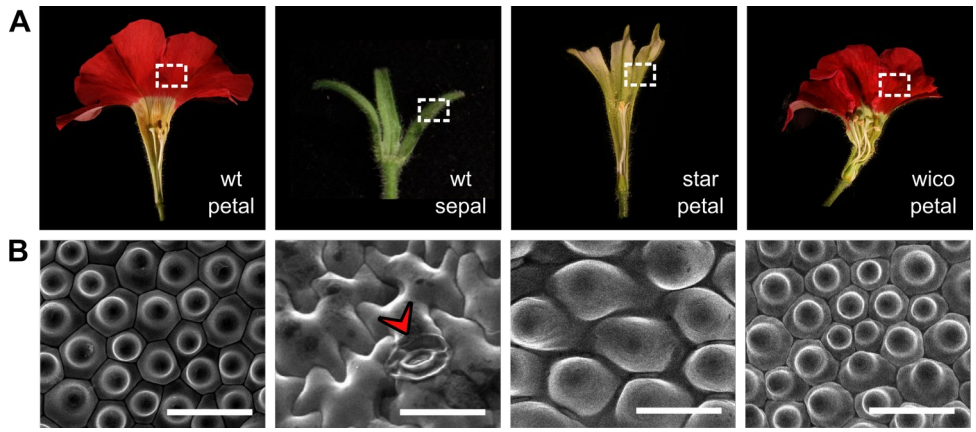

Figure 3-3: Non-cell-autonomous effects influence cell identity in the star petal epidermis. A: Corollas and sepals from wt, star and wico flowers, cut open in half. A dotted square indicates the region observed by scanning electron microscopy. **B:** Scanning electron micrographs of wt, star and wico petal limbs, and wt sepals. The red arrow indicates a stomata. Scale bar: 30 µm.

One may wonder if the star and wico flowers are merely a peculiarity found in petunia and if any conclusions drawn with this system will be general. In snapdragon and Arabidopsis flowers, periclinal chimeras for orthologs of *PhDEF* (*DEF* and *AP3* respectively) or *PhGLO1/PhGLO2* (*GLO* and *PI* respectively) have been previously obtained (Perbal et al., 1996; Vincent et al., 2003; Efremova et al., 2001; Bouhidel and Irish, 1996; Jenik and Irish, 2001; Urbanus et al., 2010). In snapdragon, expression of *DEF* only in the L1 layer largely restores petal development, particularly in the limbs, in contrast to the L2/L3 specific *DEF* or *GLO* expression which causes reduced limb growth (Perbal et al., 1996; Vincent et al., 2003; Efremova et al., 2001). Petals are fused into a tube in snapdragon flowers, but the tube is much more reduced than in petunia, hence conclusions on tube length restoration in the chimeras were not drawn by the authors. However, in light of our results, it is clear that snapdragon chimeras expressing *DEF* or *GLO* in the L2/L3 layers restore tube development to a higher degree than limb development, similar to what we observed. In Arabidopsis that has simple and unfused petals, petal shape and size were never fully restored when *AP3* was expressed in one cell layer only (Jenik and Irish, 2001; Urbanus et al., 2010); in contrast epidermal expression of *PI* was sufficient to restore normal petal development (Bouhidel and Irish, 1996). Therefore, it seems that epidermis-driven limb morphogenesis and mesophyll-driven tube morphogenesis is a shared property between petunia and snapdragon petals, but not shared with Arabidopsis petals. From this, and although we are well aware that there are only two examples from the literature, we might conclude that this property is shared by species from the orders of Lamiales and Solanales, to which Antirrhinum and Petunia respectively belong. This might account for about 28,000 species (Encyclopedia Britannica), i.e. about 8-9 % of flowering diversity, which is not insignificant.

I have found the star and wico flowers to constitute an interesting research system for several reasons:
- the decoupling of tube vs. limb growth should allow to identify key genes involved in the development of these sub-domains of the petal (part 2);
- the fact that *PhDEF* is expressed in one layer of the petal only allows to identify the GRN controlled by PhDEF in each of these layers, responsible for epidermis vs. mesophyll differentiation (part 2);
- the presence of non-autonomous effects grants the opportunity to investigate their molecular or mechanical basis (part 2);
- the fact that sub-domains of the petal manage to grow while others do not, in the same genetic chimera, shows that growth coordination between layers is not automatic and can be explored (part 3);
- tube and limb size have varied greatly during petunia petal evolution, which questions how morphologies manage to evolve with the constraint of clonally-independent cell layers (part 4).

2. Towards the cell-layer specific GRN controlled by PhDEF

a. Splitting into layer-specific GRNs

Petunia petal identity is defined early in all cell layers by a combination of several regulators, among which PhDEF has a prominent role (Vandenbussche et al., 2004). However in the mature petal, the epidermis and mesophyll tissues have specific growth characteristics (cell division and expansion rates, cell division orientation...) (Reale et al., 2002) and they acquire specific mature traits. For instance, petal epidermal cells are small, pigmented and conical while petal mesophyll cells are larger and loosely arranged (Glover, 2000; Chopy et al., 2021; Cavallini-Speisser et al., 2021). Moreover, it appears that several petal traits can be simultaneously specified from layer-specific *PhDEF* expression, since the star flowers are affected both in limb size, shape, pigmentation and epidermal cell identity (see later Fig. 5). Therefore the PhDEF regulatory network splits into an epidermal and a mesophyll network in which different (and likely also common) genes are regulated, driving the specification of cell layer identity and the development of the tube and the limbs, with all their specific features.

The molecular basis for this split into different GRNs could be due to pre-established differences between the L1 and L2 layers, prior to petal specification. For instance the transcriptomic, proteomic, metabolic, mechanical or chromatin states might be different between layers already from the embryonic stage, and organ identity is only superimposed on these pre-differentiated layers. Indeed in Arabidopsis, epidermal identity is established early in the embryo by various regulators, in particular HD-Zip class IV transcription factors (ML1 and PDF2 among others) (Robinson and Roeder, 2015; Takada and Iida, 2014; Abe et al., 2003). It was recently shown that *ML1* expression is maintained in the epidermis by a transcriptional feedback loop involving ceramids (lipids) specifically deposited on the outer membrane of epidermal cells; hence positional information maintains epidermal identity (Nagata et al., 2021). Therefore, during petal specification, *PhDEF* will be expressed in different cellular contexts in the two petal layers. As a result, the PhDEF protein might interact with different protein partners, leading to differential target gene regulation (Long et al., 2017). Indeed, MADS-box proteins work in protein complexes. These complexes usually involve other MADS-box proteins but several studies have shown that other families of transcription factors are occasionally involved (Bemer et al., 2017; Dornelas et al., 2011b), some of which might be cell-layer-specifically expressed. For instance, animal and yeast MADS-box proteins interact with several homeodomain proteins (Messenguy and Dubois, 2003), suggesting the attractive hypothesis that PhDEF could interact with the epidermally expressed homeodomain-containing HD-Zip class IV proteins. Alternatively and non-exclusively, as a result of layer differentiation, chromatin accessibility might be different in the L1 and L2 layers and therefore, PhDEF might not have access to the same target genes to regulate.

b. Uncovering the PhDEF layer-specific GRNs

In order to investigate how the PhDEF GRN splits into layer-specific GRNs, we are using the star and wico flowers to identify PhDEF protein partners, direct target genes and chromatin accessibility in the two layers of the petal. For this, I plan to perform co-immunoprecipitation (co-IP), chromatin-immunoprecipitation (ChIP-Seq), Assay for Transposase-Accessible Chromatin (ATAC-Seq) and single-cell RNA-Seq (scRNA-Seq) on wt, *phdef*, star and wico petals, ideally at different stages of development. This is a long-term project and for the moment, the PhD student that I am tutoring (Quentin Cavallini-Speisser) only recently performed scRNA-Seq on mature petals from wt, star and wico flowers (the *phdef* sample has failed but will be repeated soon). I am also optimizing the ChIP procedure on wt and *phdef* petal samples and recently obtained satisfactory results.

In order to obtain cell-layer-specifically expressed genes, we decided to use scRNA-Seq in wt, phdef, star and wico flowers rather than laser-assisted microdissection for instance. Indeed, laser-assisted microdissection is not entirely trivial, especially on differentiated tissues and we already experienced very low RNA yields in petunia tissues. Moreover, a single petal layer is still a mixture of several cell identities, and averaging gene expression in those different cell types diminishes the resolutive power to find interesting genes, involved in i.e. tube vs. limb growth or non-cell-autonomous processes. Finally, scRNA-Seq on wt petal tissue alone would constitute an excellent ressource for the community working on petal development. Performing scRNA-Seq entails generating petal protoplasts by enzymatic digestion of the cell wall. Based on collaborative work with Francesca Quattrocchio (University of Amsterdam), whose group has developed a protoplast-based system to study petunia petal pigmentation, Quentin has adapted a protoplast digestion assay to be fast (5h) and produce enough protoplasts for subsequent sequencing with the 10X Genomics Chromium microfluidics system (Fig. 3-4). Unfortunately, Quentin has never managed to obtain enough protoplasts for earlier petal developmental stages, so we have been focusing on mature stages only, which limits developmental conclusions (on tube or limb growth in particular) that could be drawn.

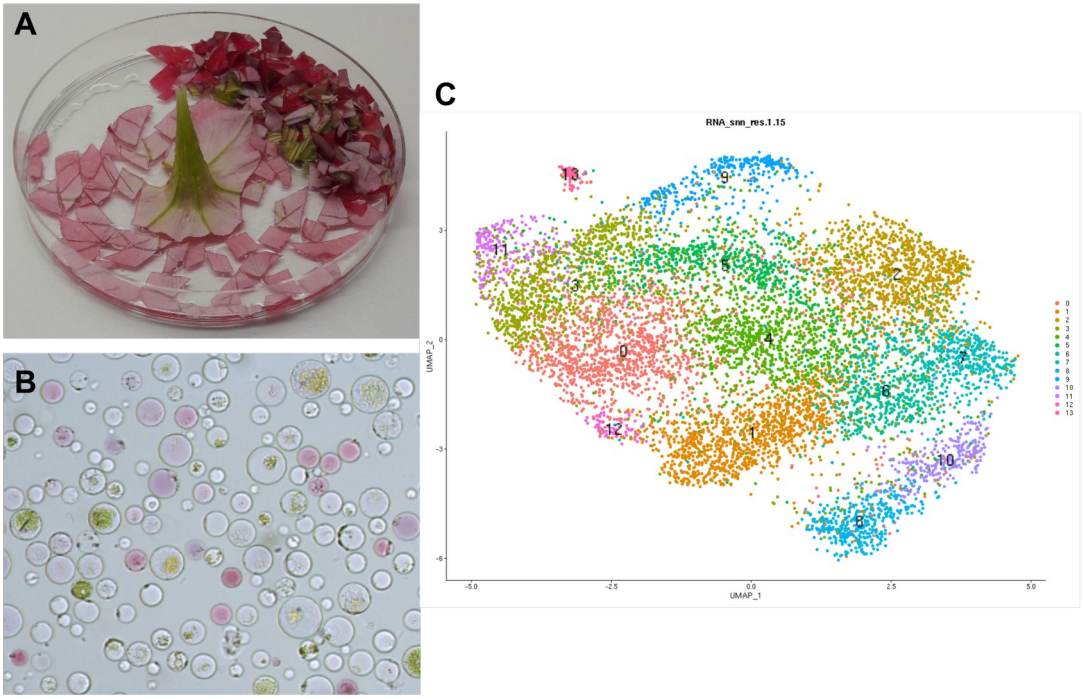

Figure 3-4: Single-cell RNA-Seq in petal tissue. A: Petals are cut into small pieces and the cell wall is digested into an enzymatic solution. **B:** Protoplasts released by the digestion are purified. From wt petals, we observe in particular pigmented protoplasts (from the limb epidermis) and photosynthetic protoplasts (from the tube mesophyll). **C:** UMAP projection revealing clusters of cell types obtained from the wt scRNA-Seq dataset. Clusters are sorted from the biggest (cluster 0) to the smallest (cluster 13) in terms of cell number.

We sequenced about 4,000-6,000 cells in the wt, star and wico petal tissue at anthesis, aiming for about 100,000 reads per cell. Although mapping of the reads still has to be improved (our petunia transcriptome is badly annotated in 3'), Quentin analyzed the reads and obtained about a dozen clusters of cell types, depending on the sample (Fig. 3-4). The identity of some of these clusters is obvious (in wt, pigmented cells in clusters 8 and 11 produce abundant anthocyanin biosynthesis genes, vascular cells in cluster 9 express several sugar SWEET transporters, tube mesophyll cells in cluster 4 express several photosynthetic genes) but the identity of other clusters remains obscure so far. Now, we will have to go back

and forth between the scRNA-Seq data and in situ hybridization experiments in petal tissue slides, in order to identify unknown clusters. Once we know the identity of clusters, we will be able to:
1) extract the number and identity of layer-specific genes and commonly expressed genes;
2) look for the presence of PhDEF binding sites and other enriched motifs in regulatory sequences of layer-specific genes, in order to find if layer-specific expression is encoded in the sequence;
3) compare clusters of the same identity between wt, *phdef*, star and wico flowers to pinpoint which genes are deregulated and might contribute to limb or tube development;
4) in the longer term, cross this data to ChIP-Seq, co-IP and ATAC-Seq data in an attempt to understand the molecular determinants of layer-specific gene expression.

c. Petal pigmentation as a model to study petal epidermal identity

One obvious phenotype of the star flowers is the absence of pigmentation in the limbs. Petal pigmentation in petunia is mostly caused by the accumulation of anthocyanins in the upper epidermis of the limbs (and in lower amounts in the lower epidermis). The regulatory and biosynthetic pathway of anthocyanins has been extensively characterized in petunia (Bombarely et al., 2016; Tornielli et al., 2009); therefore it represents a good model system to explore how epidermal-specific traits are acquired after *PhDEF* is expressed in all layers of the petal.

We performed RNA-Seq in wt, *phdef*, star and wico flowers at 3 stages of development (Fig. 3-5, A) (Chopy et al., 2021), and we found that half of all known genes from the anthocyanin biosynthetic pathway (21 out of 42) were downregulated in star and *phdef* samples. In particular, we focused our attention on the first activators of anthocyanin biosynthesis. Briefly, the earliest steps of anthocyanin production are ensured by a MBW regulatory complex composed of an R2R3-MYB transcription factor (either ANTHOCYANIN2 (AN2), AN4, DEEP PURPLE or PURPLE HAZE), AN1 (a bHLH transcription factor) and AN11 (a WD-repeat protein), which drives the expression of anthocyanin biosynthesis enzymes and proteins involved in vacuolar acidification of epidermal cells (Albert et al., 2011; de Vetten et al., 1997; Spelt et al., 2000; Quattrocchio et al., 1999, 1993). We found that *AN2* and *AN1* are both strongly down-regulated in star samples, with *AN2* being downregulated first, from stage 4 onwards, and *AN1* being downregulated from stage 8 onwards (Fig. 3-5, B). This is consistent with the fact that *AN2* is upstream of *AN1* in the pigmentation pathway: ectopic expression of *AN2* in petunia leaves is sufficient to trigger pigmentation in this tissue, and to induce *AN1* expression among others (Spelt et al., 2000; Quattrocchio et al., 1998). Therefore, we wanted to test if PhDEF might directly bind to the regulatory sequences of *AN1* and *AN2* and activate their expression, thereby triggering the whole petal pigmentation pathway.

For this, I first analyzed the genomic sequences of *AN1* and *AN2* to predict the position of CArG boxes that might be bound by PhDEF (Fig. 3-5, C). I found one good predicted CArG box in the terminator region of both *AN1* and *AN2 (AN1-bs1* and *AN2-bs3)*. These sites were confirmed to be bound by PhDEF and PhGLO1 (the two proteins work in an obligate heterodimer to bind DNA, (Riechmann et al., 1996b)) *in vitro* by gel shift assays (Fig. 3-5, D, this is the result of a collaboration with Véronique Hugouvieux, from the Laboratory for Plant and Cell Physiology (LPCV) in Grenoble). To further validate this binding by *in vivo* evidence, I recently performed chromatin immunoprecipitation (ChIP) using an antibody directed against the PhDEF protein (without its MADS domain to avoid cross-reactivity with other MADS-box proteins). This confirmed the *in vivo* binding of PhDEF to the genomic sequence of *AN2*, in the terminator region where the good *in vitro* binding site had been found (Fig. 3-5, E). The binding to *AN1* appears much weaker and not in the predicted region, therefore it is not clear if PhDEF binds *AN1* in vivo.

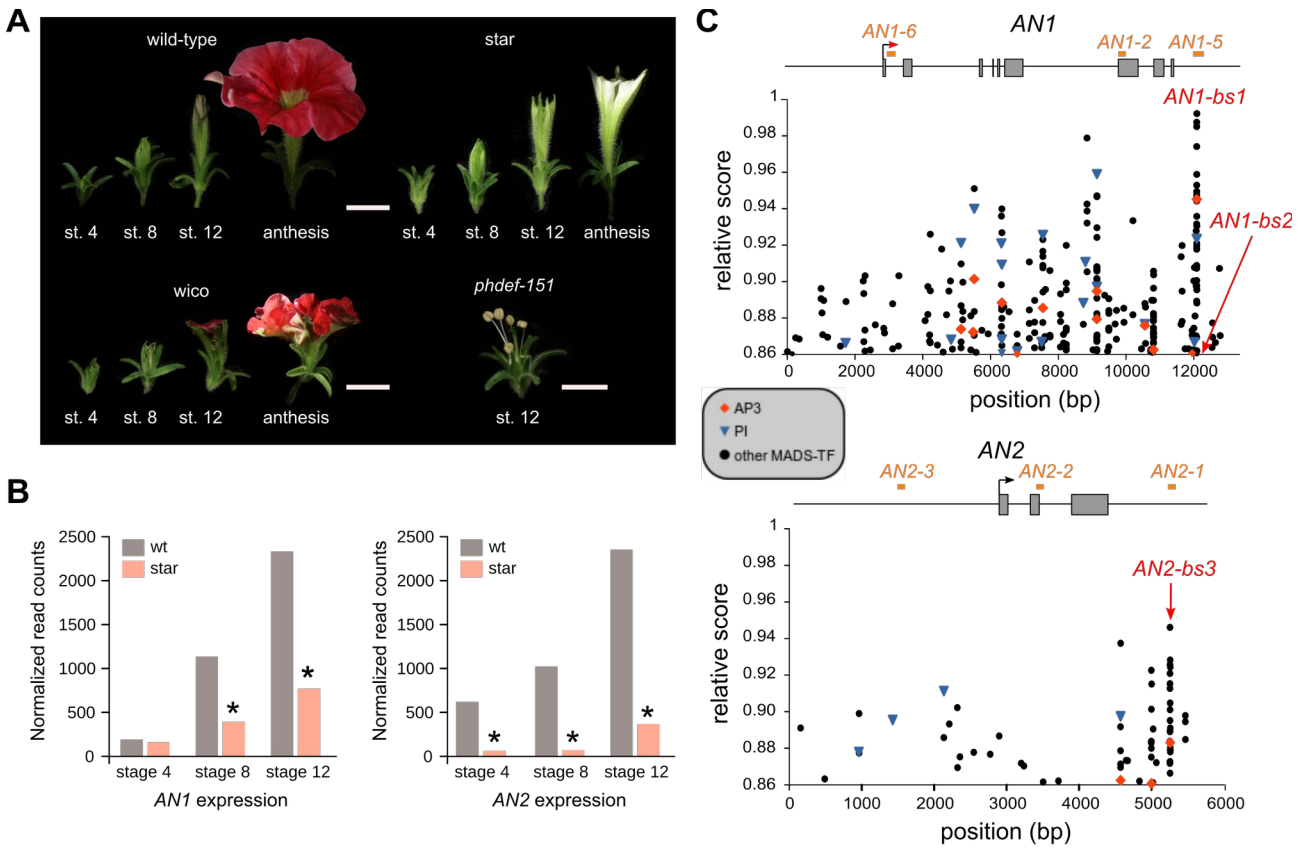

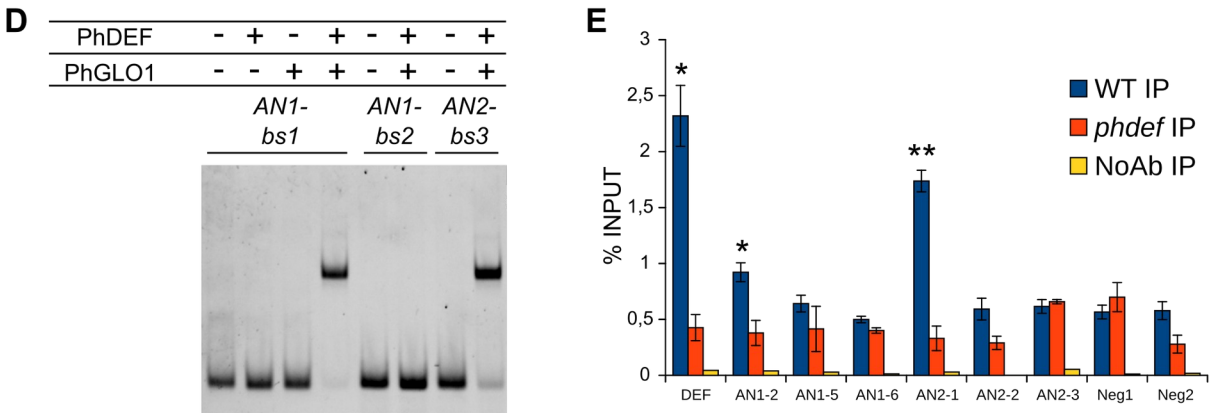

Figure 3-5: PhDEF directly binds to *AN2* regulatory regions. A: RNA-Seq was performed on wt, star and wico petals at stages 4, 8 and 12 and on *phdef* second whorl organs at stage 12. **B:** Expression of *AN1* (left) and *AN2* (right) in wt and star samples at stages 4, 8 and 12 (normalized read counts calculated by DESeq2). Stars indicate significant down-regulation. **C:** Predicted relative score (calculated by JASPAR 2020; (Fornes et al., 2020)) for AP3, PI or other MADS-box TF binding on the genomic sequence of *AN1* (up) or *AN2* (down). The gene model for *AN1* and *AN2* (START codon as an arrow, exons as grey boxes, introns and other regulatory sequences as dark lines) is aligned with the predicted binding sites. Binding sites tested by gel-shift assay are indicated in red, regions amplified by ChIP are indicated in orange. **D:** Gel-shift assay for *AN1-bs1* (test), *AN1-bs2* (negative control) and *AN2-bs3* (test) with PhDEF and/or PhGLO1 proteins produced by *in vitro* translation. **E:** Enrichment (as percentage of input) of several genomic regions after immunoprecipitation against PhDEF, in wt and *phdef* second whorl samples (NoAb is the control IP without antibody). PhDEF is known to activate its own expression by binding to a conserved binding site that lies within the DEF region amplified here. Neg1 and Neg2 correspond to two randomly selected genomic regions where no genes deregulated in *phdef* are found. Stars indicate significant enrichment of control regions as compared to the two negative controls combined.

Overall, these results indicate that PhDEF binds to the regulatory sequence of *AN2* to activate its expression in the petal. Activating *AN2* is sufficient for the accumulation of anthocyanins (Spelt et al., 2000; Quattrocchio et al., 1998); therefore PhDEF is directly responsible for pigmentation in the petal. This provides a simple mechanism for the « missing link » between organ identity and its final morphology: homeotic genes from the ABC model have been known for decades, but how they specify the many complex traits that constitute a mature organ has remained enigmatic (Dornelas et al., 2011b). Here, we have shown that PhDEF simply activates the most upstream activator of anthocyanin biosynthesis. However, why is this activation only found in the petal epidermis (and especially in the upper one), while *PhDEF* is expressed in all layers of the petal? We do not have the answer to this for the moment, but deciphering the layer-specific PhDEF GRN should help in understanding the molecular reasons for this specificity.

d. Diving into non-cell-autonomous effects

As previously shown, we have evidenced non-cell-autonomous effects in the star and wico flowers (Fig. 3-3), but the nature of these effects is unknown for the moment: small amounts of the PhDEF protein itself might be moving between layers, as was shown in a similar system in Antirrhinum (Perbal et al., 1996). This could trigger the partial acquisition of petal identity in the adjacent layer, with some petal features (formation of conical cells) being more sensitive to low PhDEF doses than others (pigmentation). But our attempts to detect the PhDEF protein by immunohistochemistry in star and wico flowers have been unsuccessful so far. Other possibilities are that another molecule (a target of PhDEF, a small signaling molecule...) travels between layers to trigger these non-cell-autonomous effects, or that they might be triggered by mechanical signals transmitted between layers. For instance, in star flowers normal growth of the mesophyll could merely drag along epidermal cells, since cells are connected by their cell walls, which could be sufficient to trigger their expansion and division. Using the scRNA-Seq data should help us understand what is happening in those cells: for instance, looking specifically at star limb epidermal cells and comparing them to *phdef* epidermal cells, should allow us to find a rather small number of deregulated genes (potentially involved in the formation of the dome observed in the star epidermal cells). Analyzing the regulatory sequence of those genes might reveal the presence of enriched motifs suggesting that these genes are commonly regulated by a factor that travels between layers, gene ontology enrichment analysis could point towards the implication in a mechanical pathway,... The star and wico flowers constitute a promising system to dive into the molecular mechanisms for non-cell-autonomous effects between petal layers.

3. How to grow with cell layers

Although cell layers are clonally independent, fully functional petals develop in a reproducible way in wild-type plants without any visible signs of tissue buckling or cracking (Maeda et al., 2014; Bemis and Torii, 2007; Rebocho et al., 2017) which would indicate growth conflicts between layers. This implies that cell layers manage to coordinate their development, through unknown molecular and/or mechanical players. In our system, the star tube and wico limbs grow seemingly normally, although *PhDEF* is expressed in one layer only. This suggests that, when expressed in one layer, *PhDEF* will at some point induce the expression of genes in the other layer (non-cell-autonomously) that ensure normal petal development. These genes might be involved in cell expansion (for instance through cell wall modification or turgor pressure building), in cell division (for

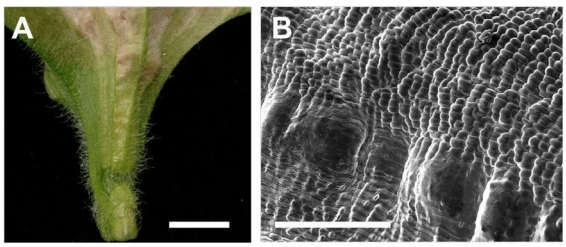

Fig. 3-6: Photograph (A, scale bar = 4 mm) and scanning electron micrograph (B, scale bar = 200 µm) of a wico tube, showing buckling of the tissue.

instance through the control of cell cycle duration) or in the specification of cell identity (for instance building conical cells in the epidermis). In contrast, the wico tube displays clear tissue buckling (Fig. 3-6), suggesting altered growth coordination and the possible existence of growth conflicts between layers.

The star and wico flowers constitute an interesting system to explore the mechanisms for coordination of development throughout layers. Results from the scRNA-Seq might reveal potential players in this process; in parallel, modeling growth of the petal as a two-layer organ, with different layers driving growth of the tube and the limb, might put forward mechanical hypotheses to later test on the flowers. I have not initiated any precise work on this topic; however, it is a possible direction to follow in the future and the fruitful environment of the RDP laboratory is ideal for this.

4. How to evolve with cell layers

Mature aerial organs have layers of differentiated cells with specific properties. For instance, the petunia petal epidermis is typically formed by small conical cells, pigmented and with a particular cuticular structure, all of these characteristics being linked with the petal's main role in pollinator attraction (Glover, 2014; Whitney et al., 2009; Moyroud and Glover, 2017). In contrast, petal mesophyll cells are large and loosely arranged, in relation with their function for nutrient and gas exchange. Acquiring layers with different identities is very likely benificial for the plant in allowing to decouple functions between layers; however the reason for developing these layers in a clonally-independent fashion, as is clearly the case in core eudicots, is enigmatic. Indeed in gymnosperms, the sister group of flowering plants, alternatively two or only one layer are found in the meristem (Gifford and Corson, 1971; Philipson, 1990; Imaichi and Hiratsuka, 2007). Still, gymnosperm leaves do form a differentiated epidermal layer without having to resort to clonally-independent layers, suggesting that positional and external cues can be sufficient to drive the acquisition of epidermal cell identity. Making organs with independent layers appears, on a first glimpse, as an unnecessary constraint for flowering plants.

Could we imagine any benefit of having clonally-independent cell layers then? We observed in petunia that growth of the petal tube and limbs are driven by different cell layers. This property grants modularity to the process of petal development, since tube and limb can develop more or less independently. Developmental modularity is generally believed to be linked with a higher potential to evolve (evolvability) by allowing for co-option of entire modules for new functions and reducing pleiotropic effects of mutations (Wagner and Altenberg, 1996; Verd et al., 2019). For instance, if we imagine that a mutation affects a gene controlling growth of mesophyll cells specifically, this would modify tube length without modifying limb area, thereby reducing the pleiotropic effect of the mutation.

Although this is highly speculative, evolution of petal morphology in the Petunia genus fits in this conceptual framework: tube length and limb area have varied independently during Petunia evolution. The Petunia genus contains around 20 wild species whose phylogeny has been reconstructed (Reck-Kortmann et al., 2014) (Fig. 3-7). A short petal tube, as is observed in *P. inflata*, is very likely the ancestral state. A long-tube clade emerged once in the genus, and is represented today by *P. axillaris* and *P. exserta* among others. *P. exserta*, with its reduced limb area and everted petals, is likely recently-derived from a *P. axillaris*-like ancestor (Sheehan et al., 2016). Several traits have coevolved at once in the Petunia genus, giving rise to distinct pollination syndromes (Galliot et al., 2006) (Fig. 3-7). For instance, *P. inflata* flowers have a short and wide tube, are pigmented by anthocyanins and do not emit much volatiles, and these traits are associated to diurnal pollination by bumblebees. In contrast, *P. axillaris* flowers have a long and narrow tube, lost their petal pigmentation but do emit large amounts of volatiles, which is associated to nocturnal pollination by hawkmoths with a long proboscis. Tube length likely restricts nectar accessibility to certain pollinators; however it is only one of the multiple traits that were modified during pollination syndrome evolution, and it

is unknown if this trait drove or only reinforced pollinator selection, leading *in fine* to reproductive isolation between emerging species (Rodrigues et al., 2018).

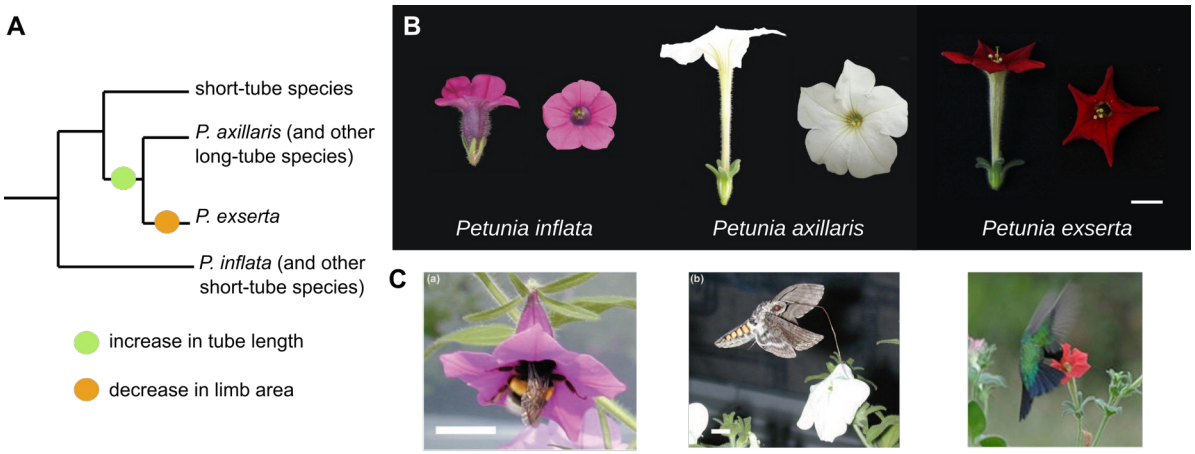

Figure 3-7: Evolution of petal morphology in Petunia. (A) Simplified phylogeny of the *Petunia* genus showing the most parcimonious interpretation for increase in tube length and decrease in limb area in the species of interest. **(B)** Top and side views of a *P. inflata*, *P. axillaris* and *P. exserta* flower. Scale bar = 1 cm. **(C)** *P. inflata* flower visited by a bumblebee, *P. axillaris* flower visited by a nocturnal hawkmoth and *P. exserta* flower visited by a hummingbird.

I am tempted to speculate that layer-specific mutations, affecting growth of one cell layer and therefore of one subdomain of the petal only, might have participated in the process of petal morphological evolution in Petunia. In the future, and if I get funding for this project, I would like to test this hypothesis by looking at cell-layer-specifically expressed genes in *P. inflata*, *P. axillaris* and *P. exserta* (by performing scRNA-Seq on petals from these species), also present in QTL intervals associated with tube length or limb area changes (Sheehan et al., 2016; Hermann et al., 2015). Testing the role of those genes on petal morphology would test the underlying hypothesis, that changes in layer-specifically expressed genes have participated in petal morphological evolution.

References

Abe, M., Katsumata, H., Komeda, Y., and Takahashi, T. (2003). Regulation of shoot epidermal cell differentiation by a pair of homeodomain proteins in Arabidopsis. Development **130**: 635–643.

Aida, M., Ishida, T., Fukaki, H., Fujisawa, H., and Tasaka, M. (1997). Genes involved in organ separation in Arabidopsis: an analysis of the cup-shaped cotyledon mutant. Plant Cell **9**: 841–857.

Airoldi, C.A. and Davies, B. (2012). Gene duplication and the evolution of plant MADS-box transcription factors. J Genet Genomics **39**: 157–165.

Albert, N.W., Lewis, D.H., Zhang, H., Schwinn, K.E., Jameson, P.E., and Davies, K.M. (2011). Members of an R2R3-MYB transcription factor family in Petunia are developmentally and environmentally regulated to control complex floral and vegetative pigmentation patterning. Plant J **65**: 771–784.

Bailey, T.L. and Elkan, C. (1995). The value of prior knowledge in discovering motifs with MEME. Proc Int Conf Intell Syst Mol Biol **3**: 21–29.

Ballerini, E.S., Min, Y., Edwards, M.B., Kramer, E.M., and Hodges, S.A. (2020). POPOVICH, encoding a C2H2 zinc-finger transcription factor, plays a central role in the development of a key innovation, floral nectar spurs, in Aquilegia. Proc Natl Acad Sci U S A **117**: 22552–22560.

Barrière, A., Gordon, K.L., and Ruvinsky, I. (2012). Coevolution within and between regulatory loci can preserve promoter function despite evolutionary rate acceleration. PLoS Genet **8**: e1002961.

Bateman, R.M. (2020). Hunting the Snark: the flawed search for mythical Jurassic angiosperms. Journal of Experimental Botany **71**: 22–35.

Bemer, M., van Dijk, A.D.J., Immink, R.G.H., and Angenent, G.C. (2017). Cross-Family Transcription Factor Interactions: An Additional Layer of Gene Regulation. Trends in Plant Science **22**: 66–80.

Bemis, S.M. and Torii, K.U. (2007). Autonomy of cell proliferation and developmental programs during Arabidopsis aboveground organ morphogenesis. Dev. Biol. **304**: 367–381.

Blázquez, M.A. and Weigel, D. (2000). Integration of floral inductive signals in Arabidopsis. Nature **404**: 889–892.

Blount, Z.D., Barrick, J.E., Davidson, C.J., and Lenski, R.E. (2012). Genomic analysis of a key innovation in an experimental Escherichia coli population. Nature **489**: 513–518.

Bombarely, A. et al. (2016). Insight into the evolution of the Solanaceae from the parental genomes of Petunia hybrida. Nat Plants **2**: 16074.

Bouhidel, K. and Irish, V.F. (1996). Cellular Interactions Mediated by the HomeoticPISTILLATAGene Determine Cell Fate in theArabidopsisFlower. Developmental Biology **174**: 22–31.

Bowman, J.L., Brüggemann, H., Lee, J.Y., and Mummenhoff, K. (1999). Evolutionary Changes in Floral Structure within Lepidium L. (Brassicaceae). Int J Plant Sci **160**: 917–929.

Cartolano, M., Castillo, R., Efremova, N., Kuckenberg, M., Zethof, J., Gerats, T., Schwarz-Sommer, Z., and Vandenbussche, M. (2007). A conserved microRNA module exerts homeotic control over Petunia hybrida and Antirrhinum majus floral organ identity. Nat Genet **39**: 901–905.

Causier, B., Castillo, R., Zhou, J., Ingram, R., Xue, Y., Schwarz-Sommer, Z., and Davies, B. (2005). Evolution in action: following function in duplicated floral homeotic genes. Curr. Biol. **15**: 1508–1512.

Causier, B., Schwarz-Sommer, Z., and Davies, B. (2010). Floral organ identity: 20 years of ABCs. Semin Cell Dev Biol **21**: 73–79.

Cavallini-Speisser, Q., Morel, P., and Monniaux, M. (2021). Petal Cellular Identities. Front Plant Sci **12**: 745507.

Chae, E., Tan, Q.K.-G., Hill, T.A., and Irish, V.F. (2008). An Arabidopsis F-box protein acts as a transcriptional co-factor to regulate floral development. Development **135**: 1235–1245.

Chahtane, H. et al. (2013). A variant of LEAFY reveals its capacity to stimulate meristem development by inducing RAX1. Plant J **74**: 678–689.

Chen, D., Yan, W., Fu, L.-Y., and Kaufmann, K. (2018). Architecture of gene regulatory networks controlling flower development in Arabidopsis thaliana. Nat Commun **9**: 4534.

Chopy, M., Cavallini-Speisser, Q., Chambrier, P., Morel, P., Just, J., Hugouvieux, V., Bento, S.R., Zubieta, C., Vandenbussche, M., and Monniaux, M. (2021). Cell layer-specific expression of the B-class MADS-box gene PhDEF drives petal tube or limb development in petunia flowers. bioRxiv: 2021.04.03.438311.

Coen, E.S. and Meyerowitz, E.M. (1991). The war of the whorls: genetic interactions controlling flower development. Nature **353**: 31–37.

Colombo, L., Franken, J., Koetje, E., van Went, J., Dons, H.J., Angenent, G.C., and van Tunen, A.J. (1995). The petunia MADS box gene FBP11 determines ovule identity. Plant Cell **7**: 1859–1868.

Corbesier, L., Vincent, C., Jang, S., Fornara, F., Fan, Q., Searle, I., Giakountis, A., Farrona, S., Gissot, L., Turnbull, C., and Coupland, G. (2007). FT protein movement contributes to long-distance signaling in floral induction of Arabidopsis. Science **316**: 1030–1033.

Delaux, P.-M. et al. (2015). Algal ancestor of land plants was preadapted for symbiosis. Proc Natl Acad Sci U S A **112**: 13390–13395.

Djordjevic, M. (2007). SELEX experiments: new prospects, applications and data analysis in inferring regulatory pathways. Biomol Eng **24**: 179–189.

Dornelas, M.C., Patreze, C.M., Angenent, G.C., and Immink, R.G.H. (2011a). MADS: the missing link between identity and growth? Trends Plant Sci **16**: 89–97.

Dornelas, M.C., Patreze, C.M., Angenent, G.C., and Immink, R.G.H. (2011b). MADS: the missing link between identity and growth? Trends in Plant Science **16**: 89–97.

Dubois, A., Raymond, O., Maene, M., Baudino, S., Langlade, N.B., Boltz, V., Vergne, P., and Bendahmane, M. (2010). Tinkering with the C-Function: A Molecular Frame for the Selection of Double Flowers in Cultivated Roses. PLOS ONE **5**: e9288.

Efremova, N., Perbal, M.-C., Yephremov, A., Hofmann, W.A., Saedler, H., and Schwarz-Sommer, Z. (2001). Epidermal control of floral organ identity by class B homeotic genes in Antirrhinum and Arabidopsis. Development **128**: 2661–2671.

Eldredge, N. and Gould, S. (1971). Punctuated Equilibria: An Alternative to Phyletic Gradualism. In Models in Paleobiology, pp. 82–115.

Encyclopedia Britannica.

Favaro, R., Pinyopich, A., Battaglia, R., Kooiker, M., Borghi, L., Ditta, G., Yanofsky, M.F., Kater, M.M., and Colombo, L. (2003). MADS-box protein complexes control carpel and ovule development in Arabidopsis. Plant Cell **15**: 2603–2611.

Fisher, S., Grice, E.A., Vinton, R.M., Bessling, S.L., and McCallion, A.S. (2006). Conservation of RET regulatory function from human to zebrafish without sequence similarity. Science **312**: 276–279.

Fornes, O. et al. (2020). JASPAR 2020: update of the open-access database of transcription factor binding profiles. Nucleic Acids Res **48**: D87–D92.

François, L., Verdenaud, M., Fu, X., Ruleman, D., Dubois, A., Vandenbussche, M., Bendahmane, A., Raymond, O., Just, J., and Bendahmane, M. (2018). A miR172 target-deficient AP2-like gene correlates with the double flower phenotype in roses. Sci Rep **8**: 12912.

Friedman, W.E. (2009). The meaning of Darwin's "abominable mystery." American Journal of Botany **96**: 5–21.

Galliot, C., Stuurman, J., and Kuhlemeier, C. (2006). The genetic dissection of floral pollination syndromes. Curr Opin Plant Biol **9**: 78–82.

Gallois, J.-L., Nora, F.R., Mizukami, Y., and Sablowski, R. (2004). WUSCHEL induces shoot stem cell activity and developmental plasticity in the root meristem. Genes Dev **18**: 375–380.

Gao, B., Chen, M., Li, X., and Zhang, J. (2019). Ancient duplications and grass-specific transposition influenced the evolution of LEAFY transcription factor genes. Commun Biol **2**: 237.

Gerats, A.G., Huits, H., Vrijlandt, E., Marana, C., Souer, E., and Beld, M. (1990). Molecular characterization of a nonautonomous transposable element (dTph1) of petunia. Plant Cell **2**: 1121–1128.

Gifford, E.M. and Corson, G.E. (1971). The shoot apex in seed plants. Bot. Rev **37**: 143–229.

Givnish, T.J. (2002). Ecological constraints on the evolution of plasticity in plants. Evolutionary Ecology **16**: 213–242.

Glover, B. (2014). Understanding Flowers and Flowering Second Edition Second Edition. (Oxford University Press: Oxford, New York).

Glover, B.J. (2000). Differentiation in plant epidermal cells. J Exp Bot **51**: 497–505.

Graeff, M., Rana, S., Marhava, P., Moret, B., and Hardtke, C.S. (2020). Local and Systemic Effects of Brassinosteroid Perception in Developing Phloem. Curr Biol **30**: 1626-1638.e3.

Hames, C., Ptchelkine, D., Grimm, C., Thevenon, E., Moyroud, E., Gerard, F., Martiel, J.-L., Benlloch, R., Parcy, F., and Muller, C.W. (2008). Structural basis for LEAFY floral switch function and similarity with helix-turn-helix proteins. EMBO J **27**: 2628–2637.

Hay, A.S. et al. (2014). Cardamine hirsuta: a versatile genetic system for comparative studies. Plant J **78**: 1–15.

Heijmans, K., Ament, K., Rijpkema, A.S., Zethof, J., Wolters-Arts, M., Gerats, T., and Vandenbussche, M. (2012). Redefining C and D in the petunia ABC. Plant Cell **24**: 2305–2317.

Heisler, M.G., Jönsson, H., Wenkel, S., and Kaufmann, K. (2022). Context-specific functions of transcription factors controlling plant development: From leaves to flowers. Curr Opin Plant Biol **69**: 102262.

Hermann, K., Klahre, U., Venail, J., Brandenburg, A., and Kuhlemeier, C. (2015). The genetics of reproductive organ morphology in two Petunia species with contrasting pollination syndromes. Planta **241**: 1241–1254.

Huang, T., Lopez-Giraldez, F., Townsend, J.P., and Irish, V.F. (2012). RBE controls microRNA164 expression to effect floral organogenesis. Development **139**: 2161–2169.

Imaichi, R. and Hiratsuka, R. (2007). Evolution of shoot apical meristem structures in vascular plants with respect to plasmodesmatal network. American Journal of Botany **94**: 1911–1921.

Jenik, P.D. and Irish, V.F. (2001). The Arabidopsis floral homeotic gene APETALA3 differentially regulates intercellular signaling required for petal and stamen development. Development **128**: 13–23.

Kang, Y.H., Breda, A., and Hardtke, C.S. (2017). Brassinosteroid signaling directs formative cell divisions and protophloem differentiation in Arabidopsis root meristems. Development **144**: 272–280.

Kater, M.M., Colombo, L., Franken, J., Busscher, M., Masiero, S., Van Lookeren Campagne, M.M., and Angenent, G.C. (1998). Multiple AGAMOUS homologs from cucumber and petunia differ in their ability to induce reproductive organ fate. Plant Cell **10**: 171–182.

Kierzkowski, D., Lenhard, M., Smith, R., and Kuhlemeier, C. (2013). Interaction between meristem tissue layers controls phyllotaxis. Dev Cell **26**: 616–628.

Krizek, B.A., Lewis, M.W., and Fletcher, J.C. (2006). RABBIT EARS is a second-whorl repressor of AGAMOUS that maintains spatial boundaries in Arabidopsis flowers. Plant J. **45**: 369–383.

Kuo, D., Licon, K., Bandyopadhyay, S., Chuang, R., Luo, C., Catalana, J., Ravasi, T., Tan, K., and Ideker, T. (2010). Coevolution within a transcriptional network by compensatory trans and cis mutations. Genome Res **20**: 1672–1678.

Kutschera, U., Bergfeld, R., and Schopfer, P. (1987). Cooperation of epidermis and inner tissues in auxin-mediated growth of maize coleoptiles. Planta **170**: 168–180.

Kutschera, U. and Niklas, K.J. (2007). The epidermal-growth-control theory of stem elongation: an old and a new perspective. J. Plant Physiol. **164**: 1395–1409.

Lai, X. et al. (2021). The LEAFY floral regulator displays pioneer transcription factor properties. Mol Plant **14**: 829–837.

Lampugnani, E.R., Kilinc, A., and Smyth, D.R. (2013). Auxin controls petal initiation in Arabidopsis. Development **140**: 185–194.

Lampugnani, E.R., Kilinc, A., and Smyth, D.R. (2012). PETAL LOSS is a boundary gene that inhibits growth between developing sepals in Arabidopsis thaliana. Plant J **71**: 724–735.

Li, J., Wang, Y., Zhang, Y., Wang, W., Irish, V.F., and Huang, T. (2016). RABBIT EARS regulates the transcription of TCP4 during petal development in Arabidopsis. J Exp Bot **67**: 6473–6480.

Liljegren, S.J., Ditta, G.S., Eshed, Y., Savidge, B., Bowman, J.L., and Yanofsky, M.F. (2000). SHATTERPROOF MADS-box genes control seed dispersal in Arabidopsis. Nature **404**: 766–770.

Litt, A. and Kramer, E.M. (2010). The ABC model and the diversification of floral organ identity. Semin Cell Dev Biol **21**: 129–137.

Liu, C., Xi, W., Shen, L., Tan, C., and Yu, H. (2009). Regulation of floral patterning by flowering time genes. Dev. Cell **16**: 711–722.

Long, Y., Stahl, Y., Weidtkamp-Peters, S., Postma, M., Zhou, W., Goedhart, J., Sánchez-Pérez, M.-I., Gadella, T.W.J., Simon, R., Scheres, B., and Blilou, I. (2017). In vivo FRET-FLIM reveals cell-type-specific protein interactions in Arabidopsis roots. Nature **548**: 97–102.

Lughadha, E.N., Govaerts, R., Belyaeva, I., Black, N., Lindon, H., Allkin, R., Magill, R.E., and Nicolson, N. (2016). Counting counts: revised estimates of numbers of accepted species of flowering plants, seed plants, vascular plants and land plants with a review of other recent estimates. Phytotaxa **272**: 82–88.

Maeda, S., Gunji, S., Hanai, K., Hirano, T., Kazama, Y., Ohbayashi, I., Abe, T., Sawa, S., Tsukaya, H., and Ferjani, A. (2014). The conflict between cell proliferation and expansion primarily affects stem organogenesis in Arabidopsis. Plant Cell Physiol **55**: 1994–2007.

Maizel, A., Busch, M.A., Tanahashi, T., Perkovic, J., Kato, M., Hasebe, M., and Weigel, D. (2005). The floral regulator LEAFY evolves by substitutions in the DNA binding domain. Science **308**: 260–263.

McKim, S.M., Routier-Kierzkowska, A.-L., Monniaux, M., Kierzkowski, D., Pieper, B., Smith, R.S., Tsiantis, M., and Hay, A. (2017). Seasonal Regulation of Petal Number. Plant Physiology **175**: 886–903.

Messenguy, F. and Dubois, E. (2003). Role of MADS box proteins and their cofactors in combinatorial control of gene expression and cell development. Gene **316**: 1–21.

Meyerowitz, E.M. (1997). Genetic Control of Cell Division Patterns in Developing Plants. Cell **88**: 299–308.

Monniaux, M., McKim, S.M., Cartolano, M., Thévenon, E., Parcy, F., Tsiantis, M., and Hay, A. (2017). Conservation vs divergence in LEAFY and APETALA1 functions between Arabidopsis thaliana and Cardamine hirsuta. New Phytol. **216**: 549–561.

Monniaux, M., Pieper, B., and Hay, A. (2016). Stochastic variation in Cardamine hirsuta petal number. Ann Bot **117**: 881–887.

Monniaux, M., Pieper, B., McKim, S.M., Routier-Kierzkowska, A.-L., Kierzkowski, D., Smith, R.S., and Hay, A. (2018). The role of APETALA1 in petal number robustness. Elife **7**.

Monniaux, M. and Vandenbussche, M. (2018). How to Evolve a Perianth: A Review of Cadastral Mechanisms for Perianth Identity. Front Plant Sci **9**: 1573.

Morel, P., Heijmans, K., Rozier, F., Zethof, J., Chamot, S., Bento, S.R., Vialette-Guiraud, A., Chambrier, P., Trehin, C., and Vandenbussche, M. (2017). Divergence of the Floral A-Function between an Asterid and a Rosid Species. Plant Cell **29**: 1605–1621.

Moyroud, E. and Glover, B.J. (2017). The Evolution of Diverse Floral Morphologies. Curr. Biol. **27**: R941–R951.

Moyroud, E., Kusters, E., Monniaux, M., Koes, R., and Parcy, F. (2010). LEAFY blossoms. Trends Plant Sci. **15**: 346–352.

Moyroud, E., Minguet, E.G., Ott, F., Yant, L., Posé, D., Monniaux, M., Blanchet, S., Bastien, O., Thévenon, E., Weigel, D., Schmid, M., and Parcy, F. (2011). Prediction of regulatory interactions from genome sequences using a biophysical model for the Arabidopsis LEAFY transcription factor. Plant Cell **23**: 1293–1306.

Moyroud, E., Monniaux, M., Thévenon, E., Dumas, R., Scutt, C.P., Frohlich, M.W., and Parcy, F. (2017). A link between LEAFY and B-gene homologues in Welwitschia mirabilis sheds light on ancestral mechanisms prefiguring floral development. New Phytol **216**: 469–481.

Nagata, K., Ishikawa, T., Kawai-Yamada, M., Takahashi, T., and Abe, M. (2021). Ceramides mediate positional signals in Arabidopsis thaliana protoderm differentiation. Development **148**.

Nitasaka, E. (2003). Insertion of an En/Spm-related transposable element into a floral homeotic gene DUPLICATED causes a double flower phenotype in the Japanese morning glory. Plant J **36**: 522–531.

Ohno, S. (1970). Evolution by Gene Duplication (Springer-Verlag).

One Thousand Plant Transcriptomes Initiative (2019). One thousand plant transcriptomes and the phylogenomics of green plants. Nature **574**: 679–685.

Pajoro, A., Biewers, S., Dougali, E., Valentim, F.L., Mendes, M.A., Porri, A., Coupland, G., Van de Peer, Y., van Dijk, A.D.J., Colombo, L., Davies, B., and Angenent, G.C. (2014). The (r)evolution of gene regulatory networks controlling Arabidopsis plant reproduction; a two decades history. J. Exp. Bot.

Parcy, F., Nilsson, O., Busch, M.A., Lee, I., and Weigel, D. (1998). A genetic framework for floral patterning. Nature **395**: 561–566.

Paris, M., Kaplan, T., Li, X.Y., Villalta, J.E., Lott, S.E., and Eisen, M.B. (2013). Extensive divergence of transcription factor binding in Drosophila embryos with highly conserved gene expression. PLoS Genet **9**: e1003748.

Pelaz, S., Ditta, G.S., Baumann, E., Wisman, E., and Yanofsky, M.F. (2000). B and C floral organ identity functions require SEPALLATA MADS-box genes. Nature **405**: 200–203.

Pelaz, S., Tapia-López, R., Alvarez-Buylla, E.R., and Yanofsky, M.F. (2001). Conversion of leaves into petals in Arabidopsis. Curr Biol **11**: 182–184.

Perbal, M.C., Haughn, G., Saedler, H., and Schwarz-Sommer, Z. (1996). Non-cell-autonomous function of the Antirrhinum floral homeotic proteins DEFICIENS and GLOBOSA is exerted by their polar cell-to-cell trafficking. Development **122**: 3433–3441.

Philipson, W.R. (1990). The significance of apical meristems in the phylogeny of land plants. Pl Syst Evol **173**: 17–38.

Pieper, B., Monniaux, M., and Hay, A. (2016). The genetic architecture of petal number in Cardamine hirsuta. New Phytol **209**: 395–406.

Pinyopich, A., Ditta, G.S., Savidge, B., Liljegren, S.J., Baumann, E., Wisman, E., and Yanofsky, M.F. (2003). Assessing the redundancy of MADS-box genes during carpel and ovule development. Nature **424**: 85–88.

Plackett, A.R., Conway, S.J., Hewett Hazelton, K.D., Rabbinowitsch, E.H., Langdale, J.A., and Di Stilio, V.S. (2018). LEAFY maintains apical stem cell activity during shoot development in the fern Ceratopteris richardii. Elife **7**: e39625.

Puzey, J.R., Gerbode, S.J., Hodges, S.A., Kramer, E.M., and Mahadevan, L. (2012). Evolution of spur-length diversity in Aquilegia petals is achieved solely through cell-shape anisotropy. Proc Biol Sci **279**: 1640–1645.

Quattrocchio, F., Wing, J., van der Woude, K., Souer, E., de Vetten, N., Mol, J., and Koes, R. (1999). Molecular analysis of the anthocyanin2 gene of petunia and its role in the evolution of flower color. Plant Cell **11**: 1433–1444.

Quattrocchio, F., Wing, J.F., Leppen, H.T.C., Mol, J.N.M., and Koes, R.E. (1993). Regulatory Genes Controlling Anthocyanin Pigmentation Are Functionally Conserved among Plant Species and Have Distinct Sets of Target Genes. Plant Cell **5**: 1497–1512.

Quattrocchio, F., Wing, J.F., van der Woude, K., Mol, J.N., and Koes, R. (1998). Analysis of bHLH and MYB domain proteins: species-specific regulatory differences are caused by divergent evolution of target anthocyanin genes. Plant J **13**: 475–488.

Reale, L., Porceddu, A., Lanfaloni, L., Moretti, C., Zenoni, S., Pezzotti, M., Romano, B., and Ferranti, F. (2002). Patterns of cell division and expansion in developing petals of Petunia hybrida. Sex Plant Reprod **15**: 123–132.

Rebocho, A.B., Southam, P., Kennaway, J.R., Bangham, J.A., and Coen, E. (2017). Generation of shape complexity through tissue conflict resolution. Elife **6**.

Reck-Kortmann, M., Silva-Arias, G.A., Segatto, A.L.A., Mader, G., Bonatto, S.L., and de Freitas, L.B. (2014). Multilocus phylogeny reconstruction: new insights into the evolutionary history of the genus Petunia. Mol Phylogenet Evol **81**: 19–28.

Riechmann, J.L., Krizek, B.A., and Meyerowitz, E.M. (1996a). Dimerization specificity of Arabidopsis MADS domain homeotic proteins APETALA1, APETALA3, PISTILLATA, and AGAMOUS. Proc Natl Acad Sci U S A **93**: 4793–4798.

Riechmann, J.L., Wang, M., and Meyerowitz, E.M. (1996b). DNA-binding properties of Arabidopsis MADS domain homeotic proteins APETALA1, APETALA3, PISTILLATA and AGAMOUS. Nucleic Acids Res **24**: 3134–3141.

Rijpkema, A.S., Royaert, S., Zethof, J., Weerden, G. van der, Gerats, T., and Vandenbussche, M. (2006). Analysis of the Petunia TM6 MADS Box Gene Reveals Functional Divergence within the DEF/AP3 Lineage. The Plant Cell **18**: 1819–1832.

Robinson, D.O. and Roeder, A.H.K. (2015). Themes and variations in cell type patterning in the plant epidermis. Curr Opin Genet Dev **32**: 55–65.

Rodrigues, D.M., Caballero-Villalobos, L., Turchetto, C., Assis Jacques, R., Kuhlemeier, C., and Freitas, L.B. (2018). Do we truly understand pollination syndromes in Petunia as much as we suppose? AoB Plants **10**.

Satina, S. and Blakeslee, A.F. (1941). Periclinal Chimeras in Datura Stramonium in Relation to Development of Leaf and Flower. American Journal of Botany **28**: 862–871.

Satina, S., Blakeslee, A.F., and Avery, A.G. (1940). Demonstration of the Three Germ Layers in the Shoot Apex of Datura by Means of Induced Polyploidy in Periclinal Chimeras. American Journal of Botany **27**: 895–905.

Sauquet, H. et al. (2017). The ancestral flower of angiosperms and its early diversification. Nat Commun **8**: 16047.

Sauquet, H. and Magallón, S. (2018). Key questions and challenges in angiosperm macroevolution. New Phytologist **0**.

Sauquet, H., Ramírez-Barahona, S., and Magallón, S. (2022). What is the age of flowering plants? Journal of Experimental Botany **73**: 3840–3853.

Savaldi-Goldstein, S. and Chory, J. (2008). Growth coordination and the shoot epidermis. Curr. Opin. Plant Biol. **11**: 42–48.

Savaldi-Goldstein, S., Peto, C., and Chory, J. (2007). The epidermis both drives and restricts plant shoot growth. Nature **446**: 199–202.

Sayou, C. et al. (2014). A promiscuous intermediate underlies the evolution of LEAFY DNA binding specificity. Science **343**: 645–648.

Scheres, B. (2001). Plant cell identity. The role of position and lineage. Plant Physiol **125**: 112–114.

Schneider, T.D. and Stephens, R.M. (1990). Sequence logos: a new way to display consensus sequences. Nucleic Acids Res **18**: 6097–6100.

Schwarz-Sommer, Z., Huijser, P., Nacken, W., Saedler, H., and Sommer, H. (1990). Genetic Control of Flower Development by Homeotic Genes in Antirrhinum majus. Science **250**: 931–936.

Sheehan, H., Moser, M., Klahre, U., Esfeld, K., Dell'Olivo, A., Mandel, T., Metzger, S., Vandenbussche, M., Freitas, L., and Kuhlemeier, C. (2016). MYB-FL controls gain and loss of floral UV absorbance, a key trait affecting pollinator preference and reproductive isolation. Nat Genet **48**: 159–166.

Sicard, A. and Lenhard, M. (2011). The selfing syndrome: a model for studying the genetic and evolutionary basis of morphological adaptation in plants. Ann Bot **107**: 1433–1443.

Soltis, P.S. and Soltis, D.E. (2016). Ancient WGD events as drivers of key innovations in angiosperms. Current Opinion in Plant Biology **30**: 159–165.

Spelt, C., Quattrocchio, F., Mol, J.N.M., and Koes, R. (2000). anthocyanin1 of Petunia Encodes a Basic Helix-Loop-Helix Protein That Directly Activates Transcription of Structural Anthocyanin Genes. The Plant Cell **12**: 1619–1631.

Stewart, R.N. and Burk, L.G. (1970). Independence of Tissues Derived from Apical Layers in Ontogeny of the Tobacco Leaf and Ovary. American Journal of Botany **57**: 1010–1016.

Takada, S. and Iida, H. (2014). Specification of epidermal cell fate in plant shoots. Front. Plant Sci. **5**.

Takeda, S., Hamamura, Y., Sakamoto, T., Kimura, S., Aida, M., and Higashiyama, T. (2022). Non-cell-autonomous regulation of petal initiation in Arabidopsis thaliana. Development **149**: dev200684.

Tanahashi, T., Sumikawa, N., Kato, M., and Hasebe, M. (2005). Diversification of gene function: homologs of the floral regulator FLO/LFY control the first zygotic cell division in the moss Physcomitrella patens. Development **132**: 1727–1736.

Theissen, G., Melzer, R., and Rümpler, F. (2016). MADS-domain transcription factors and the floral quartet model of flower development: linking plant development and evolution. Development **143**: 3259–3271.

Theissen, G. and Saedler, H. (2001). Plant biology. Floral quartets. Nature **409**: 469–471.

Tornielli, G., Koes, R., and Quattrocchio, F. (2009). The Genetics of Flower Color. In Petunia: Evolutionary, Developmental and Physiological Genetics, T. Gerats and J. Strommer, eds (Springer: New York, NY), pp. 269–299.

Tuerk, C. and Gold, L. (1990). Systematic evolution of ligands by exponential enrichment: RNA ligands to bacteriophage T4 DNA polymerase. Science **249**: 505–510.

Urbanus, S.L., Martinelli, A.P., Dinh, Q.D.P., Aizza, L.C.B., Dornelas, M.C., Angenent, G.C., and Immink, R.G.H. (2010). Intercellular transport of epidermis-expressed MADS domain transcription factors and their effect on plant morphology and floral transition. Plant J **63**: 60–72.

Vandenbussche, M., Zethof, J., Royaert, S., Weterings, K., and Gerats, T. (2004). The duplicated B-class heterodimer model: whorl-specific effects and complex genetic interactions in Petunia hybrida flower development. Plant Cell **16**: 741–754.

Verd, B., Monk, N.A., and Jaeger, J. (2019). Modularity, criticality, and evolvability of a developmental gene regulatory network. eLife **8**: e42832.

de Vetten, N., Quattrocchio, F., Mol, J., and Koes, R. (1997). The an11 locus controlling flower pigmentation in petunia encodes a novel WD-repeat protein conserved in yeast, plants, and animals. Genes Dev **11**: 1422–1434.

Vincent, C.A., Carpenter, R., and Coen, E.S. (2003). Interactions between gene activity and cell layers during floral development. The Plant Journal **33**: 765–774.

de Vries, J. and Archibald, J.M. (2018). Plant evolution: landmarks on the path to terrestrial life. New Phytol **217**: 1428–1434.

Wagner, G.P. and Altenberg, L. (1996). Perspective: Complex Adaptations and the Evolution of Evolvability. Evolution **50**: 967–976.

Whitney, H.M., Kolle, M., Andrew, P., Chittka, L., Steiner, U., and Glover, B.J. (2009). Floral iridescence, produced by diffractive optics, acts as a cue for animal pollinators. Science **323**: 130–133.

Wigge, P.A., Kim, M.C., Jaeger, K.E., Busch, W., Schmid, M., Lohmann, J.U., and Weigel, D. (2005). Integration of spatial and temporal information during floral induction in Arabidopsis. Science **309**: 1056–1059.

Wilhelmsson, P.K.I., Mühlich, C., Ullrich, K.K., and Rensing, S.A. (2017). Comprehensive Genome-Wide Classification Reveals That Many Plant-Specific Transcription Factors Evolved in Streptophyte Algae. Genome Biol Evol **9**: 3384–3397.

Winter, C.M. et al. (2011). LEAFY target genes reveal floral regulatory logic, cis motifs, and a link to biotic stimulus response. Dev. Cell **20**: 430–443.

Wuest, S.E., O'Maoileidigh, D.S., Rae, L., Kwasniewska, K., Raganelli, A., Hanczaryk, K., Lohan, A.J., Loftus, B., Graciet, E., and Wellmer, F. (2012). Molecular basis for the specification of floral organs by APETALA3 and PISTILLATA. Proc. Natl. Acad. Sci. U.S.A. **109**: 13452–13457.

Yant, L., Collani, S., Puzey, J., Levy, C., and Kramer, E.M. (2015). Molecular basis for three-dimensional elaboration of the Aquilegia petal spur. Proc. Biol. Sci. **282**: 20142778.

Yu, H., Ito, T., Wellmer, F., and Meyerowitz, E.M. (2004). Repression of AGAMOUS-LIKE 24 is a crucial step in promoting flower development. Nature Genetics **36**: 157–161.

Zhang, R., Min, Y., Holappa, L.D., Walcher-Chevillet, C.L., Duan, X., Donaldson, E., Kong, H., and Kramer, E.M. (2020). A role for the Auxin Response Factors ARF6 and ARF8 homologs in petal spur elongation and nectary maturation in Aquilegia. New Phytol **227**: 1392–1405.

Zhou, H. and von Schwartzenberg, K. (2020). Zygnematophyceae: from living algae collections to the establishment of future models. Journal of Experimental Botany **71**: 3296–3304.

for AMSR-E precipitation shown in Fig. 1F (red curve) have ~40 degrees of freedom.
18. P. J. Webster, J. L. Keller, *J. Atmos. Sci.* **32**, 1283–1301 (1975).
19. J. W. Kidson, *Mon. Weather Rev.* **114**, 1654–1663 (1986).
20. G. K. Vallis, *Atmospheric and Oceanic Fluid Dynamics* (Cambridge Univ. Press, Cambridge, 2006).
21. R. S. Lindzen, B. F. Farrell, *J. Atmos. Sci.* **37**, 1648–1654 (1980).
22. B. J. Hoskins, P. J. Valdes, *J. Atmos. Sci.* **47**, 1854–1864 (1990).
23. P. J. Kushner, I. M. Held, *Geophys. Res. Lett.* **25**, 4213–4216 (1998).
24. H. Nakamura, A. Shimpo, *J. Clim.* **17**, 1828–1844 (2004).
25. D. W. J. Thompson, T. Birner, *J. Atmos. Sci.* **69**, 1811–1823 (2012).
26. The baroclinicity is defined as the meridional slope of the isentropic surfaces relative to Earth's surface. It thus includes two components: the meridional gradient in temperature and the vertical gradient in temperature (i.e., the static stability).
27. D. G. Andrews, M. E. McIntyre, *J. Atmos. Sci.* **33**, 2031–2048 (1976).
28. The Geophysical Fluid Dynamics Laboratory (GFDL) CM3 is a coupled chemistry climate model. The analyses shown here are based on a simulation performed for the Coupled Model Intercomparison Project (CMIP5), phase 5. See (*33*). We analyzed one ensemble of the historical simulation over years 1970–2004. The aquaplanet simulation is identical to that used in (*34*). The model is integrated at T85 resolution for 21 years, with the first 2 years discarded for spin-up. All model parameters are set to the values from the control experiment of Frierson *et al*. (*34*). The idealized dry GCM is the GFDL spectral dry dynamical core of (*35*). The model does not include radiation or moisture and uses Newtonian relaxation to a zonally symmetric equilibrium temperature profile and Rayleigh damping of the low-level winds to simulate boundary layer friction. The model is integrated at T42 (42-wave triangular truncation) resolution for 6000 days with 2000 days for spin-up. Both the aquaplanet and the dry dynamical core do not have topography and are run under perpetual equinoctial conditions with no diurnal cycle.
29. C.-G. Rossby, H. C. Willett, *Science* **108**, 643–652 (1948).
30. J. Namias, *J. Meteorol.* **7**, 130–139 (1950).
31. J. M. Wallace, H.-H. Hsu, *Tellus* **37A**, 478–486 (1985).
32. D. P. Dee *et al*., *Q. J. R. Meteorol. Soc.* **137**, 553–597 (2011).
33. L. J. Donner *et al*., *J. Clim.* **24**, 3484–3519 (2011).
34. D. M. W. Frierson, I. M. Held, P. Zurita-Gotor, *J. Atmos. Sci.* **63**, 2548–2566 (2006).
35. I. M. Held, M. J. Suarez, *Bull. Am. Meteorol. Soc.* **75**, 1825–1830 (1994).

Acknowledgments: We thank R. Garreaud and J. M. Wallace for helpful discussion of the results, R. Barnes for insight into the analytic model, S. Wills for assistance with the AMSR-E data, and three anonymous reviewers for helpful comments on the manuscript. D.W.J.T. is supported by the NSF Climate Dynamics program.

Supplementary Materials

www.sciencemag.org/content/343/6171/641/suppl/DC1
Supplementary Text
Figs. S1 and S2
Reference

25 October 2013; accepted 7 January 2014
10.1126/science.1247660

A Promiscuous Intermediate Underlies the Evolution of LEAFY DNA Binding Specificity

Camille Sayou,[1,2,3,4]* Marie Monniaux,[1,2,3,4]* Max H. Nanao,[5,6]*† Edwige Moyroud,[1,2,3,4]*‡ Samuel F. Brockington,[7] Emmanuel Thévenon,[1,2,3,4] Hicham Chahtane,[1,2,3,4] Norman Warthmann,[8]§ Michael Melkonian,[9] Yong Zhang,[10] Gane Ka-Shu Wong,[10,11] Detlef Weigel,[8] François Parcy,[1,2,3,4,12]† Renaud Dumas[1,2,3,4]

Transcription factors (TFs) are key players in evolution. Changes affecting their function can yield novel life forms but may also have deleterious effects. Consequently, gene duplication events that release one gene copy from selective pressure are thought to be the common mechanism by which TFs acquire new activities. Here, we show that LEAFY, a major regulator of flower development and cell division in land plants, underwent changes to its DNA binding specificity, even though plant genomes generally contain a single copy of the *LEAFY* gene. We examined how these changes occurred at the structural level and identify an intermediate LEAFY form in hornworts that appears to adopt all different specificities. This promiscuous intermediate could have smoothed the evolutionary transitions, thereby allowing LEAFY to evolve new binding specificities while remaining a single-copy gene.

The rewiring of transcriptional networks is an important source of evolutionary novelty (*1*–*3*). Variation often occurs through changes in cis-regulatory elements, which are DNA sequences that contain binding sites for transcription factors (TFs) regulating nearby genes (*3*, *4*). There is less evidence for regulatory changes affecting the protein-coding sequence of TFs. Such changes are expected to be under highly stringent selection because they could impair the expression of many downstream targets. Gene duplication provides a solution to this dilemma, as additional TF gene copies may acquire new functions, provided that the aggregate copies fulfill the function of the original TF (*5*). Indeed, TF DNA binding specificity has been shown to diversify within multigene families (*6*, *7*). In some cases, however, TF coding genes remain as single-copy genes because of phenomena such as paralog interference (*8*), which can impede neofunctionalization. When essential TFs are maintained as single-copy genes, the extent to which they can evolve is not clear. To address this question, we examined the *LEAFY (LFY)* gene as an evolutionary model.

Except in gymnosperms, in which two paralogs (*LEAFY* and *NEEDLY*) are usually present (Fig. 1A), *LFY* exists mostly as a single-copy gene in land plants (*9*). *LFY* plays essential roles as a key regulator of floral identity in angiosperms, as well as in cell division in the moss *Physcomitrella patens* (*10*). *LFY* encodes a TF that binds DNA through a highly conserved dimeric DNA binding domain (DBD) (*11*). Despite this conservation, PpLFY1, a LFY homolog from the moss *P. patens*, is unable to bind the DNA sequence recognized by LFY from *Arabidopsis thaliana* (AtLFY) (*9*), suggesting that LFY DNA binding specificity might have changed during land plant evolution.

We mined the transcriptomes from algal species, whose origin predates the divergence of mosses and tracheophytes, and found *LFY* homologs in six species of streptophyte green algae (Fig. 1A and fig. S1) (see also supplementary materials and methods). Thus, *LFY* is not specific to land plants. Despite this extended ancestry, the LFY-DBD sequence, including the amino acids in direct contact with DNA, remains highly conserved (Fig. 1B and fig. S1). We used high-throughput SELEX (systematic evolution of ligands by exponential enrichment) (*12*) experiments to systematically analyze the DNA binding specificity of LFY proteins from each group of plants. After

[1]CNRS, Laboratoire de Physiologie Cellulaire et Végétale (LPCV), UMR 5168, 38054 Grenoble, France. [2]Université Grenoble Alpes, LPCV, F-38054 Grenoble, France. [3]Commissariat à l'Energie Atomique et aux Energies Alternatives, Direction des Sciences du Vivant, Institut de Recherches en Technologies et Sciences pour le Vivant, LPCV, F-38054 Grenoble, France. [4]Institut National de la Recherche Agronomique, LPCV, F-38054 Grenoble, France. [5]European Molecular Biology Laboratory (EMBL), 6 Rue Jules Horowitz, BP 181, 38042 Grenoble, France. [6]Unit of Virus Host-Cell Interactions, Université Grenoble Alpes–EMBL–CNRS, UMI 3265, 6 Rue Jules Horowitz, 38042 Grenoble Cedex 9, France. [7]Department of Plant Sciences, University of Cambridge, Downing Street, Cambridge CB2 3EA, UK. [8]Department of Molecular Biology, Max Planck Institute for Developmental Biology, 72076 Tübingen, Germany. [9]Botanisches Institut, Lehrstuhl I, Universität zu Köln, Biozentrum Köln, Zülpicher Strasse 47b, 50674 Köln, Germany. [10]Beijing Genomics Institute (BGI)–Shenzhen, Beishan Industrial Zone, Yantian District, Shenzhen 518083, China. [11]Department of Biological Sciences, Department of Medicine, University of Alberta, Edmonton, Alberta T6G 2E9, Canada. [12]Centre for Molecular Medicine and Therapeutics, Child and Family Research Institute, University of British Columbia, Vancouver, British Columbia V5Z 4H4, Canada.

*These authors contributed equally to this work.
†Corresponding author. E-mail: francois.parcy@cea.fr (F.P); mnanao@embl.fr (M.H.N.)
‡Present address: Department of Plant Sciences, University of Cambridge, Downing Street, Cambridge CB2 3EA, UK.
§Present address: Research School of Biology, The Australian National University, Acton, ACT 0200, Australia.

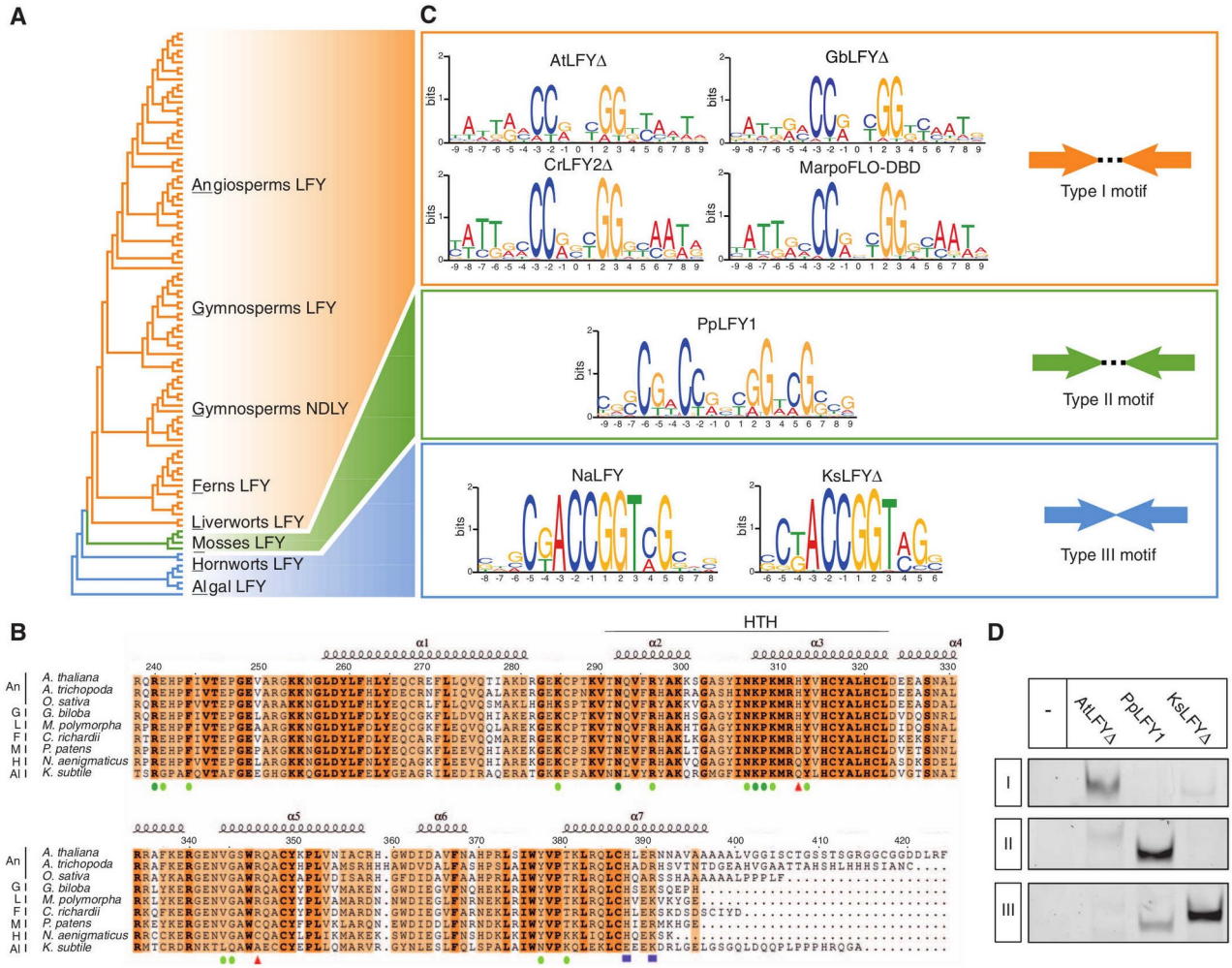

Fig. 1. Evolution of LFY DNA binding specificity. (**A**) Simplified *LEAFY* phylogeny (detailed in fig. S5). DNA binding specificities are color coded: type I, orange; type II, green; or type III, blue. (**B**) Alignment of LFY-DBDs. Amino acid numbering and secondary structure annotation (α, alpha helices; HTH, helix-turn-helix domain) are based on AtLFY from *A. thaliana*. Single-letter abbreviations for the amino acid residues are as follows: A, Ala; C, Cys; D, Asp; E, Glu; F, Phe; G, Gly; H, His; I, Ile; K, Lys; L, Leu; M, Met; N, Asn; P, Pro; Q, Gln; R, Arg; S, Ser; T, Thr; V, Val; W, Trp; and Y, Tyr. Dark green dots, DNA base contacts; light green dots, phosphate backbone contacts; red triangles, residues involved in the PpLFY1-specific DNA contacts; purple rectangles, residues involved in the interaction between DBD monomers. (**C**) SELEX motifs for AtLFYΔ, GbLFYΔ (*Ginkgo biloba*), CrLFY2Δ (*Ceratopteris richardii*), MarpoFLO-DBD (*Marchantia polymorpha*), PpLFY1 (*P. patens*), NaLFY (*N. aenigmaticus*), and KsLFYΔ (*K. subtile*) are shown. Δ denotes proteins starting at amino acid 40 (on the basis of the AtLFY sequence). Cartoons at right depict binding site organization: half-site (arrows) with or without a 3-bp spacer. (**D**) EMSA with AtLFYΔ, PpLFY1, and KsLFYΔ proteins (10 nM) and the three types (I, II, III) of DNA probes. Only the protein-DNA complexes are shown.

optimizing alignments (*13*), we found that the SELEX motifs fell into three groups (Fig. 1C and fig. S2), suggesting that LFY changed specificity at least twice.

Most LFY proteins from land plants (angiosperms, gymnosperms, ferns, and liverworts) bind the same DNA motif (type I) as AtLFY (*13*). PpLFY1, however, binds to a different motif (type II), despite possessing the same 15 DNA binding amino acids as AtLFY (Fig. 1B). These SELEX results explain why all embryophyte LFY homologs, except PpLFY1, display AtLFY-like activity when expressed in *A. thaliana* (*9*). Motifs I and II share a similar overall organization, consisting of two 8–base pair (bp) inverted half-sites separated by three nucleotides, but their peripheral positions differ. The newly identified hornwort and algal LFY proteins bind to a third motif (type III) that resembles motif II, but without the central 3-bp spacer (Fig. 1C). With AtLFY, PpLFY1, and KsLFY (from *Klebsormidium subtile*) as representative proteins of the three specificities, we confirmed that each protein displays a strong preference for one motif type (Fig. 1D, fig. S3, and table S1).

Given the broad conservation of the LFY-DBD sequence, we asked how these different specificities could be explained molecularly. We solved the crystal structure of PpLFY1-DBD bound to a motif II DNA (Fig. 2A and table S2) and compared it to the previously determined AtLFY-DBD dimer–type I DNA complex (*11*). The two ternary complexes are highly similar (root mean square deviation of protein backbone atoms of 0.6 Å). However, PpLFY1-DBD makes additional contact with DNA: Aspartic acid 312 (D312) interacts with the cytosine base (C) at position 6 of the DNA binding motif, which is the nucleotide most different between motifs I and II obtained by SELEX (Figs. 1C and 2B). In AtLFY, position 312 is occupied by a histidine residue (H312), which is pulled away from the DNA by an arginine (R345), a conformation that precludes direct H312-DNA contact. In contrast, in PpLFY1, a cysteine residue (C345) replaces R345, which does not affect the positioning of D312, thus al-

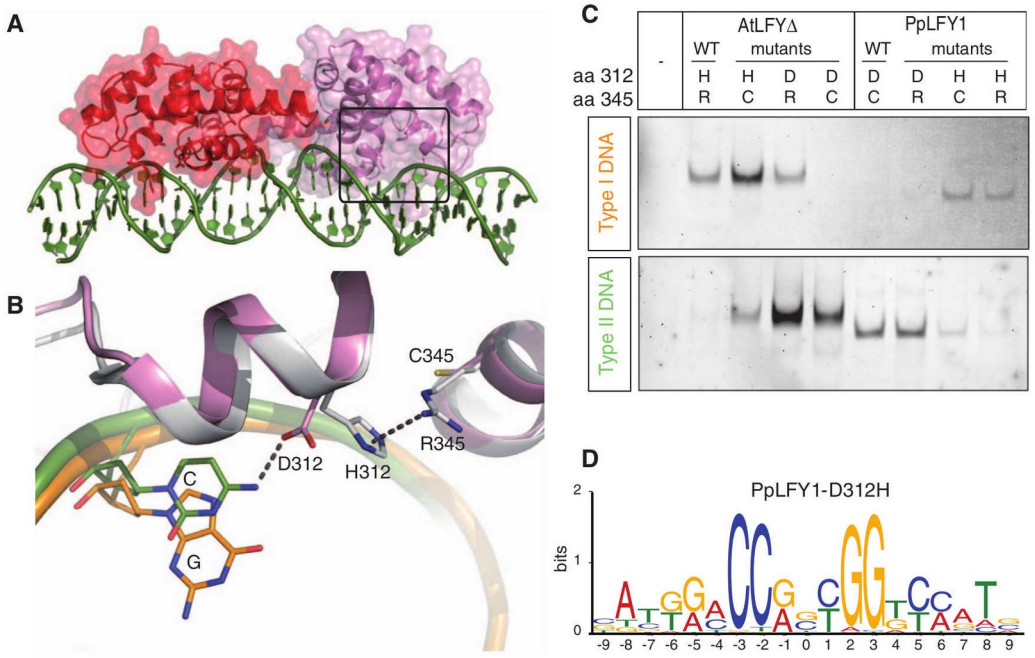

Fig. 2. Structural basis for type II specificity. (**A**) Crystal structure of PpLFY1-DBD (red and pink) bound to DNA (green). The boxed area is detailed in (B) after applying a 70° rotation. (**B**) Superimposition of AtLFY-DBD (gray)–DNA (orange) and PpLFY1-DBD (pink)–DNA (green) complexes. Specificity determinant residues and bases are represented as sticks. For amino acids: H, histidine; R, arginine; D, aspartate; C, cysteine; for DNA bases: C, cytosine; G, guanine. (**C**) Effect of specific mutations on the DNA binding specificity of AtLFYΔ and PpLFY1 in EMSA. Note that the H312-C345 combination allows binding to both motifs I and II. All proteins are at 25 nM, and only the protein-DNA complexes are shown. WT, wild type; aa, amino acid. (**D**) SELEX motif of the PpLFY1-D312H protein, bearing a strong resemblance to motif I.

lowing it to contact the cytosine base. To test the importance of positions 312 and 345, we swapped these residues between PpLFY1 and AtLFY (Fig. 2, C and D). This was sufficient to convert specificity from type I to type II and vice versa, confirming the key role of these two positions. This result is consistent with an in vivo study showing that a PpLFY1-D312H (D312H, Asp^{312}→His^{312}) mutant can bind a type I sequence and partially complement a *lfy* mutation in *A. thaliana* plants (*9*).

We next investigated binding to motif III. Motif III half-sites are similar to those of motif II (Fig. 1C), owing to the presence of a glutamine (Q) at position 312 in type III LFYs: Q is known to interact with multiple bases (*14*) (fig. S4), and the small residues present at position 345 (cysteine, alanine, or serine) allow Q312 to freely interact with position 6. Critically, motif III differs from motif II by the lack of the central 3-bp spacer (Fig. 1C). Modeling a LFY-DBD– motif III ternary complex by removing the 3-bp spacer in the type II DNA sequence (Fig. 3A) revealed that the interaction between helices α1 and α7, which stabilizes dimeric AtLFY- and PpLFY1-DBD positioning (*11*), could no longer exist for motif III.

Consistent with this observation, interacting regions of helices α1 and α7 [including the key amino acid H387 on α7 (*11*)] are highly conserved from bryophytes to angiosperms (type II and I), but are variable in algae (type III) (Fig. 1B and fig. S1). To test the importance of the α1-α7 interaction in binding to 3-bp–spaced half-sites, we mutated PpLFY1 H387 and R390 residues (which make most α1-α7 contacts). This was sufficient to shift the DNA binding preference of PpLFY1 from type II to type III (Fig. 3B). These observations suggest that LFY-DBD preferentially binds to 3-bp–spaced half-sites (motifs I and II) when the α1-α7 interaction surface is present and to motif III in the absence of this surface. Nevertheless, both the pseudosymmetry of motif III (fig. S2) and the size of LFY-DNA complexes (fig. S4) suggest that LFY binds motif III as a dimer, possibly through an alternative dimerization surface. These analyses pinpoint the molecular basis of DNA specificity changes to three amino acid sites: Positions 312 and 345 determine the half-site sequence, and position 387 determines the dimerization mode.

However, if, as shown in *P. patens* and angiosperms, LFY plays a key role throughout plant evolution, how could these changes have been tolerated? Because once arisen, they would have instantaneously modified the expression of the entire set of LFY target genes. Our *LFY* phylogeny (fig. S5) yields two insights: (i) Although we cannot completely rule out the occurrence of transient ancient duplications, all known duplication events occurred subsequent to changes in the binding specificity of the protein; therefore the *LFY* gene probably evolved new DNA binding modes independently of changes in copy number. (ii) The hornwort *LFY* lineage diverges from a phylogenetic node that lies between the type III and type I-II binding specificities. On closer examination, we realized that NaLFY from the hornwort *Nothoceros aenigmaticus* had type III specificity according to the SELEX experiment, despite having the H387 dimerization residue

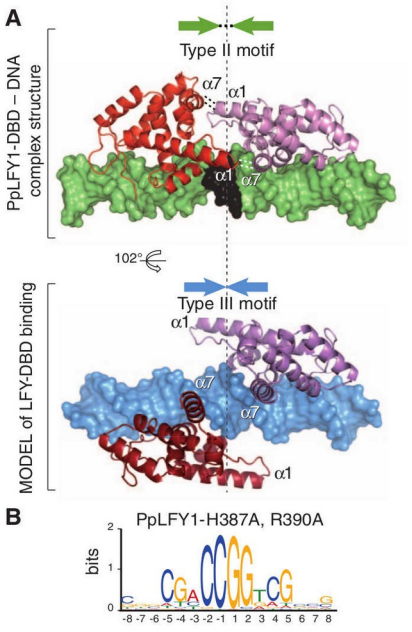

Fig. 3. Structural model for type III specificity. (**A**) (Top) PpLFY1-DBD dimer (in red and pink) bound to DNA (in green, except the black 3-bp spacer). Interactions between monomers (involving α helices α1 and α7) are shown with dashed lines. (Bottom) Modeled type III binding with DNA shown in blue. The dashed vertical line denotes the center of the pseudopalindromic DNA sequence. (**B**) SELEX motif of PpLFY1-H387A, R390A, showing a strong resemblance to motif III.

typical for type I and II specificities (Fig. 1, B and C). Using electrophoretic mobility shift assay (EMSA) experiments, we assayed NaLFY and NaLFY-DBD DNA binding and found that their dimers (fig. S6) could bind all three types of DNA motifs (Fig. 4, and figs. S3 and S7). We also established that NaLFY binding to motifs I and II was allowed by the presence of a functional α1-α7 interaction surface (Fig. 4). The SELEX experiment most likely identified only motif III because of its slightly more efficient binding to NaLFY (fig. S3 and table S1).

Our amino acid reconstruction analyses across the LFY phylogeny identify the phylogenetic location of the three specificity transitions that occurred during LFY evolution (Fig. 4 and fig. S8). Initially, the ancestral algal LFY bound motif III as a dimer (with Q312 and C345 half-site determinants). Subsequently, the evolution of the α1-α7 interaction surface generated a promiscuous LFY intermediate with two modes of DBD dimerization and a versatile glutamine residue at position 312, which bound all three types of DNA motifs. Mutations affecting positions 312 and 345 then completed the transition to type I or II specificities. Although this precise path cannot be unambiguously determined by reconstruction alone (Fig. 4 and fig. S8), the biochemical data reveal that two LFY states (Q312-C345 and H312-C345) bind to both motifs I and II (Figs. 2C and 4). Our scenario, using either of these two states as an intermediate, provides an evolutionary route through a promiscuous platform that avoids deleterious transitions. Furthermore, this scenario is equally parsimonious in the context of all alternative organismal phylogenetic hypotheses (fig. S9). Whether these transitions were accompanied by a complete change in target gene sets or whether some cis elements coevolved with DNA binding specificity (*15*) is unknown. Scanning the *P. patens* genome for PpLFY1 binding sites does not suggest any global conservation of targets but does identify several MADS-box genes potentially bound by LFY in both *Arabidopsis* and *P. patens* (table S3).

A highly conserved and essential TF evolved radical shifts in DNA binding specificity by a mechanism that does not require gene duplication. Detailed structural characterization of the different modes of DNA binding across the transition to land plants enabled us to capture LFY in a state of increased promiscuity that has persisted in *N. aenigmaticus*. This promiscuous intermediate probably facilitated the evolutionary transition between specificities, as previously shown for the evolution of metabolic enzymes or nuclear receptors (*16*–*18*). Although we have focused on the more intractable problem of evolution in single-copy TFs, it is plausible that the mechanisms we describe could also contribute to the evolution of TFs encoded by multigene families.

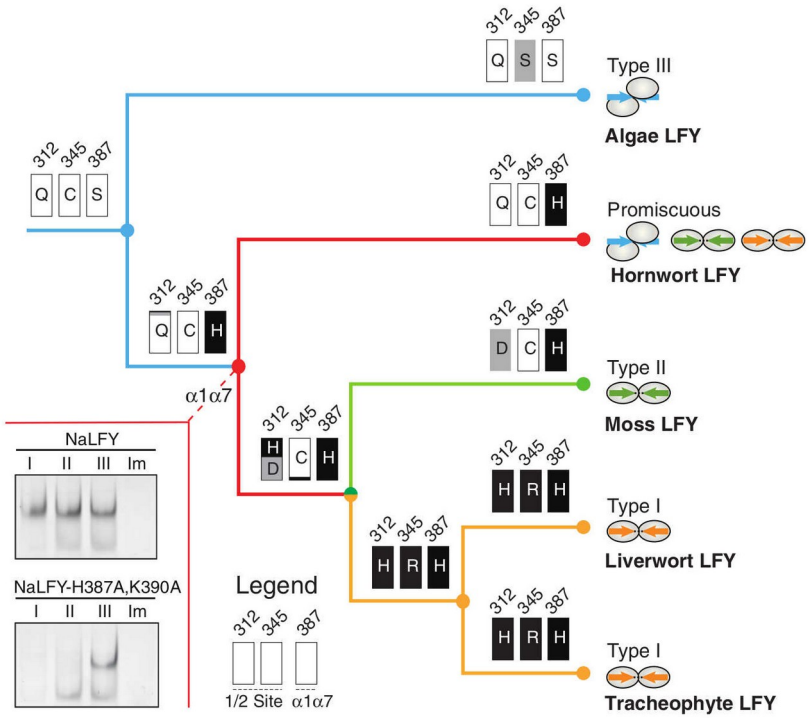

Fig. 4. Proposed evolution of LFY DNA binding specificity in green plants. The Bayesian estimation of the posterior probability of ancestral states for amino acid positions 312, 345, and 387 is depicted at the major phylogenetic nodes. Probabilities for different residues at a given position and node are indicated by the relative size of stacked boxes. The analysis shows that the ancestral LFY most likely possessed a type III specificity and that the promiscuous form arose when land plants emerged. DNA binding specificity is color-coded: type I, orange; type II, green; type III, blue; relaxed specificity, red. α1α7 refers to the α1-α7 dimerization interface. (**Inset**) NaLFY interacts with all three types of DNA binding motifs in EMSA (see also fig. S7), but not with the type I mutated probe (Im). The H387A and K390A mutations reduced the binding to type I or II motifs, but not to type III. Both proteins are at 1 μM; only the protein-DNA complexes are shown.

References and Notes

1. S. B. Carroll, *Cell* **101**, 577–580 (2000).
2. I. S. Peter, E. H. Davidson, *Cell* **144**, 970–985 (2011).
3. B. Prud'homme, N. Gompel, S. B. Carroll, *Proc. Natl. Acad. Sci. U.S.A.* **104** (suppl. 1), 8605–8612 (2007).
4. G. A. Wray, *Nat. Rev. Genet.* **8**, 206–216 (2007).
5. H. E. Hoekstra, J. A. Coyne, *Evolution* **61**, 995–1016 (2007).
6. G. Badis *et al.*, *Science* **324**, 1720–1723 (2009).
7. M. F. Berger *et al.*, *Cell* **133**, 1266–1276 (2008).
8. C. R. Baker, V. Hanson-Smith, A. D. Johnson, *Science* **342**, 104–108 (2013).
9. A. Maizel *et al.*, *Science* **308**, 260–263 (2005).
10. T. Tanahashi, N. Sumikawa, M. Kato, M. Hasebe, *Development* **132**, 1727–1736 (2005).
11. C. Hamès *et al.*, *EMBO J.* **27**, 2628–2637 (2008).
12. Y. Zhao, D. Granas, G. D. Stormo, *PLOS Comput. Biol.* **5**, e1000590 (2009).
13. E. Moyroud *et al.*, *Plant Cell* **23**, 1293–1306 (2011).
14. N. M. Luscombe, R. A. Laskowski, J. M. Thornton, *Nucleic Acids Res.* **29**, 2860–2874 (2001).
15. C. R. Baker, B. B. Tuch, A. D. Johnson, *Proc. Natl. Acad. Sci. U.S.A.* **108**, 7493–7498 (2011).
16. O. Khersonsky, C. Roodveldt, D. S. Tawfik, *Curr. Opin. Chem. Biol.* **10**, 498–508 (2006).
17. A. Aharoni *et al.*, *Nat. Genet.* **37**, 73–76 (2005).
18. G. N. Eick, J. K. Colucci, M. J. Harms, E. A. Ortlund, J. W. Thornton, *PLOS Genet.* **8**, e1003072 (2012).

Acknowledgments: We thank M. Schmid for help with sequencing; E. Masson, J. Kyozuka, M. Hasebe, C. Scutt, C. Finet, and J. C. Villarreal for sharing materials; A. Maizel and S. Rensing for discussion; and A. Maizel, R. Worsley-Hunt, A. Mathelier, M. Blazquez, O. Nilsson, C. Zubieta, and J. Chen for critical reading of the manuscript. This work was supported by funds from the Max Planck Society (D.W.), the Agence Nationale de la Recherche (grant Charmful SVSE2–2011) and Coopérations et Mobilités Internationales Rhône-Alpes (F.P.), and the FP7 P-CUBE number 227764 (R.D.). The 1000 Plants (1KP) initiative, led by G.K.-S.W., is funded by Alberta Ministry of Enterprise and Advanced Education, Alberta Innovates Technology Futures, Innovates Centre of Research Excellence, Musea Ventures, and BGI-Shenzhen. GenBank accession numbers are as follows: *AmboLFY*, KF193872; *NaLFY*, KF269532; *KsLFY*, KF269535; *CsLFY*, KF269533; *CvLFY*, KF269536; and *CyLFY*: KF269534. The Protein Data bank identification number is 4BHK for the reported crystal structure. We declare no competing financial interests.

Supplementary Materials

www.sciencemag.org/content/343/6171/645/suppl/DC1
Materials and Methods
Supplementary Text
Figs. S1 to S9
Tables S1 to S5
References (*19*–*42*)
Database S1

7 November 2013; accepted 23 December 2013
Published online 16 January 2014;
10.1126/science.1248229

Key Publication 2

eLIFE elifesciences.org

RESEARCH ARTICLE

The role of *APETALA1* in petal number robustness

Marie Monniaux[1†‡], Bjorn Pieper[1†], Sarah M McKim[2§], Anne-Lise Routier-Kierzkowska[1#], Daniel Kierzkowski[1#], Richard S Smith[1], Angela Hay[1*]

[1]Max Planck Institute for Plant Breeding Research, Cologne, Germany; [2]Plant Sciences Department, University of Oxford, Oxford, United Kingdom

Abstract Invariant floral forms are important for reproductive success and robust to natural perturbations. Petal number, for example, is invariant in *Arabidopsis thaliana* flowers. However, petal number varies in the closely related species *Cardamine hirsuta*, and the genetic basis for this difference between species is unknown. Here we show that divergence in the pleiotropic floral regulator *APETALA1* (*AP1*) can account for the species-specific difference in petal number robustness. This large effect of *AP1* is explained by epistatic interactions: *A. thaliana AP1* confers robustness by masking the phenotypic expression of quantitative trait loci controlling petal number in *C. hirsuta*. We show that *C. hirsuta AP1* fails to complement this function of *A. thaliana AP1*, conferring variable petal number, and that upstream regulatory regions of *AP1* contribute to this divergence. Moreover, variable petal number is maintained in *C. hirsuta* despite sufficient standing genetic variation in natural accessions to produce plants with four-petalled flowers.
DOI: https://doi.org/10.7554/eLife.39399.001

***For correspondence:** hay@mpipz.mpg.de

[†]These authors contributed equally to this work

Present address: [‡]Laboratoire Reproduction et Développement des Plantes, Université de Lyon, Lyon, France; [§]Division of Plant Sciences, School of Life Science, University of Dundee at the James Hutton Institute, Scotland, United Kingdom; [#]Institut de Recherche en Biologie Végétale, Département de Sciences Biologiques, Université de Montréal, Montreal, Canada

Competing interests: The authors declare that no competing interests exist.

Funding: See page 20

Received: 23 June 2018
Accepted: 11 October 2018
Published: 18 October 2018

Reviewing editor: Sheila McCormick, University of California-Berkeley, United States

Introduction

Determining the genetic basis of developmental traits, and how these evolve to generate novelties, is a major goal of evolutionary developmental biology. Developmental systems are remarkably robust to natural perturbations, such that individuals tend to develop normally despite variation in the environment or their genetic make-up (***Wagner, 2005***). Therefore, a particular challenge is to understand the developmental transitions between the robust morphology of individuals within a species, and the variation in form between species.

Petal number is a robust trait in flowering plants and usually invariant within species and even higher taxonomic orders. For example, three petals are commonly found in monocots while five petals are characteristic of many core eudicots (***Endress, 2011***; ***Specht and Bartlett, 2009***). On the other hand, petal number is much more labile in basal angiosperms (***Endress, 2001***; ***Endress, 2011***; ***Specht and Bartlett, 2009***), suggesting that this trait was canalized during angiosperm evolution to produce a stable phenotype in the face of genetic and environmental perturbation. Petals are usually required to open the flower and to help attract pollinators (***Fenster et al., 2004***; ***van Doorn and Van Meeteren, 2003***), therefore a stable number of petals could ensure a reliable display of the reproductive organs and a reproducible cue for pollinators.

The model plant *Arabidopsis thaliana* belongs to the Brassicaceae family, which are commonly called crucifers after the cross-shaped arrangement of four petals in their flowers (***Endress, 1992***). Petals acquire their identity via the combined activity of A- and B-class floral organ identity genes, according to the ABC model of flower development (***Coen and Meyerowitz, 1991***). However, less is known about the genetic control of petal number. In *A. thaliana* flowers, initiation of four petals depends on the size of the floral meristem, the establishment of boundaries that demarcate the position of petal primordia on the floral meristem, the transient formation of auxin activity maxima in

eLife digest Many plants produce flowers that attract insects to land on them. Different insects are attracted to flowers of different shapes and colors. Therefore, it is generally advantageous for plants of the same species to produce flowers that look very similar.

For example, a small weed known as Arabidopsis – which is often used in research studies – produces little white flowers that all have four petals. Thus, the number of petals in Arabidopsis flowers is said to be a 'robust' trait. However, a closely-related plant called hairy bittercress produces flowers with any number of petals between zero and four. Studying the genetic differences between Arabidopsis and hairy bittercress can help to reveal why the numbers of petals on hairy bittercress flowers vary.

A gene called *APETALA1* helps to control how petals form. Monniaux, Pieper et al. found that Arabidopsis and hairy bittercress have different versions of this gene that determine whether the number of petals may vary between individual flowers. Inserting the Arabidopsis version of *APETALA1* into hairy bittercress plants caused the plants to produce flowers that had more similar numbers of petals to each other, that is, the petal number became more robust.

Monniaux, Pieper et al. then used a statistical method called quantitative trait locus analysis to identify the precise location of regions in the hairy bittercress genome that control petal number. This showed that the Arabidopsis version of *APETALA1*, but not the hairy bittercress version, conceals the action of these genes that could alter petal number.

These findings reveal that evolutionary change in a single gene of hairy bittercress unmasked the action of other genes that caused petal number to vary. A next step will be to identify some of these genes and understand how they control petal number.

DOI: https://doi.org/10.7554/eLife.39399.002

these positions, and the general mechanisms of lateral organ outgrowth (**Huang and Irish, 2015**; **Huang and Irish, 2016** ; **Irish, 2008**). Consistent with this complexity, few *A. thaliana* mutants specifically affect petal number; among them is *petal loss* (*ptl*), which displays a variable loss of petals caused by mutation of the *PTL* trihelix transcription factor (**Brewer et al., 2004**; **Griffith et al., 1999**). Other mutants pleiotropically affect petal number, such as mutations in the MADS-box transcription factor *APETALA1* (*AP1*), which shows floral meristem identity defects in addition to variable petal loss (**Irish and Sussex, 1990**; **Mandel et al., 1992**).

Cardamine hirsuta is a close relative of *A. thaliana* that lacks a robust phenotype of four petals (**Hay et al., 2014**). Instead, *C. hirsuta* flowers display a variable number of petals, between zero and four, on a single plant (**Monniaux et al., 2016**; **Pieper et al., 2016**). This phenotype varies in response to both environmental and genetic perturbation. *C. hirsuta* flowers show seasonal variation in petal number, with spring-flowering plants producing more petals than summer-flowering plants (**McKim et al., 2017**). Seasonal cues, such as day length, winter cold, and particularly ambient temperature, all influence the number of petals produced in *C. hirsuta* flowers (**McKim et al., 2017**). Furthermore, petal number is strongly influenced by natural genetic variation in *C. hirsuta*. A polygenic architecture of small to moderate effect quantitative trait loci (QTL), that shift the trait in both directions, contribute to petal number variation in *C. hirsuta* (**Pieper et al., 2016**). Alleles of large effect and low pleiotropy were identified in genetic screens for four-petalled mutants in *C. hirsuta*, but were not detected by QTL analysis in natural accessions (**Pieper et al., 2016**). Thus, the distribution of allelic effects found in natural populations of *C. hirsuta* is more likely to maintain variation, rather than robustness, in petal number.

Petal number varies both within and between species, evolving from a robust state of four petals, typified by *A. thaliana*, to a variable state in *C. hirsuta*. Phenotypic divergence between species is necessarily derived from variation within species, but identifying these evolutionary transitions is not a straight-forward task. This is because similar phenotypes that vary within and between species may or may not be caused by similar genetic mechanisms. For example, the same light-pigmentation alleles that are fixed in a yellow-bodied *Drosophila* species, segregate in a closely related brown-bodied species and contribute to clinal variation in its body colour (**Wittkopp et al., 2009**). However, in another example, genes responsible for leaf shape differences between *A. thaliana* and *C.*

hirsuta were not detected as leaf shape QTL in *C. hirsuta* (**Cartolano et al., 2015**). Therefore, to understand how petal number variation is produced and how it evolved, it is important to investigate both the genetic basis of variation within species and divergence between species. For example, to address questions such as: How many genes contribute to trait divergence between species? How large are their effects? Do they have pleiotropic functions? How do they interact with genes causing variation in natural populations?

A simple prediction about robust phenotypes, such as petal number in *A. thaliana*, is that they are invariant because genetic variation is reduced by stabilizing selection on the phenotype. On the other hand, a developmental pathway might be robust because certain alleles prevent the phenotypic effects of new mutations. This would effectively buffer the phenotype and hide underlying genetic variation. Previous studies of vulva development in *Caenorhabditis* (**Félix, 2007**), and eye development in cavefish (**Rohner et al., 2013**), support the latter view, showing that there is extensive, selectable genetic variation affecting robust phenotypes, which can be exposed by genetic or environmental perturbation. Moreover, studies that use gene expression as a trait, have mapped QTL that influence variance rather than mean expression level (**Hulse and Cai, 2013**), and identified selection acting on expression noise rather than mean level (**Metzger et al., 2015**). However, there are few examples (**Rohner et al., 2013**) where the genetic basis of morphological differences between species can be traced to the release of cryptic variation.

In this study, we investigate the evolutionary transition from a robust phenotype of four petals, typified by *A. thaliana*, to a variable petal number in *C. hirsuta*. We show that divergence in the pleiotropic floral regulator *AP1* can account for the difference in petal number robustness between species. This large effect of *AP1* is explained by epistatic interactions: *A. thaliana AP1* masks the phenotypic expression of all petal number QTL in *C. hirsuta* and, in this way, confers robustness. We show that *C. hirsuta AP1* fails to complement this function of *A. thaliana AP1*, conferring variable petal number, and that upstream regulatory regions of *AP1* contribute to this divergence.

Results

Petal number variation in *C. hirsuta* flowers

The flowers of *A. thaliana* and other Brassicaceae species are readily distinguished by their four petals. This phenotype is robust to natural genetic variation; for example, flowers from genetically diverse *A. thaliana* accessions consistently produce four petals (**Figure 1a**). *C. hirsuta* lacks this robustness and shows variation in petal number. For example, we found similar frequencies of each petal number between zero and four in flowers from 39 *C. hirsuta* accessions sampled from across the species range (**Figure 1b**) (**Hay et al., 2014**). Therefore, petal number varies within *C. hirsuta* and is a species-level trait that distinguishes *C. hirsuta* from *A. thaliana*.

Petals initiate in the second whorl of *A. thaliana* and *C. hirsuta* flowers, each positioned between two outer sepals, with the inner whorls being occupied by male and female reproductive organs (stamens and carpels) (**McKim et al., 2017**; **Smyth et al., 1990**). Small petal primordia are readily observed in the second whorl of *A. thaliana* floral buds, located between first-whorl sepals and third-whorl stamens (**Figure 1c,d**). In contrast to this, petal primordia were often missing in *C. hirsuta* flowers at similar developmental stages (**Figure 1e**). Instead, we observed a flat surface in the second whorl with no indication of outgrowths (**Figure 1f**). However, when we found petal primordia in *C. hirsuta* flowers, their development appeared indistinguishable from those in *A. thaliana* (**Figure 1—figure supplement 1**). These petals occupied any of the four positions available in the second whorl, with a slightly higher frequency in abaxial positions (**Figure 1—figure supplement 2**). Therefore, the number of petals in a *C. hirsuta* flower is determined at early stages of petal initiation and outgrowth.

Auxin activity maxima fail to form in whorl two of *C. hirsuta* floral meristems

To study the earliest stages of petal initiation, we tracked floral meristem development using time-lapse confocal laser scanning microscopy and analysed growth in these 4-dimensional image stacks (**Barbier de Reuille et al., 2015**). We followed the formation of auxin activity maxima during petal initiation in *A. thaliana* and *C. hirsuta* using the *DR5::VENUS* and *DR5v2::VENUS* auxin activity

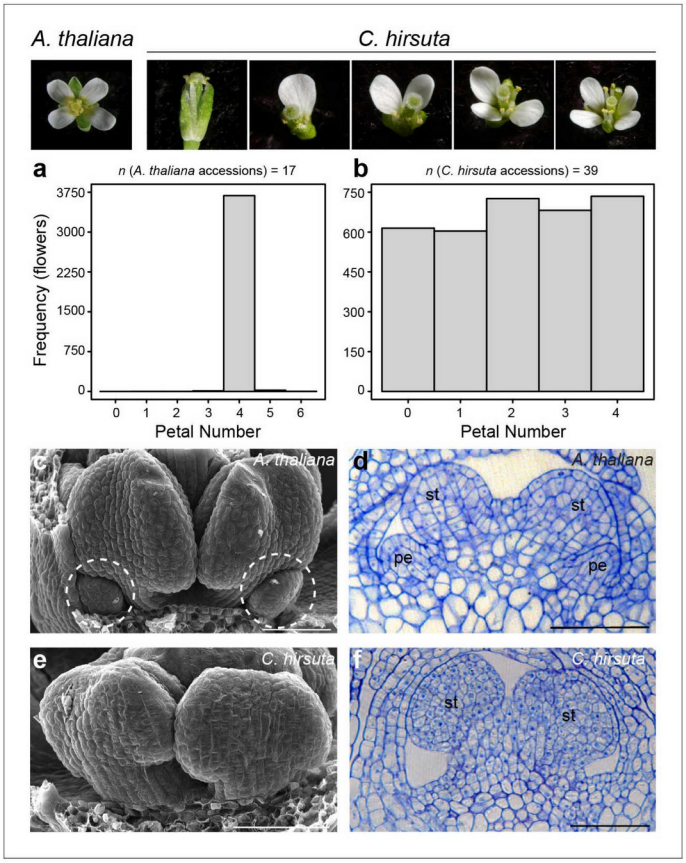

Figure 1. Petal number is robust in *A. thaliana* and variable in *C. hirsuta*. Four-petalled *A. thaliana* flower compared with *C. hirsuta* flowers containing 0, 1, 2, 3 or 4 petals. (**a, b**) Histograms showing petal number on the x-axis and frequency of flowers of the y-axis for (**a**) 17 *A. thaliana* accessions (*n* = 3725 flowers from 149 plants) and (**b**) 39 *C. hirsuta* accessions (*n* = 3362 flowers from 143 plants). (**c, e**) Scanning electron micrographs of stage eight flowers with covering sepals dissected away to show medial stamen primordia and small petal primordia (dashed circles) present in *A. thaliana* (**c**) and absent in *C. hirsuta* (**e**). (**d, f**) Longitudinal sections of stage eight flowers showing small petal primordia present in *A. thaliana* (**d**) and absent in *C. hirsuta* (**f**). Abbreviations: pe, petal; st, stamen. Scale bars: 20 μm (**c–f**).

DOI: https://doi.org/10.7554/eLife.39399.003

The following figure supplements are available for figure 1:

Figure supplement 1. Scanning electron micrograph of a *C. hirsuta* stage eight flower.

DOI: https://doi.org/10.7554/eLife.39399.004

Figure supplement 2. Petal position in *C. hirsuta* flowers (*n* = 144 flowers, flower numbers 1 – 25).

DOI: https://doi.org/10.7554/eLife.39399.005

sensors (***Barkoulas et al., 2008***; ***Heisler et al., 2005***; ***Liao et al., 2015***). At sites of petal initiation in *A. thaliana*, auxin activity maxima formed in 2 – 3 epidermal cells on the floral meristem flank prior to growth of these cells (***Figure 2a,b***; 83% *DR5::VENUS* observation rate, ***Figure 2—figure supplement 1***). However, in *C. hirsuta*, auxin activity maxima often failed to form on the floral meristem, and instead were either absent or aberrantly located in the first whorl between sepals (***Figure 2c,d***; 36% *DR5v2::VENUS* observation rate, ***Figure 2—figure supplement 1***). Therefore, four sites of petal

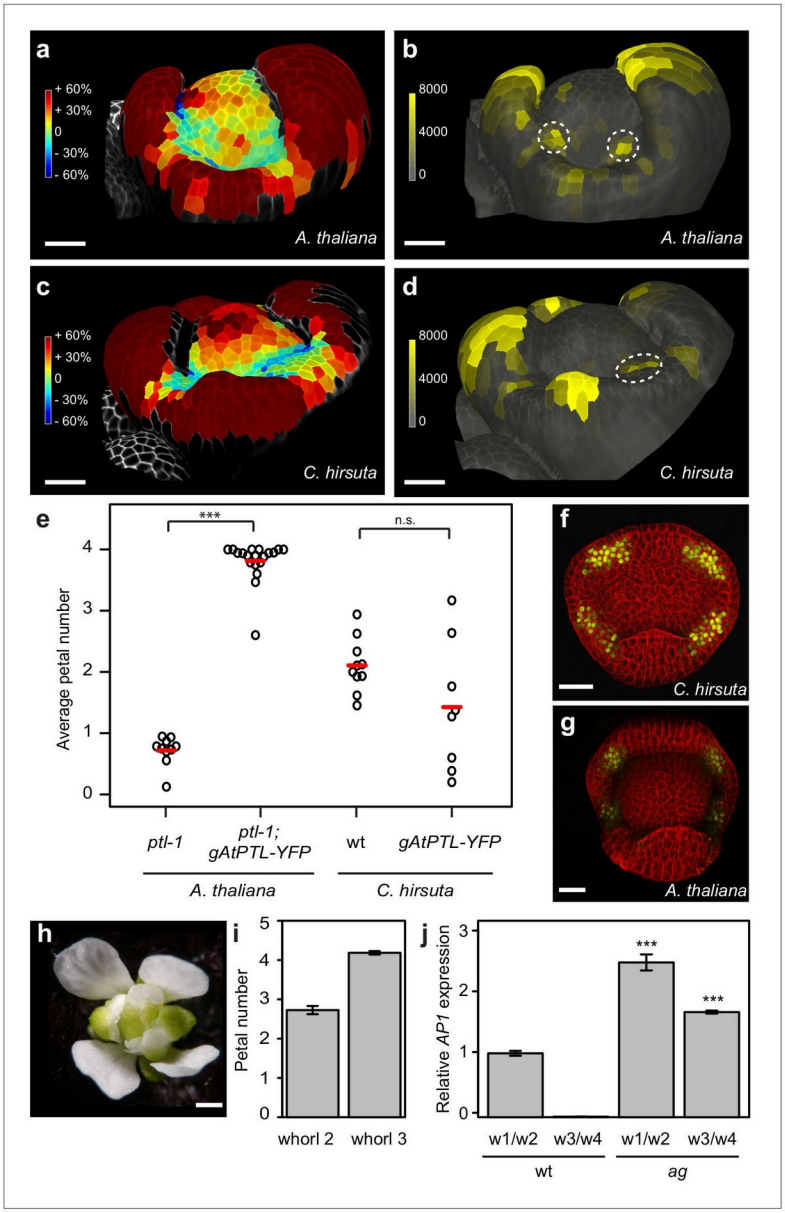

Figure 2. Auxin activity maxima fail to form in whorl two of *C. hirsuta* floral meristems. (**a–d**) Heat maps of change in relative cell area of floral primordia over 24 hr of growth (**a, c**) and surface projections of *DR5::VENUS* expression (**b, d**) in *A. thaliana* (**a, b**) and *C. hirsuta* (**c, d**). Colour bars: percentage increase (warm colours) and decrease (cool colours) of cell area (**a, c**) and signal intensity (yellow) in arbitrary units (**b, d**). Dashed circles indicate expression maxima that correspond to initiating petals. Floral primordia are shown in side view facing a lateral sepal. (**e**) Beeswarm plot of average petal number in *A. thaliana ptl-1* (n = 149 flowers, 10 plants) and *ptl-1; AtPTL::AtPTL:YFP* (n = 266 flowers, 19 independent insertion lines), and *C. hirsuta* Ox (n = 145 flowers, 10 plants) and *AtPTL::AtPTL:YFP* (n = 110 flowers, eight independent insertion lines). Red lines indicate means. (**f, g**) CLSM

Figure 2 continued on next page

Figure 2 continued

projections showing *AtPTL::AtPTL:YFP* expression (yellow) in the regions between sepals in stage 3–4 flowers of *C. hirsuta* (**f**) and *A. thaliana* (**g**). (**h**) *C. hirsuta ag* flower. (**i**) Barplot of mean petal number in whorls 2 and 3 of *C. hirsuta ag* flowers (n = 136 flowers, four plants). Note that mean stamen number is distributed between 4 – 5 in *C. hirsuta*, reflecting variation in lateral stamen number (***Hay et al., 2014***), and third whorl petals show similar variation in *ag*. (**j**) Relative expression of *C. hirsuta AP1* in floral organs pooled from whorls 1, 2 (w1/w2) and whorls 3, 4 (w3/w4), in Ox compared to *ag* flowers, determined by quantitative RT-PCR and reported as means of three biological replicates (Student's *t*-test: p<0.001). Error bars represent s.e.m. Scale bars: 20 μm (**a–d, f–g**), 0.5 mm (**h**).

DOI: https://doi.org/10.7554/eLife.39399.006

The following figure supplements are available for figure 2:

Figure supplement 1. CLSM time-lapse series of *DR5::VENUS* in *A. thaliana* and *DR5v2::VENUS* in *C. hirsuta* flowers.

DOI: https://doi.org/10.7554/eLife.39399.007

Figure supplement 2. Representative flowers.

DOI: https://doi.org/10.7554/eLife.39399.008

Figure supplement 3. In situ hybridization of *C. hirsuta PTL*.

DOI: https://doi.org/10.7554/eLife.39399.009

initiation are usually marked by auxin activity maxima in the second whorl of the floral meristem in *A. thaliana*, but not *C. hirsuta*.

The *ptl* mutant in *A. thaliana* mimics the variable petal number found in *C. hirsuta* and shows a similar distribution of auxin activity during petal initiation as wild-type *C. hirsuta* (***Figure 2d***) (***Griffith et al., 1999***; ***Lampugnani et al., 2013***). Therefore, we tested whether differences in *PTL* function could explain why petal number is robust in *A. thaliana* but variable in *C. hirsuta*. A functional fusion protein of *A. thaliana* PTL (AtPTL::AtPTL:YFP) was sufficient to restore four petals in the *ptl* mutant, but did not alter petal number when expressed in *C. hirsuta* (***Figure 2e***; ***Figure 2—figure supplement 2***). Given that AtPTL::AtPTL:YFP expressed correctly in the regions between sepals in *C. hirsuta* and *A. thaliana* flowers (***Figure 2f,g***), similar to the endogenous *PTL* transcripts in *C. hirsuta* and *A. thaliana* (***Figure 2—figure supplement 3***) (***Brewer et al., 2004***; ***Lampugnani et al., 2012***; ***Lampugnani et al., 2013***), these results indicate that differences in *PTL* function are unlikely to account for the variation in petal number between *C. hirsuta* and *A. thaliana*.

Petals are defined by both their identity and position within a flower. To test whether the variable number of petals in *C. hirsuta* is dependent on their identity or on the location where they arise in the second whorl, we used the homeotic mutant *agamous* (*ag*), to alter floral organ identity. In *C. hirsuta ag* mutants, four petals replaced the four stamens normally found in the third whorl of wild-type flowers, while petal number remained variable and lower than four in the second whorl (***Figure 2h,i***). This means that floral organs with petal identity show no variation in number if they arise outside the second whorl. As predicted by the ABC model (***Coen and Meyerowitz, 1991***), we found *AP1* ectopically expressed in third whorl petals of *ag* mutants in *C. hirsuta* (***Figure 2j***). Therefore, ectopic expression of *AP1* is associated with an invariant number of petals, whereas endogenous *AP1* expression in whorl two of the *C. hirsuta* floral meristem is associated with variable petal number.

A. thaliana AP1 confers robust petal number in *C. hirsuta* and masks natural variation

We reasoned that *AP1* might be a good candidate to contribute to petal number variation in *C. hirsuta*, particularly given that *ap1* mutants in both *C. hirsuta* and *A. thaliana* show variable petal loss (***Bowman et al., 1993***; ***Monniaux et al., 2017***). To test this possibility, we used a genomic construct of *A. thaliana AP1* (*AtAP1::AtAP1:GFP* (***Urbanus et al., 2009***)), which was sufficient to restore four petals in the *ap1* mutant (Mann-Whitney *U* test, p=1.07e-06) and eliminate the ectopic flowers that characterize the partial loss of floral meristem identity of *ap1* mutants (Mann-Whitney *U* test, p=2.92e-06; ***Figure 3a–c***). We found that this transgene was sufficient to convert *C. hirsuta* petal number from variable to robust, elevating petal number towards the *A. thaliana* value of four petals (pairwise Mann-Whitney *U* test with Bonferroni correction, p=2.4e-08; ***Figure 3a,d,e***). In contrast to

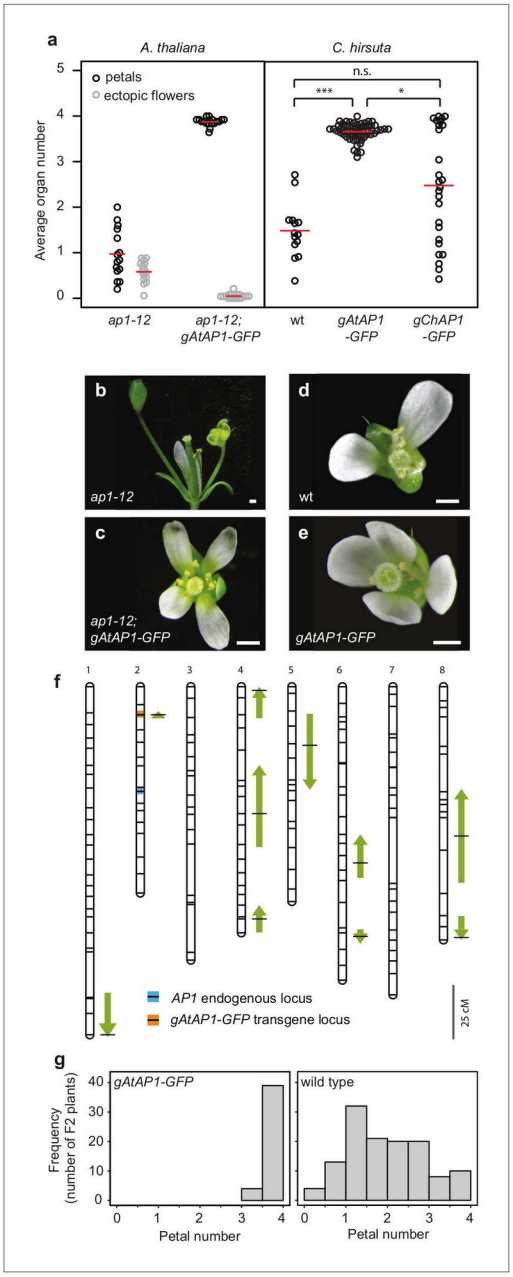

Figure 3. *A. thaliana AP1* confers robust petal number in *C. hirsuta* and masks natural variation. (**a**) Beeswarm plot of average petal number (black) and average number of ectopic flowers (grey) in *A. thaliana ap1-12* (*n* = 375 flowers, 15 plants) and *ap1-12; gAtAP1-GFP* (*AtAP1::AtAP1:GFP; n* = 472 flowers, 19 plants, two independent insertion lines), and average petal number (black) in *C. hirsuta* wild-type (wt; *n* = 331 flowers, 14 plants), *gAtAP1-GFP* (*n* = 1286 flowers, 57 plants, five independent insertion lines) and *gChAP1-GFP* (*ChAP1::ChAP1:GFP*) (*n* = 628

Figure 3 continued on next page

Figure 3 continued

flowers, 26 plants, two independent insertion lines). Red lines indicate means. Differences between *C. hirsuta* genotypes assessed by pairwise Mann-Whitney U test with Bonferroni correction: ***p=2.4e-08; *p=0.015; n.s. p=0.07. (**b–e**) Representative flowers of *A. thaliana ap1-12* (**b**), *ap1-12; gAtAP1-GFP* (**c**), and *C. hirsuta* wild type (**d**), *gAtAP1-GFP* (**e**). Scale bars: 0.5 mm. (**f**) QTL for average petal number detected in the *C. hirsuta* Ox *gAtAP1-GFP* × Nz F2 mapping population are shown as arrows on the 8 chromosomes of the genetic map. Positions with the most significant effects are indicated by horizontal black lines and the length of the arrows is scaled to the 2 (Log(p)) interval for each QTL. Arrow direction indicates whether the Ox allele for each QTL increases (upward pointing) or decreases (downward pointing) petal number. Positions of the *AP1* endogenous locus (blue line) and the *gAtAP1-GFP* transgene (orange line) are indicated on the genetic map. Scale bar: 25 cM. (**g**) Distribution of average petal number in plants of the Ox × Nz F2 population that segregate homozygous for the *gAtAP1-GFP* transgene (left histogram) or without the transgene (right histogram).

DOI: https://doi.org/10.7554/eLife.39399.010

this, the distribution of petal number remained variable in *C. hirsuta* lines expressing the endogenous *AP1* locus (*ChAP1::ChAP1:GFP*; pairwise Mann-Whitney *U* test with Bonferroni correction, p=0.07: ***Figure 3a***). This suggests that the function of the endogenous *AP1* locus to confer four petals is attenuated in *C. hirsuta*. Therefore, divergence in *AP1* function likely contributed to the variation in petal number between *A. thaliana* and *C. hirsuta*.

This raises the question whether petal number variation both between and within species may be caused by similar genetic changes. If *AP1* divergence contributed to petal number variation between species, do *AP1* polymorphisms contribute to this phenotype within *C. hirsuta*? To address this question, we inspected the locations of petal number QTL previously identified in five mapping populations derived from bi-parental crosses of different *C. hirsuta* accessions (***Pieper et al., 2016***), and an additional population constructed in this study (***Figure 3f***). We found that none of the QTL mapped to the *AP1* locus, which was represented by a specific genetic marker on chromosome 2 (***Figure 3f***, ***Table 1***) (***Pieper et al., 2016***). Therefore, allelic variation at *AP1* does not contribute to the quantitative variation in petal number mapped in *C. hirsuta*.

However, an alternative possibility is that *AP1* divergence indirectly caused petal number to vary within *C. hirsuta* by altering the robustness of this phenotype to genetic variation. Given that petal number is a canalized trait in *A. thaliana* and robust to genetic variation (***Figure 1a***), we hypothesized that *AP1* divergence may have decanalized petal number in *C. hirsuta*, giving phenotypic expression to formerly cryptic variation (***Figure 1b***) (***Félix, 2007***; ***Paaby and Rockman, 2014***). A key prediction of this hypothesis is that *A. thaliana AP1* should canalize petal number in *C. hirsuta* via

Table 1. *A. thaliana AP1* masks the effects of *C. hirsuta* petal number QTL

QTL	Chromosome	Position	QTL effects			
		(cM)	Wild-type plants		*gAtAP1* homozygous plants	
			additive	dominance	additive	dominance
Q1	1	147.8	−0.18	0.28	-	-
Q2 (*gAtAP1*)	2	11.9	n.a.	n.a.	n.a.	n.a.
Q3	4	1.6	-	0.32	-	-
Q4	4	53.9	−0.19	-	-	-
Q5	4	98.6	−0.33	-	-	-
Q6	5	25.7	0.28	-	-	-
Q7	6	74.8	−0.28	-	-	-
Q8	6	116.6	0.82	-	-	-
Q9	8	63.5	−0.27	-	-	-
Q10	8	105.6	0.38	-	-	-

n.a. – not available because the effects of all other QTL were determined conditional on zygosity at this QTL. '– '– No significant effect.

DOI: https://doi.org/10.7554/eLife.39399.011

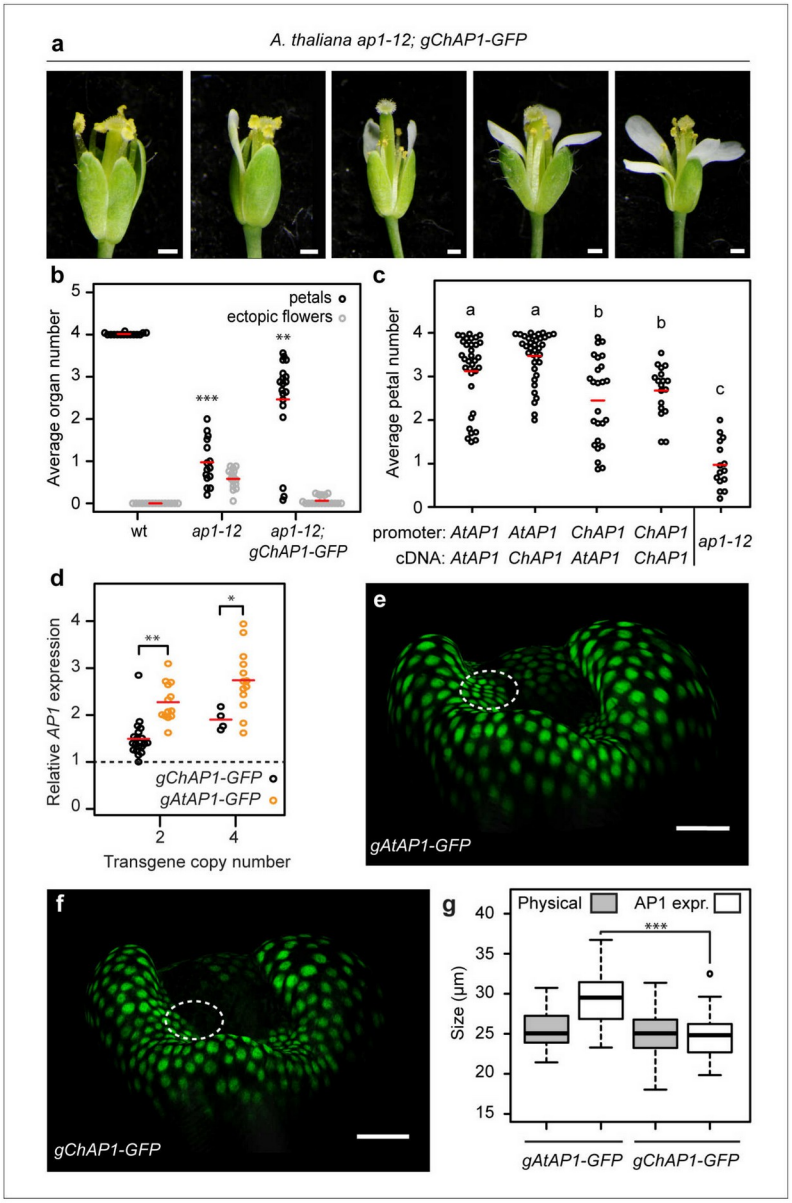

Figure 4. *AP1* divergence contributes to species-specific petal number. (**a**) *A. thaliana* flowers of *ap1-12; gChAP1-GFP* (*ChAP1::ChAP1:GFP*) genotype. (**b**) Beeswarm plot of average petal number (black) and average number of ectopic flowers (grey) in *A. thaliana* wild-type (*n* = 369 flowers, 15 plants), *ap1-12* (*n* = 375 flowers, 15 plants) and *ap1-12; gChAP1-GFP* (*n* = 598 flowers, 25 plants, two independent insertion lines). Red lines indicate means. Levene's test showed that the variance in petal number differed between wild-type and *ap1-12* (***p=5.588e-05) and wild-type and *ap1-12; gChAP1-GFP* (**p=0.005823), but not between *ap1-12* and *ap1-–12; gChAP1-GFP* (p=0.282). (**c**) Beeswarm plot of average petal number in *A. thaliana ap1-12* plants either untransformed or transformed with chimeric *AP1* constructs comprising the promoter sequences from either *AtAP1* (*A. thaliana*) or *ChAP1* (*C. hirsuta*) and the cDNA sequences from either *AtAP1* or *ChAP1*. A two-way ANOVA test on ranked data

Figure 4 continued on next page

Figure 4 continued

showed a significant effect of promoter sequence on petal number (p=9.45e-08) but no effect of coding sequence (p=0.103) and no interaction effect between the promoter and coding sequences (p=0.258). Post-hoc Tukey's HSD tests showed that *AP1* constructs containing the *A. thaliana* promoter had significantly higher petal number than those containing the *C. hirsuta* promoter, and all transgenic genotypes had higher petal number than *ap1-12* at 0.05 level of significance. *ap1-12: n* = 375 flowers, 15 plants; *ap1-12; pAtAP1::AtAP1: n* = 1454 flowers, 37 plants, 10 independent insertion lines; *ap1-12; pAtAP1::ChAP1: n* = 1414 flowers, 36 plants, nine independent insertion lines; *ap1-12; pChAP1::AtAP1: n* = 986 flowers, 25 plants, five independent insertion lines; *ap1-12; pChAP1::ChAP1: n* = 717 flowers, 18 plants, five independent insertion lines. (**d**) Beeswarm plot of relative *AP1* expression levels in inflorescences of *C. hirsuta* transgenic lines of *gChAP1-GFP* (black) and *gAtAP1-GFP* (orange) with 2 or four transgene copies. *AP1* expression is quantified by qRT-PCR in three biological replicates of each sample and expressed relative to *AP1* expression in wild-type inflorescences (dashed line). Relative *AP1* expression is higher for *gAtAP1-GFP* lines, both for two (Student's *t*-test, p<0.01) and four (p<0.05) transgene copies. *n* = 26 plants from six independent insertion lines for *gAtAP1-GFP*; n = 24 plants from five independent insertion lines for *gChAP1-GFP*. (**e–f**) Surface projections showing nuclear expression (green) of *gAtAP1-GFP* (**d**) and *gChAP1-GFP* (**e**) in stage 4 *C. hirsuta* flowers viewed from the lateral sepal. The dashed circle indicates the petal initiation domain on the floral meristem. (**g**) Boxplot of the size of inter-sepal regions (Physical) and the extent of AP1 expression along these transects into whorl 2 (AP1 expr) in *C. hirsuta* stage four floral meristems of *gAtAP1-GFP* and *gChAP1-GFP*. Size of the AP1 expression domain differs significantly between genotypes (Wilcoxon test, p<0.001; *n* = 7 samples each genotype) but physical size does not (p=0.44). Box and whiskers: quartiles, circles: outliers, black lines: median. Scale bars: 0.5 mm (**a**), 20 µm (**e, f**).

DOI: https://doi.org/10.7554/eLife.39399.012

The following figure supplements are available for figure 4:

Figure supplement 1. Quantification of ectopic flowers produced by chimeric *AP1* constructs complementing *A. thaliana ap1-12*.

DOI: https://doi.org/10.7554/eLife.39399.013

Figure supplement 2. Example of a time-lapse series for *AtAP1::AtAP1:GFP* and *ChAP1::ChAP1:GFP* flowers in *C. hirsuta*.

DOI: https://doi.org/10.7554/eLife.39399.014

Figure supplement 3. Quantitative image analysis of *C. hirsuta* stage-4 flower meristems expressing *AtAP1::AtAP1:GFP*.

DOI: https://doi.org/10.7554/eLife.39399.015

Figure supplement 4. Measurements of the physical boundary size and the AP1 expression boundary size (as defined in ***Figure 4—figure supplement 3***) in 7 samples of *AtAP1::AtAP1:GFP* and *ChAP1::ChAP1:GFP* stage-4 flowers in *C. hirsuta*.

DOI: https://doi.org/10.7554/eLife.39399.016

Figure supplement 5. Variability of measurements of the physical boundary size and the AP1 expression boundary size, as defined in ***Figure 4—figure supplement 3***.

DOI: https://doi.org/10.7554/eLife.39399.017

Figure supplement 6. Measurements of the lateral and median lengths of the flower and of the meristem, and the meristem area (as defined in ***Figure 4—figure supplement 3***) in 7 samples of *AtAP1::AtAP1:GFP* and *ChAP1::ChAP1:GFP* stage-4 flowers in *C. hirsuta*.

DOI: https://doi.org/10.7554/eLife.39399.018

Figure supplement 7. CLSM projections of *C. hirsuta* (**a**) and *A. thaliana* (**b**) stage four flowers co-expressing *gAtAP1-GFP* (green) and *gChAP1-RFP* (red).

DOI: https://doi.org/10.7554/eLife.39399.019

epistatic interactions with petal number QTL. We tested this genetic prediction in an F2 population created by crossing *C. hirsuta* Ox containing the *A. thaliana AP1* genomic locus (*AtAP1::AtAP1:GFP*), with the Nz accession (***Figure 3f***). We detected nine petal number QTL in addition to the *A. thaliana AP1* transgene locus (***Table 1***, ***Figure 3f***). Strikingly, the allelic effects of these 9 QTL were undetectable in the presence of the *A. thaliana AP1* genomic locus (***Table 1***). This epistasis was readily observed in the distribution of petal number between plants homozygous for the *A. thaliana AP1* transgene, which had four petals, and plants that lacked the transgene, which had variable petal number (***Figure 3g***). Thus, *A. thaliana AP1* canalized *C. hirsuta* petal number by masking the phenotypic effects of at least 9 QTL.

Changes in *AP1* expression contribute to species-specific petal number

Our findings suggest that the *AP1* genes from *A. thaliana* and *C. hirsuta* may have a differential ability to confer four petals. To test whether or not *C. hirsuta AP1* could fully complement the function of *A. thaliana AP1*, we introduced a *ChAP1::ChAP1:GFP* transgene into an *ap1* mutant background in *A. thaliana*. Rather than restoring four petals like *ap1-12; AtAP1::AtAP1:GFP* (**Figure 3a**), we found that the distribution of petal number remained variable in *ap1-12; ChAP1::ChAP1:GFP* flowers (homogeneity of variance accepted by Levene's test, p=0.282; **Figure 4a,b**), mimicking the variable petal number found in *C. hirsuta*. Petal number varied between zero and four, and the average petal number was significantly lower in *ap1* plants expressing the *AP1* genomic clone from *C. hirsuta* rather than *A. thaliana* (**Figures 3a** and **4a,b**, Mann-Whitney *U* test p=2.08e-07). In contrast, *ChAP1::ChAP1:GFP* expression was sufficient to reduce the ectopic flowers in *ap1* mutants (**Figure 4b**), indicating that *AP1* divergence between *C. hirsuta* and *A. thaliana* affected petal number independently of floral meristem identity. Therefore, the results of these gene swaps indicate that *C. hirsuta AP1* has a reduced ability to promote four petals when compared to *A. thaliana AP1*.

Next, we considered the relative contributions of regulatory and coding sequences to this species-specific difference in *AP1* function. To address this question, we expressed endogenous and chimeric versions of *A. thaliana* and *C. hirsuta AP1*, swapping the promoter and coding sequences, in an *ap1* mutant background in *A. thaliana*. We found that petal number was significantly elevated by the *A. thaliana AP1* promoter, compared to the *C. hirsuta AP1* promoter, irrespective of the *AP1* coding sequence driven by these promoters (**Figure 4c**). Whereas all constructs functioned equivalently to rescue the ectopic flowers found in *ap1* mutants (**Figure 4—figure supplement 1**). Therefore, functional differences in *AP1* that are responsible for petal number variation between *A. thaliana* and *C. hirsuta*, are more likely to reside in regulatory regions of the gene rather than coding sequences.

Species-specific *AP1* expression

Since upstream regulatory regions contributed to *AP1* divergence, we investigated whether expression differed between *C. hirsuta* and *A. thaliana AP1*. We reasoned that the reduced function of *C. hirsuta AP1* to promote four petals may reflect reduced levels of gene expression. To test this prediction, we compared *AP1* expression between *C. hirsuta* lines with matched copy numbers of either *AtAP1::AtAP1:GFP* or *ChAP1::ChAP1:GFP* transgenes, and found that expression levels were significantly lower in floral tissues of *ChAP1::ChAP1:GFP* than *AtAP1::AtAP1:GFP* lines (**Figure 4d**). To visualize the spatiotemporal dynamics of expression, we localized AP1::AP1:GFP fusion proteins from each species in the four-dimensional context of the growing *C. hirsuta* flower (**Figure 4—figure supplement 2**). In stage four floral buds, we observed *A. thaliana* AP1::AP1:GFP nuclear signal in the sepal whorl and on the flanks of the floral meristem, in the small regions where petals initiate in whorl two (**Figure 4e**). In contrast to this, *C. hirsuta* AP1::AP1:GFP was essentially restricted to the sepal whorl throughout stages 4 and 5 (**Figure 4f**, **Figure 4—figure supplement 2**). Using top-view, two-dimensional snapshots of these curved surface images, we measured how far the AP1::AP1:GFP signal extended into whorl two in each transgenic line (**Figure 4—figure supplements 3–5**). We found that the expression of *A. thaliana* AP1::AP1:GFP extended significantly further than *C. hirsuta* AP1::AP1:GFP (approximately 5 µm, **Figure 4g**). Moreover, we found no significant change in size or geometry between flowers expressing either the *A. thaliana* or *C. hirsuta AP1* genomic constructs (**Figure 4g**, **Figure 4—figure supplement 6**). This contrasts with the changes in growth and maturation of floral buds that are associated with the regulation of *C. hirsuta* petal number by seasonal changes in temperature (**McKim et al., 2017**). Therefore, the expression domain of *ChAP1::ChAP1:GFP* is reduced compared to *AtAP1::AtAP1:GFP*, comprising fewer cells in the petal whorl on the flanks of the floral meristem in *C. hirsuta*.

By co-localizing the expression of both *AtAP1::AtAP1:GFP* and *ChAP1::ChAP1:RFP* in stage 4 flowers of *C. hirsuta* and *A. thaliana*, we also found that *C. hirsuta* AP1::AP1:RFP expression is enriched in the regions between sepals (**Figure 4—figure supplement 7**). Since peaks of auxin activity are displaced away from the petal whorl to the region between sepals in *C. hirsuta* flowers (**Figure 2d**), and since distortions of this region have been shown to influence petal initiation in *A. thaliana* (**Baker et al., 2005**; **Lampugnani et al., 2012**; **Lampugnani et al., 2013**; **Laufs et al., 2004**;

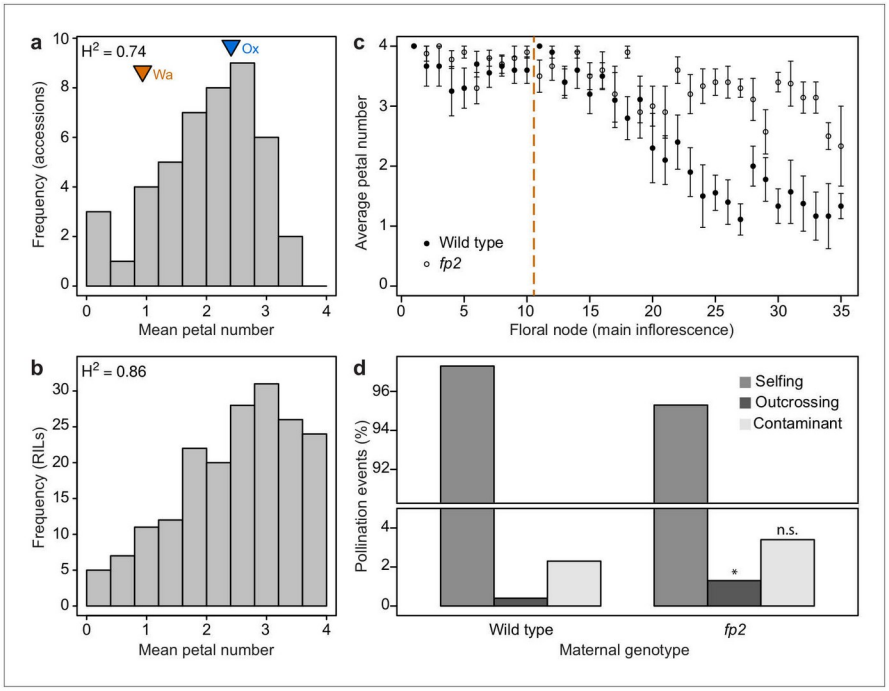

Figure 5. Petal number distributions differ between natural and experimental populations of *C. hirsuta* and outcrossing frequency associates with petal number. (**a–b**) Distributions of *C. hirsuta* petal number in 45 natural accessions (**a**) and a population of RILs derived from Ox and Wa accessions (b, reproduced from (***Pieper et al., 2016***)). Mean petal number of Ox and Wa are indicated in (**a**). (**c**) Average petal number (±s.e.m.) at every floral node in homozygous wild-type and *fp2* plants (genotyped at SNP:2:2905982) in field conditions (n = 10 plants from each genotype). Flowers 1–10 were removed from every plant (indicated by dashed line) since petal number in these flowers did not differ significantly between genotypes ($p>0.05$, Mann-Whitney U test). Seeds produced from remaining flowers on the main inflorescence were harvested. (**d**) Progeny of 10 wild-type and 10 *fp2* mothers were genotyped at SNP:2:2905982 to determine their paternity (n = 1703 wild-type and 1610 *fp2* seedlings). Pollination events were considered as selfing when the genotype of the progeny corresponded to the maternal genotype; outcrossing when the genotype of the progeny was heterozygous; and contaminant when the genotype of the progeny corresponded to the other parental genotype. These were likely seed contaminants from the outside of collection bags. Rates of outcrossing were significantly different between genotypes, $p<0.05$, whereas rates of contaminations were not $p>0.05$ (Chi-square test with Yates' continuity correction). Moreover, outcrossing and contaminations per parent plant were not correlated (r^2 = 0.025), suggesting that they are independent events.

DOI: https://doi.org/10.7554/eLife.39399.020

The following figure supplements are available for figure 5:

Figure supplement 1. Measurement of fitness traits in wild-type (Ox) and *AtAP1::AtAP1:GFP* plants.

DOI: https://doi.org/10.7554/eLife.39399.021

Figure supplement 2. Field experiment to paternity-test progeny of *C. hirsuta* wild-type and *four petals2* (*fp2*) genotypes.

DOI: https://doi.org/10.7554/eLife.39399.022

Mallory et al., 2004), the enrichment of *C. hirsuta AP1* in this domain might be relevant for petal number variation in *C. hirsuta*.

Maintaining variable petal number in *C. hirsuta*

Our findings suggest that petal number is a robust phenotype in *A. thaliana* that became decanalized in *C. hirsuta*, such that *AP1* divergence allowed previously cryptic loci to quantitatively affect petal number. Allelic variation at these QTL maintains the distribution of petal numbers found among natural accessions of *C. hirsuta* (***Pieper et al., 2016***). A striking feature of this distribution is the absence of natural accessions with four petals (***Figure 5a***). Moreover, few accessions have an

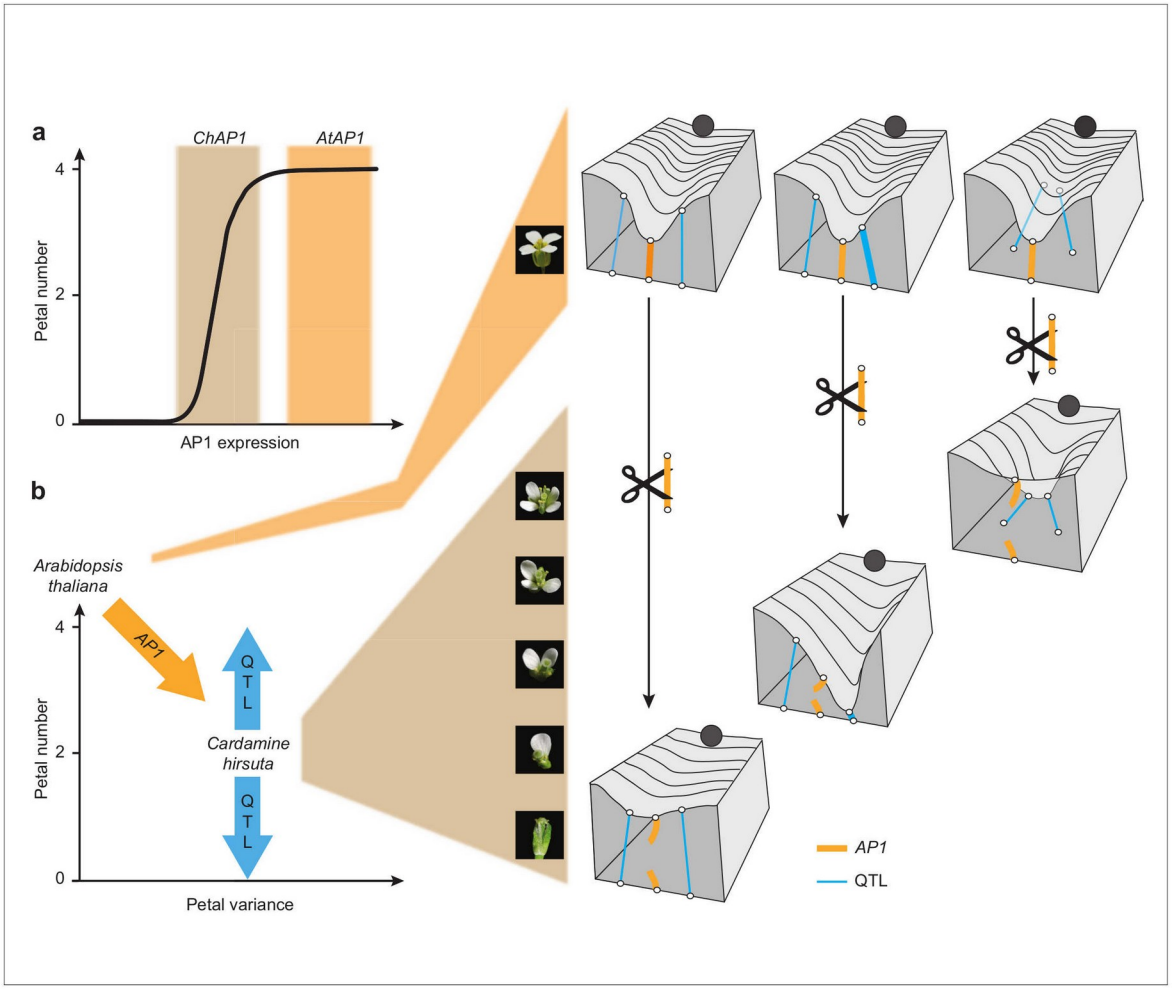

Figure 6. Cartoons depicting the proposed role of *AP1* in phenotypic buffering and canalization. (**a**) Non-linear relationship between *AP1* expression and petal number (black line). The range of *AtAP1* expression (orange) is within a zone of high phenotypic robustness, while the range of *ChAP1* expression (brown) is outside of this robust zone, such that petal number is sensitive to perturbations. (**b**) Left: decanalization of petal number in *C. hirsuta* from an invariant phenotype of four petals, typified by *A. thaliana*. *AP1* divergence (orange arrow) allowed phenotypic expression of QTL (blue arrows) in the *C. hirsuta* genome to quantitatively affect petal number. Right: cartoons of Waddington's landscape depicting petal number as a canalized phenotype in *A. thaliana* (ball rolls down path of least resistance shaped by canals in the landscape); this landscape is underpinned by a genetic network including *AP1* (orange rope) and QTL (blue ropes). Decanalization of petal number in *C. hirsuta* involved regulatory changes in *AP1* (cut orange rope) that relaxed its epistasis over QTL that cause petal number to vary (deformations in the landscape). Based on (***Waddington, 1957***; ***Paaby and Rockman, 2014***).

DOI: https://doi.org/10.7554/eLife.39399.023

average petal number approaching four (***Figure 5a***). To explore the genetic basis of this phenotypic distribution, we constructed experimental populations from founder accessions with phenotypes close to the mean (arrowheads, ***Figure 5a***). These recombinant inbred populations contained a high frequency of lines with high average petal numbers, including four petals (***Figure 5b***, and other examples in (***Pieper et al., 2016***)). This shows that there is sufficient standing genetic variation to produce phenotypes through recombination that are not observed in natural accessions.

To explore this finding, we reasoned that producing four-petalled flowers could incur an energetic cost. However, in standard growth conditions, we could not detect any difference in seed output between *C. hirsuta* wild-type and *AtAP1::AtAP1:GFP* plants that differed in petal number (***Figure 5—figure supplement 1***). Alternatively, variable petal number could be the cause or consequence of variation in other trait(s) that contribute to maintaining petal number within its variable range. Given that petals are responsible for the opening of most flowers (***van Doorn and Van Meeteren, 2003***), thus allowing cross-pollination, we tested whether petal number was associated with outcrossing rate in *C. hirsuta*. Using field conditions to grow two genotypes that differed significantly in petal number (2.65 ± 0.08 vs 3.45 ± 0.05, Mann-Whitney *U* test $p<0.001$; ***Figure 5c***, ***Figure 5—figure supplement 2***), we paternity-tested the progeny of these plants and found a significantly higher outcrossing rate in the genotype with higher petal number (Chi-square test $p<0.05$, Monte-Carlo permutation test $p<0.001$, ***Figure 5d***, ***Figure 5—figure supplement 2***). Therefore, outcrossing frequency is associated with petal number in *C. hirsuta*.

Discussion

In this study, we identified *AP1* as a gene of major effect in the evolutionary transition from a robust phenotype of four petals, typified by *A. thaliana*, to a variable petal number in *C. hirsuta*. Despite this large effect, *AP1* polymorphisms do not contribute directly to within-species variation in *C. hirsuta* petal number. Instead, the decanalization of petal number in *C. hirsuta* involved regulatory changes in *AP1* that relaxed its epistasis over alleles that cause petal number to vary. Therefore, our results suggest that *AP1* divergence likely exposed cryptic genetic variation in *C. hirsuta* that contributes directly to maintaining variable petal number within natural accessions of *C. hirsuta*.

AP1 is an important regulator of *A. thaliana* flower development, acting early to initiate flowers and later to specify floral organs (***Bowman et al., 1993***; ***Irish and Sussex, 1990***; ***Mandel et al., 1992***). It functions predominantly as a transcriptional repressor during floral initiation and later as an activator during sepal and petal initiation, and has been described as a 'true hub' in the gene regulatory network that initiates flower development (***Kaufmann et al., 2010***). We found that *AP1* genes from *A. thaliana* and *C. hirsuta* diverged in their ability to specify an invariant number of four petals. This difference mapped broadly to upstream regulatory rather than coding regions of *AP1*, and did not alter the function of *AP1* in flower initiation or sepal specification; suggesting that regulatory sequence divergence can disable specific linkages in gene regulatory networks while maintaining pleiotropic functions in other tissues (***Rebeiz and Tsiantis, 2017***).

We showed that differences in *AP1* expression are associated with the functional divergence in *AP1* between *A. thaliana* and *C. hirsuta*. Specifically, *C. hirsuta AP1* transcript levels are reduced in floral tissues and protein abundance is reduced in the small regions of stage four flowers where petals initiate. Robustness to variation in developmental systems is often a consequence of nonlinear dose-response curves between gene activity and phenotype (***Félix and Barkoulas, 2015***). For example, vulva development in *Caenorhabditis elegans* is robust to genetic variation in *lin-3* expression, such that 15–50 *lin-3* mRNA molecules defines a robust range that allows wild-type cell fate patterning, bounded by two thresholds, beyond which the phenotype varies (***Barkoulas et al., 2013***). We propose that the expression of *A. thaliana AP1* defines a robust range where petal number is buffered against perturbations (***Figure 6a***). *C. hirsuta AP1* is expressed below this threshold, such that petal number varies in response to genetic, environmental, and stochastic perturbations (***Figure 6a***) (***McKim et al., 2017***; ***Monniaux et al., 2016***; ***Pieper et al., 2016***).

Waddington's model of canalization invokes a similar concept of phenotypic buffering against natural variation. In his classical metaphor of marbles rolling down canals, he depicted the surface of the landscape being pulled down by guy ropes and fastened to anchors that represented genes (***Waddington, 1957***). Like this, the genetic underpinnings of the landscape may vary, but produce a consistent phenotype (e.g. *A. thaliana* petal number, ***Figure 6b***) (***Paaby and Rockman, 2014***). Petal number is invariant among natural accessions of *A. thaliana*, reflecting its robustness to genetic variation. However, we could change *A. thaliana* petal number to variable by complementing *ap1* mutants with the *AP1* genomic locus from *C. hirsuta*. These flowers mimicked the variable petal number found in *C. hirsuta*, suggesting that there may be variability in the gene regulatory network controlling petal number in *A. thaliana* that is hidden beneath the uniformity of wild-type development.

In *C. hirsuta*, petal number is decanalized, such that natural genetic variation deforms Waddington's landscape, producing a variable phenotype (**Figure 6b**). We mapped this natural variation to specific QTL in the *C. hirsuta* genome and showed that introducing the *A. thaliana AP1* locus masked the effects of all QTL. Therefore, petal number was effectively canalized in *C. hirsuta* via epistasis of *A. thaliana AP1* over existing QTL. Based on these results, we propose that *AP1* divergence perturbed the genetic equilibrium in *C. hirsuta* that confers petal number robustness. Given the large effect of the *A. thaliana AP1* locus on petal number, it is interesting that endogenous *AP1* polymorphisms do not contribute directly to petal number variation in *C. hirsuta*. Rather, it is the ability of *AP1* to exert epistasis over other loci that diverged between *A. thaliana* and *C. hirsuta* (**Figure 6b**). We propose that this change in genetic interactions was the likely mechanism by which cryptic variation was exposed in *C. hirsuta*, contributing to the evolution of variable petal number.

Materials and methods

Key resources table

Reagent type (species) or resource	Designation	Source or reference	Identifiers	Additional information
Gene (*Cardamine hirsuta*)	*AP1*	**Gan et al. (2016)**	CARHR062020	
Gene (*C. hirsuta*)	*PTL*	**Gan et al. (2016)**	CARHR209620	
Gene (*C. hirsuta*)	*AG*	**Gan et al. (2016)**	CARHR225900	
Gene (*C. hirsuta*)	*Clathrin/AP2M*	**Gan et al. (2016)**	CARHR174880	
Biological sample (*C. hirsuta*)	Ox	**Hay and Tsiantis (2006)**	herbarium specimen voucher Hay 1 (OXF)	
Biological sample (*Arabidopsis thaliana*)	Col-0		CS60000	
Genetic reagent (*A.thaliana*)	pDR5rev::3XVENUS-N7	**Heisler et al., 2005**		
Genetic reagent (*C. hirsuta*)	pDR5rev::3XVENUS-N7	**Barkoulas et al., 2008**		
Genetic reagent (*C. hirsuta*)	DR5-v2::3xVenus	**Liao et al., 2015**		
Genetic reagent (*A.thaliana*)	*ap1-12*	N6232		
Genetic reagent (*A.thaliana*)	*ptl-1*	N276		
Genetic reagent (*C. hirsuta*)	*ag-1*	this paper		EMS mutant
Genetic reagent (*C. hirsuta*)	*fp2*	**Pieper et al. (2016)**		
Genetic reagent (*A.thaliana*)	AtPTL::AtPTL:YFP	this paper		2.9 kb genomic sequence of PTL
Genetic reagent (*A.thaliana*)	AtPTL::AtPTL:YFP; ptl-1	this paper		2.9 kb genomic sequence of PTL
Genetic reagent (*C. hirsuta*)	AtPTL::AtPTL:YFP	this paper		2.9 kb genomic sequence of PTL
Genetic reagent (*A.thaliana*)	AtAP1::AtAP1:GFP	**Urbanus et al., 2009**		
Genetic reagent (*C. hirsuta*)	AtAP1::AtAP1:GFP	**Urbanus et al., 2009**		
Genetic reagent (*C. hirsuta*)	ChAP1::ChAP1:GFP	**Monniaux et al., 2017**		

Continued on next page

Continued

Reagent type (species) or resource	Designation	Source or reference	Identifiers	Additional information
Genetic reagent (*A. thaliana*)	ChAP1::ChAP1:GFP; ap1-12	**Monniaux et al., 2017**		
Genetic reagent (*A. thaliana*)	AtAP1::AtAP1:GFP; ap1-12	**Urbanus et al., 2009**		
Genetic reagent (*A. thaliana*)	ChAP1::ChAP1:RFP; AtAP1::AtAP1:GFP	this paper		6.6 kb genomic sequence of AP1
Genetic reagent (*C. hirsuta*)	ChAP1::ChAP1:RFP; AtAP1::AtAP1:GFP	this paper		6.6 kb genomic sequence of AP1
Genetic reagent (*A. thaliana*)	pAtAP1::AtAP1; ap1-12	this paper		2.9 kb promoter sequence of AP1 driving AP1 cDNA
Genetic reagent (*A. thaliana*)	pAtAP1::ChAP1; ap1-12	this paper		2.9 kb promoter sequence of AP1 driving AP1 cDNA
Genetic reagent (*A. thaliana*)	pChAP1::ChAP1; ap1-12	this paper		2.9 kb promoter sequence of AP1 driving AP1 cDNA
Genetic reagent (*A. thaliana*)	pChAP1::AtAP1; ap1-12	this paper		2.9 kb promoter sequence of AP1 driving AP1 cDNA
Genetic reagent (*C. hirsuta*)	Ox gAtAP1-GFP × Nz F2	this paper		312 individuals used for QTL analysis
Software	MorphoGraphX	**Barbier de Reuille et al., 2015**		

Accession numbers and plant material

The wild-type genotype in *C. hirsuta* is the reference Oxford (Ox) accession, herbarium specimen voucher Hay 1 (OXF) (**Hay and Tsiantis, 2006**), and in *A. thaliana*, the reference Col-0 accession. *DR5::VENUS* transgenic lines in *A. thaliana* (**Heisler et al., 2005**) and *C. hirsuta* (**Barkoulas et al., 2008**) have been described previously. NASC accession numbers for *A. thaliana* mutants: *ap1-12* (N6232), *ptl-1* (N276). Additional *A. thaliana* and *C. hirsuta* accessions have been described previously (**1001 Genomes Consortium. Electronic address: magnus.nordborg@gmi.oeaw.ac.at and 1001 Genomes Consortium, 2016**; **Hay et al., 2014**). *C. hirsuta* genome assembly gene identifiers: *ChAP1* (CARHR062020), *ChPTL* (CARHR209620), *ChAG* (CARHR225900), *Clathrin/AP2M* (CARHR174880) (**Gan et al., 2016**).

Plant growth conditions and petal number scoring

All plants were grown in long day conditions unless otherwise stated. Greenhouse: 16 hr light (22°C), 8 hr dark (20°C); controlled environment room long days: 16 hr light (21°C), 8 hr dark (20°C) and short days: 10 hr light (21°C), 14 hr dark (21°C); growth cabinet short days: 8 hr light (22°C), 16 hr dark (20°C). Petal number was generally scored on 10–15 plants from each genotype, except when scoring the T1 generation of transgenic lines. Flowers were scored every second day by removing them from the plant with tweezers, and observing them with a head band magnifier or stereo microscope. For the *C. hirsuta ag* mutant, flowers from four plants were removed every second day and scored with a binocular loop. Whorl one was removed to allow scoring of whorl two organs, which were then removed to score whorl three organs.

EMS mutagenesis and *ag* mutant isolation

C. hirsuta Ox seeds were mutagenized by agitation with ethyl methanesulfonate (EMS, Sigma), sown on soil, harvested as pools of five M1 plants, and M2 plants were screened for floral phenotypes as described previously (**Pieper et al., 2016**). The *four petals 2* (*fp2*) (**Pieper et al., 2016**) and *agamous* (*ag-1*) mutants were isolated and backcrossed twice to Ox. The *ag-1* sequence bears a C to T single nucleotide change predicted to convert a Gln residue to a stop codon and produce a truncated 33 AA protein. Expressing an *AtAG:GFP* translational fusion (gift from G. Angenent (**Urbanus et al., 2009**)) complemented the *C. hirsuta ag-1* mutant phenotype.

Quantitative RT-PCR (qPCR) and transgene copy number determination

Five and ten flowers from one plant of *C. hirsuta* wild-type and *ag-1*, respectively, were pooled to generate one biological replicate for RNA extraction. Three biological replicates were generated per genotype. For quantification of *AP1* expression levels in *C. hirsuta AtAP1::AtAP1:GFP* and *ChAP1::ChAP1:GFP* lines, a secondary inflorescence from 29 and 24 plants from five independent lines, respectively, was used for RNA extraction, together with three wild-type biological replicates. For these plants, transgene copy number was determined from genomic DNA by a Taqman qPCR assay using the Hygromycin resistance gene (IDna Genetics, Norwich, UK). RNA was extracted using Spectrum Plant Total RNA kit (Sigma) and DNA was digested by on-column DNase I digestion (Sigma). Reverse Transcription was performed with SuperScript III Reverse Transcriptase (ThermoFisher Scientific) using 1 µg of RNA template. Quantitative PCR was performed with the Power SYBR Green Master Mix (ThermoFisher Scientific) with the following primers: AP1-qPCR-F (5'- CCAGAGGCATTA TCTTGGGGAAGACTTG) and AP1-qPCR-R (5'- GCTCATTGATGGACTCGTACATAAGTTGGT) to amplify either *ChAP1* or *AtAP1*, and Clathrin-qPCR-F (5'- TCGATTGCTTGGTTTGGAAGATAAGA) and Clathrin-qPCR-R (5'- TTCTCTCCCATTGTTGAGATCAACTC) to amplify the reference gene *Clathrin/AP2M*. Expression was calculated with the ΔΔCt method (**Pfaffl, 2001**), normalized against the reference gene, and expressed relative to wild-type levels.

Transgenic plant construction

For the *AtPTL::AtPTL:YFP* construct, a 2.8 kb *PTL* promoter up to the second exon, driving functional *PTL* expression (**Lampugnani et al., 2012**), was amplified with primers pPTL-F (5'-ATATA TTGAGAAGAGATTAAAAACTTAG) and pPTL-R (5'-GTATCCATGTTCCTCGGACA) from Col-0 genomic DNA and cloned into the multiSite Gateway donor vector pDONR-P4-P1R. The full 2.9 kb genomic sequence of *PTL* was amplified with primers gPTL-F (5'-ATGGATCAAGATCAGCATC) and gPTL-R (5'-CTGATTCTCTTCTTTACTGAGC) from Col-0 genomic DNA and cloned into the multiSite Gateway donor vector pDONR-221. The *YFP* coding sequence was cloned into the multiSite Gateway donor vector pDONR-P2R-P3. The *AtPTL::AtPTL:YFP* construct was created by recombining together the three previous vectors into the pGII-0229 destination vector, as described in the MultiSite Gateway manual (Thermo Fisher Scientific). Eight and nineteen independent lines of *AtPTL::AtPTL:YFP* were generated in *C. hirsuta* wild type and *A. thaliana ptl-1* respectively. Petal number was scored on all independent lines in the T1 generation, together with *C. hirsuta* wild type and *A. thaliana ptl-1*.

Twenty independent lines of *AtAP1::AtAP1:GFP* (gift from G. Angenent (**Urbanus et al., 2009**)) were generated in *C. hirsuta* wild-type and *A. thaliana ap1-12* backgrounds. This translational fusion contains a 6.6 kb genomic fragment of *A. thaliana AP1* including 3 kb of regulatory sequence upstream of the translational start. *ChAP1::ChAP1:GFP* was previously described (**Monniaux et al., 2017**) and contains a comparable 6.6 kb genomic fragment of *C. hirsuta AP1*. Ten independent lines of *ChAP1::ChAP1:GFP* were generated in *C. hirsuta* wild type and *A. thaliana ap1-12*. For all the *AP1*-related lines, petal number was scored on 2 to 5 single-insertion homozygous T3 lines, together with wild-type *C. hirsuta* and *A. thaliana ap1-12*.

ChAP1::ChAP1:RFP was constructed in the modified destination vector pB7RWG2 (gift from M. Kater (**Gregis et al., 2009**)) by recombining the same *C. hirsuta AP1* genomic fragment used above. Six independent lines were generated in *A. thaliana AtAP1::AtAP1:GFP* for co-localisation studies. Four independent lines were generated in *C. hirsuta* and selected for strong expression in the third generation. Homozygous plants were crossed to an *AtAP1::AtAP1:GFP* strong expressing line for co-localisation studies.

The *pAtAP1::AtAP1*, *pAtAP1::ChAP1*, *pChAP1::AtAP1* and *pChAP1::ChAP1* constructs were generated by three-fragment multi-site Gateway in the pGII-0227 destination vector. The *AtAP1* and *ChAP1* promoters contain 2.9 kb upstream of the start codon and were amplified with primers pAtAP1-F (5'- CGAACGTGGTGGTTAGAAGA) and pAtAP1-R (5'-TTTTGATCCTTTTTTAAGAAAC TT), and primers pChAP1-F (5'-CATATAGCTTGGATCATGCTC) and pChAP1-R (5'-TTTGATCCTA TTTTGAGAAACTTCTT) respectively. Ten independent lines, with five plants per line, were scored for petal and ectopic flower number together with *A. thaliana* wild type and *ap1-12*. Lines with a clear *ap1-12* phenotype were considered not to be complemented by the transgene and were removed from the analysis.

The *DR5-v2::3xVENUS* plasmid was a gift from Dolf Weijers (**Liao et al., 2015**). Eleven independent insertion lines were generated in *C. hirsuta* wild type. All lines were checked for expression in the T1 generation and two representative lines were selected to image by time-lapse CLSM in the T2 generation.

All binary vectors were transformed into *C. hirsuta* or *A. thaliana* by *Agrobacterium tumefaciens* (strains GV3101 or C58)-mediated floral dip.

Scanning electron microscopy (SEM)

Shoot apices were induced to flower by a shift from short to long day conditions and fixed in FAA, post-fixed in osmium tetraoxide, dehydrated, critical point dried and dissected before coating with gold/palladium for viewing in a JSM-5510 microscope (JEOL). Floral primordia were staged according to (**Smyth et al., 1990**).

Confocal laser scanning microscopy (CLSM) and quantitative image analysis

Time-lapse imaging was performed using 4–5 week old plants grown on soil in long day conditions. The inflorescence was cut and flowers were dissected off to uncover young floral primordia at the shoot apex. Dissected shoots (around 0.5 cm long sections) were transferred to ½ MS medium supplemented with 1.5% plant agar, 1% sucrose and 0.1% Plant Preservative Mixture (Plant Cell Technology). To outline cells, samples were stained with 0.1% propidium iodide (PI, Sigma) for 2 – 5 min before each observation. Floral primordia were immersed in water and imaged from the top at 24 hr intervals. Confocal imaging was performed using a Leica SP8 up-right confocal microscope equipped with a long working-distance water immersion objective (L 40x/0.8 W) (Leica) and HyD hybrid detectors (Leica). Excitation was achieved using an argon laser with 514 nm for VENUS and PI. Images were collected at 526 – 545 nm for VENUS, and 600 – 660 nm for PI. Between imaging, samples were transferred to a growth cabinet and cultured in vitro in standard long day conditions at 20°C. Confocal image stacks of time-lapse series were analyzed using MorphoGraphX software (**Barbier de Reuille et al., 2015**; **Kierzkowski et al., 2012**). The outer 10 Full datasets of *A. thaliana* and *C. hirsuta* time-lapse series used to track growth and *DR5::VENUS* and *DR5v2::VENUS* expression shown in ***Figure 2—figure supplement 1***. To measure physical boundary size and size of AP1-GFP expression, the epidermal (2 to 5 µm) GFP signal was projected on the surface of the sample with MorphoGraphX. Top-view snapshots of the flower meristem with GFP-projected signal were acquired and subsequently analyzed with FiJi (**Schindelin et al., 2012**) as described in ***Figure 4—figure supplement 3***.

Histology and in situ hybridization

Shoot apices were induced to flower by a shift from short to long day conditions. Digoxigenin-labeled antisense RNA probes to *C. hirsuta ChPTL* were generated by mixing together three synthetic probes covering the whole *ChPTL* cDNA (GenScript HK Limited, USA). 8 – 10 µm inflorescence cross-sections were fixed, embedded in paraffin and hybridized with the *ChPTL* probe as previously described (**Vlad et al., 2014**). The signal was observed and images were acquired with a Zeiss AxioImager.M2 light microscope equipped with an Axiocam HR color camera. To cover the entire hybridization pattern in depth, images of two consecutive sections were registered and minimal projections generated using the image processing package Fiji (**Schindelin et al., 2012**). Cropping, gamma and colour correction were done using Photoshop CS5 and performed on entire images only. For semi-thin sections, apices were fixed in 2.5% glutaraldehyde in phosphate buffer, dehydrated, step-wise infiltrated with and embedded in TAAB Low Viscosity resin (TAAB) and 1.5 µm sections were stained with 0.05% toluidine blue.

Quantitative trait locus (QTL) analysis

QTL analysis of petal number was performed on a *C. hirsuta* F2 population derived from a cross between an *AtAP1::AtAP1:GFP* transgenic line in the Ox accession and the Nz accession. Petal number was quantified in 312 individuals that were pre-screened by PCR amplification of the *GFP* sequence such that approximately 1/4 of the plants were wild-type. The first 25 flowers on each plant were removed on the day they opened and petal number was counted using a dissecting

microscope. The 312 F2 plants were genotyped with 155 Sequenom markers (Welcome Trust Center for Human Genetics, High Throughput Genomics, Oxford, UK) designed to cover the whole genome according to an early version of the *C. hirsuta* genome assembly (**Gan et al., 2016**), and a dCAPS marker was generated for the *C. hirsuta AP1* locus using primers AP1cisF1 (5'-TCCCTAAAACCGC TCTTAGC) and AP1cisR1 (5'-AGAGAGATAAAGAAGAGTTCAGGC) and the restriction enzyme *Alu*I. The genetic map was made using JoinMap 4 (**Van Ooijen, 2006**), including the genotype for *AtAP1::AtAP1:GFP* as a dominant marker to determine the location of the transgene, and had a total length of 910 centiMorgans in eight linkage groups. QTL analyses were performed with Genstat 13th Edition (VSN International, Hemel Hempstead, UK) using all 312 F2 plants. Genetic predictors were calculated with a maximum distance of 2 cM between them from the molecular marker data and the genetic map. Average petal number per F2 plant was used as a phenotype for QTL analysis. Simple interval mapping and composite interval mapping were performed. The latter procedure was repeated several times while adding and/or removing cofactors until no further improvement could be made. The resulting set of 10 cofactors was used in a final QTL model to estimate QTL effects. A model with nine cofactors, when excluding the *AtAP1::AtAP1:*GFP locus, was fitted to data from F2 plants that were either homozygous for the *AtAP1::AtAP1:*GFP transgene or wild-type.

Field experiment and paternity testing of *C. hirsuta* wild type and *four petals 2* (*fp2*)

Seeds from Ox and *fp2* (**Pieper et al., 2016**) were stratified for 1 week at 4°C and sown on 15.03.2016 on hydrated Jiffy plugs. Seedlings were first grown in a greenhouse without temperature or light control, and later transferred to the field on 13.04.2016. More details on experimental design can be found in **Figure 5** and **Figure 5—figure supplement 2**. Genomic DNA was extracted from parent and progeny plants with Edwards Buffer and isopropanol precipitation and amplified with primers m458 (5'-GCCTAATCTTGCACAACACGAAATCT) and m459 (5'-GATTCTAAAGTTCTG TCAAAAGGAGAAACC**T**GA), designed with dCAPS Finder (http://helix.wustl.edu/dcaps/dcaps.html), to genotype SNP:2:2905982 by dCAPS. PCR was performed with Mango *Taq* polymerase (Bioline) under the following conditions: initial denaturation of 5 min at 95°C, 40 cycles of 30 s at 95°C, 30 s at 56°C and 30 s at 72°C, final extension of 10 min at 72°C. 1/5th volume of the reaction was digested with 2.5 units of *Dde*I (New England Biolabs) for 2 hr at 37°C and migrated on a 3% agarose gel to resolve the uncut 141 bp amplicon for *fp2*, and the two cut fragments of 116 bp and 25 bp for Ox.

Fitness measurements

40 plants of *C. hirsuta* wild type and a homozygous T4 line of *AtAP1::AtAP1:GFP* were grown in a greenhouse with standard conditions (20°C, long days). 20 of these plants were scored for petal number, and the other 20 were bagged carefully to recover all seeds. A fraction of the seeds was counted and weighed with the seed analyser MARVIN (GTA Sensorik GmbH) and total seed number was estimated by proportionality with the total seed weight.

Acknowledgements

We thank M Tsiantis for sharing unpublished *C. hirsuta* accessions and for helpful discussions and continuous support throughout this work. We thank P Huijser and R Berndtgen for assistance with *in situ* hybridisation, C Rojas for assistance with field experiments, W Faigl, G Angenent, M Kater, D Weijers and the Arabidopsis Biological Resource Center for materials, J Baker and M Kalda for photography, and S Laurent, M Abraham, and D Bailey for advice. This work was supported by Biotechnology and Biological Sciences Research Council grant BB/H01313X/1 to AH and Human Frontiers Science Program grant RGP0008/2013 to RS. AH was supported by a Royal Society University Research Fellowship and the Max Planck Society W2 Minerva programme, MM and SM by European Molecular Biology Organization Long Term Fellowships, SM by a National Science and Engineering Research Council of Canada Post-Doctoral Fellowship, and DK by Deutsche Forschungsgemeinschaft SFB 680 grant to M Tsiantis.

Additional information

Funding

Funder	Grant reference number	Author
Biotechnology and Biological Sciences Research Council	BB/H01313X/1	Angela Hay
Human Frontier Science Program	RGP0008/2013	Richard S Smith
Royal Society	University Research Fellowship	Angela Hay
Max-Planck-Gesellschaft	W2 Minerva Fellowship	Angela Hay
European Molecular Biology Organization	Long Term Fellowship	Marie Monniaux Sarah M McKim
Natural Sciences and Engineering Research Council of Canada	Post-Doctoral Fellowship	Sarah M McKim

The funders had no role in study design, data collection and interpretation, or the decision to submit the work for publication.

Author contributions

Marie Monniaux, Investigation, Visualization, Writing—original draft, Writing—review and editing; Bjorn Pieper, Investigation, Visualization, Writing—review and editing; Sarah M McKim, Daniel Kierzkowski, Investigation; Anne-Lise Routier-Kierzkowska, Investigation, Visualization; Richard S Smith, Supervision, Funding acquisition; Angela Hay, Conceptualization, Supervision, Funding acquisition, Investigation, Writing—original draft, Project administration, Writing—review and editing

Author ORCIDs

Marie Monniaux http://orcid.org/0000-0001-6847-3902
Bjorn Pieper http://orcid.org/0000-0002-0357-6254
Sarah M McKim http://orcid.org/0000-0002-8893-9498
Richard S Smith http://orcid.org/0000-0001-9220-0787
Angela Hay http://orcid.org/0000-0003-4609-5490

Decision letter and Author response

Decision letter https://doi.org/10.7554/eLife.39399.028
Author response https://doi.org/10.7554/eLife.39399.029

Additional files

Supplementary files

- Transparent reporting form

DOI: https://doi.org/10.7554/eLife.39399.024

Data availability

All data generated or analysed during this study are included in the manuscript and supporting files.

References

1001 Genomes Consortium. Electronic address: magnus.nordborg@gmi.oeaw.ac.at, 1001 Genomes Consortium. 2016. 1,135 genomes reveal the global pattern of polymorphism in *Arabidopsis thaliana*. *Cell* **166**: 481–491. DOI: https://doi.org/10.1016/j.cell.2016.05.063, PMID: 27293186

Baker CC, Sieber P, Wellmer F, Meyerowitz EM. 2005. The *early extra petals1* mutant uncovers a role for microRNA miR164c in regulating petal number in Arabidopsis. *Current Biology* **15**:303–315. DOI: https://doi.org/10.1016/j.cub.2005.02.017, PMID: 15723790

Barbier de Reuille P, Routier-Kierzkowska A-L, Kierzkowski D, Bassel GW, Schüpbach T, Tauriello G, Bajpai N, Strauss S, Weber A, Kiss A, Burian A, Hofhuis H, Sapala A, Lipowczan M, Heimlicher MB, Robinson S, Bayer EM, Basler K, Koumoutsakos P, Roeder AHK, et al. 2015. MorphoGraphX: a platform for quantifying morphogenesis in 4D. *eLife* **4**:e05864. DOI: https://doi.org/10.7554/eLife.05864

Barkoulas M, Hay A, Kougioumoutzi E, Tsiantis M. 2008. A developmental framework for dissected leaf formation in the Arabidopsis relative *Cardamine hirsuta*. *Nature Genetics* **40**:1136–1141. DOI: https://doi.org/10.1038/ng.189, PMID: 19165928

Barkoulas M, van Zon JS, Milloz J, van Oudenaarden A, Félix MA. 2013. Robustness and epistasis in the *C. elegans* vulval signaling network revealed by pathway dosage modulation. *Developmental Cell* **24**:64–75. DOI: https://doi.org/10.1016/j.devcel.2012.12.001, PMID: 23328399

Bowman JL, Alvarez J, Weigel D, Meyerowitz EM, Smyth DR. 1993. Control of flower development in *Arabidopsis thaliana* by *APETALA1* and interacting genes. *Development* **119**:721–743.

Brewer PB, Howles PA, Dorian K, Griffith ME, Ishida T, Kaplan-Levy RN, Kilinc A, Smyth DR. 2004. *PETAL LOSS*, a trihelix transcription factor gene, regulates perianth architecture in the Arabidopsis flower. *Development* **131**:4035–4045. DOI: https://doi.org/10.1242/dev.01279, PMID: 15269176

Cartolano M, Pieper B, Lempe J, Tattersall A, Huijser P, Tresch A, Darrah PR, Hay A, Tsiantis M. 2015. Heterochrony underpins natural variation in *Cardamine hirsuta* leaf form. *PNAS* **112**:10539–10544. DOI: https://doi.org/10.1073/pnas.1419791112, PMID: 26243877

Coen ES, Meyerowitz EM. 1991. The war of the whorls: genetic interactions controlling flower development. *Nature* **353**:31–37. DOI: https://doi.org/10.1038/353031a0, PMID: 1715520

Endress PK. 1992. Evolution and floral diversity: the phylogenetic surroundings of Arabidopsis and Antirrhinum. *International Journal of Plant Sciences* **153**:S106–S122. DOI: https://doi.org/10.1086/297069

Endress PK. 2001. Origins of flower morphology. *Journal of Experimental Zoology* **291**:105–115. DOI: https://doi.org/10.1002/jez.1063, PMID: 11479912

Endress PK. 2011. Evolutionary diversification of the flowers in angiosperms. *American Journal of Botany* **98**:370–396. DOI: https://doi.org/10.3732/ajb.1000299, PMID: 21613132

Félix MA. 2007. Cryptic quantitative evolution of the vulva intercellular signaling network in Caenorhabditis. *Current Biology* **17**:103–114. DOI: https://doi.org/10.1016/j.cub.2006.12.024, PMID: 17240335

Félix MA, Barkoulas M. 2015. Pervasive robustness in biological systems. *Nature Reviews Genetics* **16**:483–496. DOI: https://doi.org/10.1038/nrg3949, PMID: 26184598

Fenster CB, Armbruster WS, Wilson P, Dudash MR, Thomson JD. 2004. Pollination syndromes and floral specialization. *Annual Review of Ecology, Evolution, and Systematics* **35**:375–403. DOI: https://doi.org/10.1146/annurev.ecolsys.34.011802.132347

Gan X, Hay A, Kwantes M, Haberer G, Hallab A, Ioio RD, Hofhuis H, Pieper B, Cartolano M, Neumann U, Nikolov LA, Song B, Hajheidari M, Briskine R, Kougioumoutzi E, Vlad D, Broholm S, Hein J, Meksem K, Lightfoot D, et al. 2016. The Cardamine hirsuta genome offers insight into the evolution of morphological diversity. *Nature Plants* **2**:16167. DOI: https://doi.org/10.1038/nplants.2016.167, PMID: 27797353

Gregis V, Sessa A, Dorca-Fornell C, Kater MM. 2009. The Arabidopsis floral meristem identity genes *AP1*, *AGL24* and *SVP* directly repress class B and C floral homeotic genes. *The Plant Journal* **60**:626–637. DOI: https://doi.org/10.1111/j.1365-313X.2009.03985.x, PMID: 19656343

Griffith ME, da Silva Conceição A, Smyth DR. 1999. *PETAL LOSS* gene regulates initiation and orientation of second whorl organs in the Arabidopsis flower. *Development* **126**:5635–5644. PMID: 10572040

Hay A, Tsiantis M. 2006. The genetic basis for differences in leaf form between *Arabidopsis thaliana* and its wild relative *Cardamine hirsuta*. *Nature Genetics* **38**:942–947. DOI: https://doi.org/10.1038/ng1835, PMID: 16823378

Hay AS, Pieper B, Cooke E, Mandáková T, Cartolano M, Tattersall AD, Ioio RD, McGowan SJ, Barkoulas M, Galinha C, Rast MI, Hofhuis H, Then C, Plieske J, Ganal M, Mott R, Martinez-Garcia JF, Carine MA, Scotland RW, Gan X, et al. 2014. *Cardamine hirsuta*: a versatile genetic system for comparative studies. *The Plant Journal* **78**:1–15. DOI: https://doi.org/10.1111/tpj.12447, PMID: 24460550

Heisler MG, Ohno C, Das P, Sieber P, Reddy GV, Long JA, Meyerowitz EM. 2005. Patterns of auxin transport and gene expression during primordium development revealed by live imaging of the Arabidopsis inflorescence meristem. *Current Biology* **15**:1899–1911. DOI: https://doi.org/10.1016/j.cub.2005.09.052, PMID: 16271866

Huang T, Irish VF. 2015. Temporal control of plant organ growth by TCP transcription factors. *Current Biology* **25**:1765–1770. DOI: https://doi.org/10.1016/j.cub.2015.05.024, PMID: 26073137

Huang T, Irish VF. 2016. Gene networks controlling petal organogenesis. *Journal of Experimental Botany* **67**:61–68. DOI: https://doi.org/10.1093/jxb/erv444, PMID: 26428062

Hulse AM, Cai JJ. 2013. Genetic variants contribute to gene expression variability in humans. *Genetics* **193**:95–108. DOI: https://doi.org/10.1534/genetics.112.146779, PMID: 23150607

Irish VF, Sussex IM. 1990. Function of the *apetala-1* gene during Arabidopsis floral development. *The Plant Cell Online* **2**:741–753. DOI: https://doi.org/10.1105/tpc.2.8.741, PMID: 1983792

Irish VF. 2008. The Arabidopsis petal: a model for plant organogenesis. *Trends in Plant Science* **13**:430–436. DOI: https://doi.org/10.1016/j.tplants.2008.05.006, PMID: 18603466

Kaufmann K, Wellmer F, Muiño JM, Ferrier T, Wuest SE, Kumar V, Serrano-Mislata A, Madueño F, Krajewski P, Meyerowitz EM, Angenent GC, Riechmann JL. 2010. Orchestration of floral initiation by APETALA1. *Science* **328**:85–89. DOI: https://doi.org/10.1126/science.1185244, PMID: 20360106

Kierzkowski D, Nakayama N, Routier-Kierzkowska AL, Weber A, Bayer E, Schorderet M, Reinhardt D, Kuhlemeier C, Smith RS. 2012. Elastic domains regulate growth and organogenesis in the plant shoot apical meristem. *Science* **335**:1096–1099. DOI: https://doi.org/10.1126/science.1213100, PMID: 22383847

Lampugnani ER, Kilinc A, Smyth DR. 2012. *PETAL LOSS* is a boundary gene that inhibits growth between developing sepals in *Arabidopsis thaliana*. *The Plant Journal* **71**:724–735. DOI: https://doi.org/10.1111/j.1365-313X.2012.05023.x, PMID: 22507233

Lampugnani ER, Kilinc A, Smyth DR. 2013. Auxin controls petal initiation in Arabidopsis. *Development* **140**:185–194. DOI: https://doi.org/10.1242/dev.084582, PMID: 23175631

Laufs P, Peaucelle A, Morin H, Traas J. 2004. MicroRNA regulation of the *CUC* genes is required for boundary size control in Arabidopsis meristems. *Development* **131**:4311–4322. DOI: https://doi.org/10.1242/dev.01320, PMID: 15294871

Liao CY, Smet W, Brunoud G, Yoshida S, Vernoux T, Weijers D. 2015. Reporters for sensitive and quantitative measurement of auxin response. *Nature Methods* **12**:207–210. DOI: https://doi.org/10.1038/nmeth.3279, PMID: 25643149

Mallory AC, Dugas DV, Bartel DP, Bartel B. 2004. MicroRNA regulation of NAC-domain targets is required for proper formation and separation of adjacent embryonic, vegetative, and floral organs. *Current Biology* **14**:1035–1046. DOI: https://doi.org/10.1016/j.cub.2004.06.022, PMID: 15202996

Mandel MA, Gustafson-Brown C, Savidge B, Yanofsky MF. 1992. Molecular characterization of the Arabidopsis floral homeotic gene *APETALA1*. *Nature* **360**:273–277. DOI: https://doi.org/10.1038/360273a0, PMID: 1359429

McKim SM, Routier-Kierzkowska A-L, Monniaux M, Kierzkowski D, Pieper B, Smith RS, Tsiantis M, Hay A. 2017. Seasonal regulation of petal number. *Plant Physiology* **175**:00563. DOI: https://doi.org/10.1104/pp.17.00563

Metzger BP, Yuan DC, Gruber JD, Duveau F, Wittkopp PJ. 2015. Selection on noise constrains variation in a eukaryotic promoter. *Nature* **521**:344–347. DOI: https://doi.org/10.1038/nature14244, PMID: 25778704

Monniaux M, Pieper B, Hay A. 2016. Stochastic variation in *Cardamine hirsuta* petal number. *Annals of Botany* **117**:881–887. DOI: https://doi.org/10.1093/aob/mcv131, PMID: 26346720

Monniaux M, McKim SM, Cartolano M, Thévenon E, Parcy F, Tsiantis M, Hay A. 2017. Conservation vs divergence in *LEAFY* and *APETALA1* functions between *Arabidopsis thaliana* and *Cardamine hirsuta*. *The New Phytologist* **216**:549–561. DOI: https://doi.org/10.1111/nph.14419, PMID: 28098947

Paaby AB, Rockman MV. 2014. Cryptic genetic variation: evolution's hidden substrate. *Nature Reviews Genetics* **15**:247–258. DOI: https://doi.org/10.1038/nrg3688, PMID: 24614309

Pfaffl MW. 2001. A new mathematical model for relative quantification in real-time RT-PCR. *Nucleic Acids Research* **29**:e45. DOI: https://doi.org/10.1093/nar/29.9.e45, PMID: 11328886

Pieper B, Monniaux M, Hay A. 2016. The genetic architecture of petal number in *Cardamine hirsuta*. *New Phytologist* **209**:395–406. DOI: https://doi.org/10.1111/nph.13586, PMID: 26268614

Rebeiz M, Tsiantis M. 2017. Enhancer evolution and the origins of morphological novelty. *Current Opinion in Genetics & Development* **45**:115–123. DOI: https://doi.org/10.1016/j.gde.2017.04.006, PMID: 28527813

Rohner N, Jarosz DF, Kowalko JE, Yoshizawa M, Jeffery WR, Borowsky RL, Lindquist S, Tabin CJ. 2013. Cryptic variation in morphological evolution: HSP90 as a capacitor for loss of eyes in cavefish. *Science* **342**:1372–1375. DOI: https://doi.org/10.1126/science.1240276, PMID: 24337296

Schindelin J, Arganda-Carreras I, Frise E, Kaynig V, Longair M, Pietzsch T, Preibisch S, Rueden C, Saalfeld S, Schmid B, Tinevez JY, White DJ, Hartenstein V, Eliceiri K, Tomancak P, Cardona A. 2012. Fiji: an open-source platform for biological-image analysis. *Nature Methods* **9**:676–682. DOI: https://doi.org/10.1038/nmeth.2019, PMID: 22743772

Smyth DR, Bowman JL, Meyerowitz EM. 1990. Early flower development in Arabidopsis. *The Plant Cell Online* **2**:755–767. DOI: https://doi.org/10.1105/tpc.2.8.755, PMID: 2152125

Specht CD, Bartlett ME. 2009. Flower evolution: the origin and subsequent diversification of the angiosperm flower. *Annual Review of Ecology, Evolution, and Systematics* **40**:217–243. DOI: https://doi.org/10.1146/annurev.ecolsys.110308.120203

Urbanus SL, de Folter S, Shchennikova AV, Kaufmann K, Immink RG, Angenent GC. 2009. In planta localisation patterns of MADS domain proteins during floral development in *Arabidopsis thaliana*. *BMC Plant Biology* **9**:5. DOI: https://doi.org/10.1186/1471-2229-9-5, PMID: 19138429

van Doorn WG, Van Meeteren U. 2003. Flower opening and closure: a review. *Journal of Experimental Botany* **54**:1801–1812. DOI: https://doi.org/10.1093/jxb/erg213, PMID: 12869518

Van Ooijen JW. 2006. *Joinmap 4 Software for the Calculation of Genetic Linkage Maps in Experimental Populations*. Wageningen, Netherlands: Kyazma B.V.

Vlad D, Kierzkowski D, Rast MI, Vuolo F, Dello Ioio R, Galinha C, Gan X, Hajheidari M, Hay A, Smith RS, Huijser P, Bailey CD, Tsiantis M. 2014. Leaf shape evolution through duplication, regulatory diversification, and loss of a homeobox gene. *Science* **343**:780–783. DOI: https://doi.org/10.1126/science.1248384, PMID: 24531971

Waddington CH. 1957. *The Strategy of the Genes; a Discussion of Some Aspects of Theoretical Biology*. London: Allen & Unwin.

Wagner A. 2005. *Robustness and Evolvability in Living Systems*. Princeton, NJ, USA: Princeton University Press.

Wittkopp PJ, Stewart EE, Arnold LL, Neidert AH, Haerum BK, Thompson EM, Akhras S, Smith-Winberry G, Shefner L. 2009. Intraspecific polymorphism to interspecific divergence: genetics of pigmentation in Drosophila. *Science* **326**:540–544. DOI: https://doi.org/10.1126/science.1176980, PMID: 19900891

Key Publication 3

Cell layer-specific expression of the B-class MADS-box gene *PhDEF* drives petal tube or limb development in petunia flowers

Chopy M.[1,2], Cavallini-Speisser Q.[1], Chambrier P.[1], Morel P.[1], Just J.[1], Hugouvieux V.[3], Rodrigues Bento S.[1], Zubieta C.[3], Vandenbussche M.[1,*] and Monniaux M.[1,*]

[1] Laboratoire de Reproduction et Développement des Plantes, Université de Lyon, ENS de Lyon, UCB Lyon 1, CNRS, INRAE, 69007 Lyon, France.

[2] Current address: Institute of Plant Sciences, University of Bern, Altenbergrain 21, Bern, CH-3013, Switzerland.

[3] Laboratoire de Physiologie Cellulaire et Végétale, Université Grenoble-Alpes, CNRS, CEA, INRAE, IRIG-DBSCI, 38000 Grenoble, France.

* Authors for correspondence: michiel.vandenbussche@ens-lyon.fr, marie.monniaux@ens-lyon.fr

ABSTRACT

Floral homeotic MADS-box transcription factors ensure the correct development of floral organs with all their mature features, i.e. organ shape, size, colour and cellular identity. Furthermore, all plant organs develop from clonally-independent cell layers, deriving from the meristematic epidermal (L1) and internal (L2 and L3) layers. How cells from these distinct layers acquire their floral identities and coordinate their growth to ensure reproducible organ development is unclear. Here we study the development of the *Petunia x hybrida* (petunia) corolla, which consists of five fused petals forming a tube and pigmented limbs. We present petunia flowers expressing the B-class MADS-box gene *PhDEF* in the epidermis or in the mesophyll of the petal only, that we called wico and star respectively. Strikingly, the wico flowers form a very small tube while their limbs are almost normal, and the star flowers form a normal tube but very reduced and unpigmented limbs. Therefore, the star and wico phenotypes indicate that in the petunia petal, the epidermis mainly drives limb growth and pigmentation while the mesophyll mainly drives tube growth. As a first step towards the identification of candidate genes involved in specification of petal layer identities and tube/limb development, we sequenced the star and wico whole petal transcriptome at three developmental stages. Among downregulated genes in star petals, we found the major regulator of anthocyanin biosynthesis *ANTHOCYANIN 1 (AN1),* and we showed that, *in vitro*, PhDEF directly binds to its terminator sequence, suggesting that it might regulate its expression. Altogether this study shows that layer-specific expression of *PhDEF* drives petunia tube or limb development in a highly modular fashion, which adds an extra layer of complexity to the petal development process.

INTRODUCTION

All plant aerial organs derive from clonally-distinct layers, named L1, L2 and L3 in the shoot apical meristem (SAM) (Satina et al., 1940). Within the L1 and L2 layers, cells divide anticlinally, thereby maintaining a clear layered structure in all aerial organs produced by the SAM (Meyerowitz, 1997; Stewart and Burk, 1970; Scheres, 2001). Already at the meristematic stage, cell layers express different genes and thereby have their own identity (Yadav et al., 2014). For flower formation, floral organ identity will be appended on top of layer identity by the combinatorial expression of homeotic floral genes, most of which are MADS-box genes (Coen and Meyerowitz, 1991; Schwarz-Sommer et al., 1990). How these master floral regulators specify all floral organ features, such as organ size, shape, pigmentation, and cellular characteristics, while maintaining layer-specific features, remains unknown.

Petals are often the most conspicuous organs of the flower, and they display a tremendous diversity in size, shape and pigmentation across flowering plants (Moyroud and Glover, 2017). Floral organ identity is specified by a combination of A-, B- and C-class identity genes as proposed by the classical ABC model established on *Arabidopsis thaliana* (Arabidopsis) and *Antirrhinum majus* (snapdragon), and B-class genes are particularly important for petal identity (Coen and Meyerowitz, 1991; Schwarz-Sommer et al., 1990). B-class proteins, belonging to MADS-box transcription factors, are grouped in the DEF/AP3 and the GLO/PI subfamilies, named after the snapdragon/Arabidopsis B-class proteins DEFICIENS/APETALA3 and GLOBOSA/PISTILLATA (Purugganan et al., 1995; Theißen et al., 1996). These proteins act as obligate heterodimers consisting of one DEF/AP3 and one GLO/PI protein, and this complex activates its own expression for maintenance of high expression levels all along petal and stamen development (Tröbner et al., 1992). In petunia, gene duplication has generated four B-class genes, namely *PhDEF* and *PhTM6* belonging to the *DEF/AP3* subfamily, and *PhGLO1* and *PhGLO2* belonging to the *GLO/PI* subfamily (Vandenbussche et al., 2004; Rijpkema et al., 2006; van der Krol et al., 1993; Angenent et al., 1992). Mutating the two members of each subfamily (*phdef phtm6* or *phglo1 phglo2* double mutants) produces a classical B-function mutant phenotype with homeotic transformation of petals into sepals and stamens into carpels (Vandenbussche et al., 2004; Rijpkema et al., 2006). Additionally, gene copies within the *DEF/AP3* subfamily have subfunctionalized: while *PhDEF* exhibits a classical B-class expression pattern largely restricted to developing petals and stamens, atypically *PhTM6* is mainly expressed in stamens and carpels, and its upregulation depends on the petunia C-function genes (Rijpkema et al., 2006; Heijmans et al., 2012). As a consequence, the single *phdef* mutant displays a homeotic conversion of petals into sepals, while the stamens are

unaffected due to redundancy with *PhTM6* (Rijpkema et al., 2006). The petunia *phdef* mutant is therefore an interesting model to study the mechanism of petal identity specification alone since it displays a single-whorl complete homeotic transformation, which is quite rare for floral homeotic mutants that generally show defects in two adjacent whorls.

Flowers from the *Petunia* genus develop five petals, that arise as individual primordia and fuse congenitally. Mature petals are fully fused and the corolla is organized in two distinct domains: the tube and the limbs. Variation in the relative size of these subdomains of the corolla are observed between wild species of *Petunia*, where flowers with a long tube grant nectar access to long-tongued hawkmoths or hummingbirds, while wide and short tubes are easily accessible to bees (Galliot et al., 2006). The short- and long-tube species cluster separately on a phylogeny made from 20 wild *Petunia* species, and the short-tube phenotype is likely the ancestral one (Reck-Kortmann et al., 2014). Pollinator preference assays and field observations have confirmed that tube length and limb size are discriminated by pollinators and thereby might play a role in reproductive isolation, together with multiple other traits of the pollination syndromes such as limb pigmentation (Venail et al., 2010; Hoballah et al., 2007; Galliot et al., 2006).

Although the petunia petal tube and limbs seem to play important ecological roles, the mechanisms driving their development are mostly unknown. Tube and limb develop as relatively independent entities in flowers from the Solanaceae family, to which petunia belongs: for instance, tube length and limb width are uncorrelated traits in intra-specific crosses performed in *Nicotiana* and *Jaltomata* (Bissell and Diggle, 2008; Kostyun et al., 2019). Moreover, tube and limb identities can be acquired independently: this is strikingly observed in the petunia *blind* mutant, a partial A-class mutant, that forms an almost wild-type tube topped by functional anthers (Cartolano et al., 2007). Apart from the petal identity genes, the molecular players involved in petunia tube or limb growth are mostly unknown. General growth factors affect petal development as a whole (both tube and limbs) together with other vegetative or reproductive traits (Vandenbussche et al., 2009; Terry et al., 2019; Brandoli et al., 2020), but to our knowledge, only one gene has been found to specifically affect growth of one subdomain of the petal: downregulation of *PhEXP1*, encoding an α-expansin expressed in petunia petal limbs, leads to a specific decrease in limb area without affecting tube length (Zenoni et al., 2004). Therefore, the mechanisms of petunia tube and limb growth remain to be fully explored. In contrast, the genetic and molecular bases of petunia petal pigmentation are extremely well characterized, thanks to the plethora of mutants that have been isolated over decades of breeding and research (Bombarely et al., 2016; Tornielli et al., 2009). Petunia limb pigmentation is mainly due to the presence of anthocyanins in the vacuole of epidermal cells. Briefly, the earliest steps of anthocyanin production are ensured by a MBW

regulatory complex composed of ANTHOCYANIN1 (AN1, a bHLH transcription factor), AN11 (a WD-repeat protein) and an R2R3-MYB transcription factor (either AN2, AN4, DEEP PURPLE or PURPLE HAZE), which drives the expression of anthocyanin biosynthesis enzymes and proteins involved in vacuolar acidification of epidermal cells (Koes et al., 2005; Albert et al., 2011). How this pathway is activated, after regulators such as PhDEF have specified petal identity, has not been determined so far.

In this work, we present petunia flowers with strongly affected tube or limb development, that we respectively named wico and star, and that spontaneously arose from plants mutant for *PhDEF*. We provide genetic and molecular evidence that these contrasting flower phenotypes both are periclinal chimeras, resulting from the layer-specific transposon excision of the *phdef-151* allele, restoring *PhDEF* activity either in the epidermis or in the mesophyll of the petal. The star and wico phenotypes indicate that in the petunia petal, the epidermis mainly drives limb growth and pigmentation while the mesophyll mainly drives tube growth. This is seemingly different from previous studies in *Antirrhinum majus* flowers, where *def* periclinal chimeras led the authors to conclude that epidermal *DEF* expression was making a major contribution to petal morphology (Perbal et al., 1996; Vincent et al., 2003; Efremova et al., 2001). We characterized in detail the star and wico petal phenotypes at the tissue and cellular scale, and found evidence for non-cell-autonomous effects affecting cell identity between layers. We sequenced the total petal transcriptome from wild-type, wico and star flowers at three developmental stages, and we found that a large proportion of the genes involved in anthocyanin production were downregulated in star petal samples, as could be expected from their white petals. We further showed that PhDEF directly binds *in vitro* to the terminator region of *AN1,* thereby possibly regulating its expression and triggering the early steps of limb pigmentation. Our results and our unique star and wico material promise to improve our understanding of tube and limb development in petunia, and address the broader question of how organ identity and cell layer identity superimpose during organ development.

Results

Spontaneous appearance of two phenotypically distinct classes of partial revertants from the *phdef-151* locus

Previously described null alleles for the *PhDEF* gene (also named *GP* or *pMADS1*) were obtained by either ethyl methanesulfonate (EMS) mutagenesis (de Vlaming et al., 1984; Rijpkema et al., 2006) or by γ-radiation (van der Krol et al., 1993). In our sequence-indexed *dTph1* transposon mutant population in the W138 genetic background (Vandenbussche et al., 2008), we identified a new mutant allele of *PhDEF*, named *phdef-151*, referring to the *dTph1* insertion position 151 bp downstream of the ATG in first exon of the *PhDEF* gene, disrupting the MADS-domain. As observed for previously identified *phdef* null alleles, *phdef-151* flowers display a complete homeotic conversion of petals into sepals (Fig. 1A-D). *phdef-151* is thus very likely a null mutant allele.

While growing homozygous *phdef-151* individuals during several seasons, we repeatedly observed the spontaneous appearance of inflorescence side branches that developed flowers with a partial restoration of petal development (Fig. 1E-H, Fig. S1). Interestingly, these partially revertant flowers could be classified as belonging to either one of two contrasting phenotypic classes, that we named star and wico. For both phenotypic classes, we obtained more than 10 independent reversion events. The star flowers (Fig. 1E, F), named in reference to their star-shaped petals, grow an elongated tube similar to wild-type flowers, but their limbs are underdeveloped: they appear to mainly grow around the mid-vein with reduced lateral expansion, hence losing the typical round shape of wild-type limbs. Moreover, they do not display pigmentation, apart from occasional red sectors (Fig. S1B-F). We quantified these changes in flower morphology and found that total limb area was reduced almost 5-fold in star flowers (Fig. 1K). In contrast total tube length was only slightly reduced in star as compared to wild type (Fig. 1J), and this was mainly due to a reduction in length of domain D1, corresponding to the part of the tube fused with stamens (as defined in (Stuurman et al., 2004), Fig. 1I), while length of the rest of the tube (domain D2) remained unchanged (Fig. 1J, Fig. S2). As a result, the ratio between limb area and tube length, which we use as a simple measure for overall corolla morphology, is reduced about 4-fold in star flowers as compared to wild type (Fig. 1L). The wico flowers, named after their wide corolla, grow round-shaped and pigmented limbs while their tube remains very small (Fig. 1G, H). Limb pigmentation ranged from pink to bright red, and green sepaloid tissue was observed around the mid-veins, especially on the abaxial side of the petals (Fig. S1H-P). Total tube length was reduced about 3-fold in wico flowers, with domain D1 being absent since stamens were totally unfused to the tube (Fig.

S2), while domain D2 was significantly reduced in size (Fig. 1J). Limb area was also about 2-fold reduced in wico as compared to wild type flowers (Fig. 1K), but the ratio between limb area and tube length was higher than in wild type (Fig. 1L), indicating the larger contribution of limb tissue to total corolla morphology in wico. In summary, the star flowers form an almost normal tube but small, misshaped and unpigmented limbs, while the wico flowers form almost normally shaped and pigmented limbs but a tube strongly reduced in length. These contrasting phenotypes suggest that tube and limb development can be uncoupled in petunia flowers, at least to some degree.

The star and wico flowers result from excision of the *dTph1* transposon from the *phdef-151* locus

Reversion of a mutant phenotype towards a partial or a complete wild-type phenotype is classically observed in unstable transposon insertion mutant alleles. In the petunia W138 line from which *phdef-151* originates, the *dTph1* transposon is actively transposing (Gerats et al., 1990). We assumed therefore that the star and wico flowers were caused by the excision of *dTph1* from the *PhDEF* locus. *dTph1* transposition is generally accompanied by an 8-bp duplication of the target site upon insertion, and excision can have various outcomes depending on the length and nature of the remaining footprint (van Houwelingen et al., 1999). Hence we first hypothesized that the distinct star and wico phenotypes were caused by different types of alterations of the *PhDEF* coding sequence after the excision of *dTph1*.

To test this hypothesis, we characterized the *phdef-151* locus from in total 14 star and 14 wico independent reversion events. For this we extracted genomic DNA from sepals or petals of star and wico flowers, and we amplified the part of the *PhDEF* locus containing the *dTph1* transposon with primers flanking the insertion site (Fig. 2A). All samples produced a mixture of *PhDEF* fragments, some containing the *dTph1* transposon and some where *dTph1* had been excised (Fig. 2B). We specifically sequenced the small fragments resulting from *dTph1* excision in star and wico petal samples, including *phdef-151* second whorl organs as a control (Fig. 2C). In *phdef-151* the *dTph1*-excised alleles were always out-of-frame, with either 7 or 8 additional nucleotides as compared to the wild-type sequence. Due to a reading frame shift, both of these alleles are expected to produce an early truncated protein likely not functional (Fig. 2C), in line with the normal *phdef* mutant phenotype observed in these plants. In contrast, in both star and wico flowers we could find either wild-type sequences (found 1 time and 3 times independently in star and wico flowers respectively) or in-frame footprint alleles consisting of various additions of 6 nucleotides (alleles further named *PhDEF+6*, found 13 times and 11 times independently in star and wico flowers respectively, Fig. 2C). These last insertions are predicted to result in proteins with 2 additional

amino-acids inserted towards the end of the DNA-binding MADS domain (Fig. 2C). Together these results demonstrate that wico and star revertant flowers depend on the presence of an in-frame *def-151* derived excision allele that partially restores petal development. In contrast to our initial expectations however, there was no correlation between the sequence of the locus after excision and the phenotype of the flower, and both star and wico flowers could be found with a wild-type *PhDEF* excision allele or with an identical *PhDEF+6* allele (e.g. the 6-bp GTCTGG footprint allele was frequently found both in wico and star flowers). This indicates that the phenotypic difference between the star and wico flowers cannot be explained by a differently modified *PhDEF* sequence after *dTph1* excision. Secondly, since the *phdef* mutation is fully recessive (Vandenbussche et al., 2004), the presence of one transposon mutant allele combined with the wild-type revertant sequence, normally should lead to wild-type flowers. Together this implied that another molecular mechanism is causing the difference between wico and star flowers.

The star and wico phenotypes are not heritable

To further explore the genetic basis of the star and wico phenotypes, we analyzed the progeny after selfing of a series of independent wico and star flowers (Table 1). Because all wico and star flowers were heterozygous at the *PhDEF* locus (they still carried the original transposon allele in a heterozygous state), both the original transposon allele and the in-frame footprint allele were expected to segregate independently in the progeny of these flowers. Remarkably however, neither the star nor the wico phenotypes turned out to be heritable. First of all, we found that the progeny of the wico flowers almost exclusively displayed a *phdef* mutant phenotype, undistinguishable from the parental *phdef-151* allele. In line with that, no 6-bp footprint alleles could be detected in these plants, indicating that the in-frame wico footprint alleles were not transmitted to the progeny. This suggested that the gametes generated by the wico flowers exclusively carried the mutant *phdef-151* allele, hence resulting in homozygous *phdef-151* mutants in the progeny.

On the other hand, both the original transposon allele and the in-frame footprint allele were found to segregate independently in the progeny of star flowers as was expected, but despite that, the star phenotype itself was not transmitted to the progeny. The progeny of the star flowers with a *PhDEF+6* allele yielded three different phenotypic classes (in a proportion close to 1:1:2; Table 1): plants displaying a *phdef* phenotype, plants having wild-type flowers, and plants carrying flowers with a wild-type architecture but with reduced pigmentation, further referred to as « pink wild-type » (Fig. S3). We genotyped the *PhDEF* locus in plants descendant from one star parent and carrying flowers with a wild-type architecture (Table S2). We found that all plants with a pink wild-type phenotype were heterozgyous with an out-of-frame *phdef* allele and an in-frame *PhDEF+6*

allele, while fully red wild-type flowers had in-frame *PhDEF+6* alleles at the homozygous state. This indicates that the PhDEF protein with 2 additional amino acids is not 100% fully functional, as it leads to a reduction in limb pigmentation when combined with an out-of-frame allele. The fact that it can ensure normal petal development when at the homozygous state indicates that this is dosage dependent. In summary, the segregation ratio shows that the star gametes carried either the *phdef-151* allele or an in-frame *PhDEF* allele at a 1:1 ratio, and hence that the germ cells generating these gametes were heterozygous for these two alleles. Therefore, analysis of the star and wico progeny informed us about the genotype of the parental germ cells, and the non-heritability of the star and wico phenotypes suggested that these flowers were genetic mosaics.

Cell layer-specific *PhDEF* expression correlates with the wico and star phenotypes

Excision of *dTph1* from a gene can occur at different times during plant development: if happening at the zygotic stage, then the whole plant will have a *dTph1*-excised allele. If excision occurs later, this will result in a genetic mosaic (chimera) with a subset of cells carrying the *dTph1* insertion at the homozygous state and others having a *dTph1*-excised allele. This typically leads to branches or flowers with a wild-type phenotype on a mutant mother plant (supposing a recessive mutation). Furthermore, since all plant organs are organized in clonally-independent cell layers, excision can happen in one cell layer only, thereby creating a periclinal chimera, *i.e.* a branch or flower where cell layers have different genotypes (Frank and Chitwood, 2016; De Keukeleire et al., 2001).

Several pieces of evidence suggested that the star and wico flowers were periclinal chimeras: (1) when amplifying the *PhDEF* fragment spanning the *dTph1* excision site, the intensity of the bands obtained from the sepal and the petal tissues were consistently different, likely reflecting the quantity of *dTph1*-excised fragment found in the original tissue (Fig. 2B). This suggested that in wico flowers the *dTph1*-excised fragment was more present in petals than in sepals, and the opposite for star flowers. Sepals generally have a much thicker mesophyll than petals, therefore the relative contribution of the epidermis (L1-derived) and mesophyll (L2-derived) tissues is different. Thus this result tended to indicate that in wico and star flowers the excision happened in the epidermal and mesophyll layers respectively. (2) The non-heritability of the star and wico phenotypes and the genotype of their germ cells suggested that L2-derived cells, to which germ cells belong, had a different genotype than L1-derived cells. For instance, we found that germ cells were homozygous mutant for *phdef-151* in wico, which should result in a *phdef* phenotype if the epidermal tissue had the same genotype. (3) Finally, periclinal chimeras for *DEF* were already obtained in *Antirrhinum majus* and were found to partially restore petal development, suggesting

that similar processes could be at stake here (Vincent et al., 2003; Perbal et al., 1996; Efremova et al., 2001).

To investigate if the star and wico flowers were indeed the result of a layer-specific excision of *dTph1* from *PhDEF*, we localized the *PhDEF* transcript in these flowers by *in situ* hybridization (Fig. 3, Fig. S4). In wild-type flowers, the *PhDEF* transcript is first detected in the stamen initiation domain, then shortly after in incipient stamen and petal primordia (Fig. 3A, B). At all stages observed, *PhDEF* expression appears quite homogeneous in all cell layers of the organs, with a stronger expression in the distal part of the petal (Fig. 3C, Fig. S4C). In star flowers, the dynamics of *PhDEF* expression was similar to wild-type flowers, but strikingly *PhDEF* expression was absent from the L1 and epidermis (Fig. 3D-F, Fig. S4D-F). At the petal margins, underlying layers were also devoid of *PhDEF* expression (Fig. 3F), which likely corresponds to the restricted petal area where cells of L1 origin divide periclinally and invade the mesophyll (Satina and Blakeslee, 1941). In wico flowers we observed the exact opposite situation to the star flowers, with *PhDEF* expression restricted to the L1 and epidermis, all throughout petal development (Fig. 3G-I, Fig. S4G-I). Thus the star and wico flowers are respectively the result of an early *dTph1* excision event in one cell from the L2 or L1 meristematic layer, resulting in a chimeric flower expressing *PhDEF* only in the mesophyll (L2-derived cells) or in the epidermis (L1-derived cells) of petals. Considering the star and wico phenotypes, these results suggest that the epidermis is the main driver for limb growth, shape and pigmentation, while the mesophyll mainly drives tube growth.

Non-autonomous effects of layer-specific *PhDEF* expression on cell identity

Knowing the genetic basis of the star and wico phenotypes, we wondered how layer-specific *PhDEF* expression affects the determination of cell identity, in the layer where *PhDEF* is expressed (cell-autonomous effect) but also in the layer devoid of *PhDEF* expression (non-cell-autonomous effect). For this, we focused on star petals and examined the appearance of their epidermal cells by scanning electron microscopy, to compare with wild-type petals and sepals, and wico petals (Fig. 4A, B, Fig. S5C, D).

On the adaxial side of the wild-type petal, cells from the limb are round and adopt the classical conical shape found in many angiosperm petals, while cells from the tube are elongated with a central cone (Fig. 4B). In contrast, the adaxial epidermis of wild-type sepals (indistinguishable from *phdef-151* second whorl organs) displays typical leaf-like features (Morel et al., 2019), with puzzle-shaped cells interspersed with stomata and trichomes (Fig. 4B). Epidermal cell shape thus appears as a good parameter to discriminate epidermal cell identity between petals and sepals. In star petal tubes, epidermal cells have a similar appearance as in a wild-type petal tube

but are slightly less elongated (Fig. 4B, D). In contrast, cells from the adaxial side of the star limbs are domed, reminiscent of wild-type conical cells, but they appear flatter and are about 3-times larger (Fig. 4C). We occasionally observed pigmented revertant sectors on star flowers, resulting from an additional independent *dTph1* excision in the epidermis, generating wild-type sectors on a star flower (Fig. S5A). These sectors allow the immediate comparison between star and wild-type epidermal cells on a single sample, confirming the difference in conical cell size, shape and colour (Fig. S5A-D). Moreover, the star limbs occasionally form trichomes on their abaxial epidermis (Fig. S5C), which is a typical sepal feature that is normally not observed on petal limbs. Altogether these observations suggest that epidermal cells from star limbs have an intermediate identity between petal and sepal cells. Since star petals do not express *PhDEF* in their epidermis, these observations show that non-cell-autonomous effects are at stake to specify cell identity. The interpretation of these effects is summarized in Fig. S6.

In wico petals, epidermal limb cells are conical, similar to wild-type cells from the same area, although slightly bigger (Fig. 4B, C). In contrast, cells from the tube, albeit displaying similar shape than wild-type cells, are strongly reduced in length (Fig. 4B, D). This suggests that in addition to the absence of the D1 region of the tube (Fig.S2), a defect in cell elongation in the D2 region is, at least partly, responsible for overall tube length reduction in wico petals. Also, we observed after peeling the epidermis from wico petal limbs (at the base of the limbs or along the petal midveins) that the underlying mesophyll was chloroplastic, similar to a sepal mesophyll and in striking contrast with the white mesophyll of wild-type petal limbs (Fig. 4E). This suggests that mesophyll identity in wico petals in similar to the one of sepals, and hence that it is defined cell-autonomously, although additional histology analyses would be required to examine cell identity in more details.

We wondered if the non-cell-autonomous effects that we observed between layers in the star petals were also influencing cell identity within a layer. The revertant sectors observed on star flowers showed a very abrupt transition between pigmented and non pigmented epidermal cells (Fig. S5B), together with a quite sharp transition in conical cell shape and size (Fig. S5C). In particular, we found a clear file of pigmented cells on a star petal and the scanning electron micrograph revealed that these cells were also conical, in stark contrast with the flat surrounding cells of the petal mid-vein (Fig. S5D). Therefore we conclude that within the epidermal layer, cell shape and pigmentation are defined cell-autonomously, suggesting that different processes are at stake for cell-cell communication between and within layers.

Transcriptome sequencing of star and wico petals

To better understand the molecular basis for the star and wico phenotypes, we performed RNA-Seq on total petal tissue at three developmental stages, including wild-type and *phdef-151* samples. We chose an early stage (stage 4 as defined in (Reale et al., 2002)) when no major difference between genotypes is visible by eye, an intermediate stage (stage 8) when tube length is at half its final size, suggesting that tube growth is still active, and a late stage (stage 12) before limbs are fully expanded, suggesting that limb growth is still active (Fig. 5A). For *phdef-151* we only sequenced second-whorl sepal tissue at stage 12. Principal component analysis showed that developmental stage is the first contributor to variation in gene expression, while genotype corresponds to the second axis of variation (Fig. 5B). All samples clustered separately except wico and wild-type samples which were globally highly similar at all stages. We analyzed one-to-one differential gene expression between mutant and wild-type samples with DESeq2 (Love et al., 2014) and we found on average 5,816 deregulated genes in *phdef-151*, as compared to 1,853 and 1,115 deregulated genes in star and wico respectively, when averaging for all stages (Fig. 5C, Table S3). There were generally more downregulated genes than upregulated ones in mutant or chimeric genotypes, and the number of deregulated genes increased with ageing of the petal in both star and wico (Fig. 5C). A large proportion of genes (58-61%) deregulated in star or wico samples at stage 12 were also deregulated in *phdef-151* samples at the same stage (Fig. 5D), as expected since star and wico flowers are mutant for *PhDEF* in one cell layer. Genes uniquely deregulated in star or wico flowers represented 36% of deregulated genes for each, and only 16-29% of deregulated genes were jointly deregulated in star and wico flowers, consistent with the very different phenotypes of these flowers. These proportions indicate that the star and wico phenotypes are mostly subtended by the deregulation of sets of genes also deregulated in *phdef-151*, together with the deregulation of a unique set of genes set for each genotype. Altogether these transcriptomes constitute a promising dataset to identify genes involved in the establishment of petal epidermis and mesophyll identities, and in tube and limb development.

PhDEF directly binds *in vitro* to the terminator region of *AN1*, encoding a major regulator of petal pigmentation

To evaluate the potential for our transcriptomic dataset to decipher the gene regulatory networks underlying petal development, we decided to focus our attention on genes involved in petal pigmentation. Indeed, the players and regulatory pathways involved in anthocyanin biosynthesis in the petal epidermis have been extremely well described but their relationship with the specifiers of

petal identity, to whom PhDEF belongs, is so far unknown. The absence of pigmentation in star petals, the restoration of pigmentation in late revertant sectors and the phenotype of the pink wild-type flowers prompted us to investigate the direct link between *PhDEF* expression and petal pigmentation. For this, we examined the 504 genes down-regulated in both *phdef-151* and star samples (at any stage) but not deregulated in wico samples (Table S4), and we found 24 anthocyanin-related genes in this gene set (out of a total of 41 in the whole genome), which constitutes an exceptionally high enrichment for this gene function ($p < 0.001$, Fisher's exact test). In particular, we found the genes encoding the major regulators ANTHOCYANIN1 (AN1), AN2, PH4 and DEEP PURPLE, as well as many genes encoding anthocyanin biosynthesis enzymes, in this dataset. We hypothesized that, since *PhDEF* is expressed throughout petal development, the most upstream genes in the anthocyanin production pathway might be direct targets of PhDEF. Of particular interest for us were the genes *AN1* and *AN2*, encoding transcription factors taking part in the MBW regulatory complex triggering anthocyanin biosynthesis in the limbs (Spelt et al., 2000; Quattrocchio et al., 1999), whereas *DEEP PURPLE* is mostly involved in tube pigmentation (Albert et al., 2011), and *PH4* in vacuolar acidification of petal epidermal cells but has no role in anthocyanin production (Quattrocchio et al., 2006). Therefore, we aimed to test if PhDEF could be a direct activator of *AN1* or *AN2* expression.

We first attempted to predict PhDEF binding on the genomic sequences of *AN1* and *AN2*. For this, we used the high-quality transcription factor (TF) binding profile database Jaspar (Fornes et al., 2020; Sandelin et al., 2004), using position weight matrices for each TF to compute relative binding scores that should reflect *in vitro* binding preferences (Stormo, 2013). The exact DNA-binding specificity of PhDEF has not been characterized, but only the one of its Arabidopsis homologs AP3 and PI (Riechmann et al., 1996b). Therefore, since PhDEF DNA-binding specificity might be slightly different to those of AP3 and PI, we decided to predict binding for all MADS-box TFs available in Jaspar 2020, accounting for 23 binding profiles (Fornes et al., 2020). This approach should identify high-confidence CArG boxes (the binding site for MADS-box proteins), and we still payed a special attention to AP3 and PI predicted binding sites (Fig. 6). As a validation of this strategy, we analyzed the genomic sequence of *PhDEF* and found a high-confidence CArG box in the *PhDEF* promoter (visible by the presence of good predicted binding sites for several MADS-box proteins and therefore appearing as a clear black line in Fig. 6A, and indicated by a red arrow), also predicted to be a high-affinity binding site for both AP3 and PI, lying in a region shown to be important both for *AP3* petal-specific expression and for its auto-activation in Arabidopsis, and extremely conserved between distantly-related flowering plants (Wuest et al., 2012; Hill et al., 1998; Rijpkema et al., 2006). We next applied this predictive approach to the genomic sequences of

AN1 and *AN2*. The genomic region of *AN1* appears to be a good binding environment for MADS-box proteins, with several high-confidence CArG boxes predicted (Fig. 6B). In particular, we predicted a binding site (*AN1-bs1*) with a very high score, for all MADS-box proteins and for AP3 and PI in particular, in the terminator region of the *AN1* gene. In contrast, in the genomic region of *AN2* we found only sites with moderate binding scores (Fig. S7), therefore we decided not to investigate this gene any further.

To determine if PhDEF could indeed bind to *AN1-bs1* and potentially regulate *AN1* expression, we performed gel shift assays using *in vitro* translated PhDEF and/or PhGLO1 proteins (Fig. 6C). We found that, when incubating a 60-bp fragment containing *AN1-bs*1 in its center with either PhDEF or PhGLO1, no shift in migration was visible, meaning that neither protein could bind to this site alone. However when incubating *AN1-bs1* with both PhDEF and PhGLO1 proteins, we observed a clear shift in migration, consistent with the obligate heterodimerization of these proteins for DNA binding (Riechmann et al., 1996a). A control 60-bp fragment named *AN1-bs2*, also located in the *AN1* terminator region but predicted to have a very low binding score (relative score under 0.8 both for AP3 and PI), was indeed not bound by the PhDEF + PhGLO1 proteins, showing that our assay was specific. Therefore PhDEF, when dimerized with PhGLO1, is able to bind to a putative regulatory region in *AN1*, suggesting that it might regulate *AN1* expression. Although additional assays are needed to validate this binding *in vivo* and the regulatory action of PhDEF + PhGLO1 on *AN1*, this constitutes to our knowledge the first evidence of a putative direct link between petal identity regulators and petal pigmentation.

hypothesized that the petunia petal is formed similarly. Consistently, we only obtained two phenotypic classes, star and wico, suggesting that L3-specific *PhDEF* expression probably might only lead to a *phdef* mutant phenotype.

Different cell layers drive tube and limb growth

The star and wico phenotypes revealed that in petunia petals, the epidermis is the main driver for limb growth while the mesophyll is the main driver for tube growth. Kutschera and others proposed the epidermal-growth-control theory (Kutschera and Niklas, 2007; Kutschera et al., 1987), where the epidermis is under tension and restricts growth from the inner tissues; therefore, the inner tissues drive organ growth but the epidermis determines the final size of the organ. This theory has been based on physical experiments performed on the shoot from several organisms: inner tissues expand when they are separated from the epidermis that retracts. However, this is opposed by genetic evidence suggesting that the epidermis can also be an active driver of shoot growth, and that signaling between layers coordinates growth at the organ level (Savaldi-Goldstein et al., 2007). Moreover, seemingly opposing conclusions have been drawn using different mutants and genetic systems (Savaldi-Goldstein and Chory, 2008), leading to the idea that any layer could be driving organ growth, depending on the species, the organ or the gene studied. In the case of the petunia petal, it is not entirely surprising that the epidermis would be the active driver of limb growth, since the limb mesophyll tissue is thin and lacunous. In particular, petal edges whose mesophyll tissue is L1-derived, can only grow if L1-derived cells are actively expanding or dividing. The fact that the tube growth is L2-driven is consistent with its tissue architecture (large mesophyll cells with less lacunes than in the limbs) and as such, it behaves more like a shoot.

Observing these apparently conflicting growth behaviours, one may wonder how general our observations are. In *Antirrhinum majus* (Antirrhinum) and Arabidopsis, periclinal chimeras for orthologs of *PhDEF* (*DEF* and *AP3* respectively) or *PhGLO1/PhGLO2* (*GLO* and *PI* respectively) have been previously obtained (Perbal et al., 1996; Vincent et al., 2003; Efremova et al., 2001; Bouhidel and Irish, 1996; Jenik and Irish, 2001). In Antirrhinum, expression of *DEF* only in the L1 layer largely restores petal development, particularly in the limbs, in contrast to the L2/L3 specific *DEF* or *GLO* expression which causes reduced limb growth (Perbal et al., 1996; Vincent et al., 2003; Efremova et al., 2001). Petals are fused into a tube in Antirrhinum flowers, but the tube is much more reduced than in petunia, hence conclusions on tube length restoration in the chimeras were not drawn by the authors. However, in light of our results, it is clear that Antirrhinum chimeras expressing *DEF* or *GLO* in the L2/L3 layers restore tube development to a higher degree than limb

development, similar to what we observed. In Arabidopsis that has simple and unfused petals, petal shape and size were never fully restored when *AP3* was expressed in one cell layer only (Jenik and Irish, 2001); in contrast epidermal expression of *PI* was sufficient to restore normal petal development (Bouhidel and Irish, 1996). Therefore, it seems that epidermis-driven limb growth and mesophyll-driven tube growth is a shared property between petunia and Antirrhinum petals. We could thus infer that this property applies to the whole clade of euasterids I to which the two species belong. Interestingly, euasterids mainly form flowers whose petals are fused into a tube, with a likely single origin for petal fusion (Zhong and Preston, 2015), suggesting the attractive but highly speculative hypothesis that petal fusion and layer-driven growth of tube vs. limbs could have arisen simultaneously.

Autonomous and non-autonomous effects of *PhDEF* expression on petal traits

Our study revealed that petal traits were affected differently by layer-specific *PhDEF* expression (Fig. S6). For instance, epidermal pigmentation is a clearly autonomous trait, since star petals are not pigmented except when wild-type revertant sectors arise. On the contrary, epidermal cell shape appears to behave as a partially autonomous trait since star epidermal cells are domed, but larger and flatter than wild-type conical cells. Finally, organ size and shape are specified non-autonomously in sub-domains of the petal: *PhDEF* expression in the L1 or L2 is sufficient to specify correct shape of the limbs or correct size and shape of the tube respectively, suggesting that in these petal domains, layer-specific *PhDEF* expression is sufficient to signal cells from the other layer to grow normally. The mechanisms for this inter-layer communication remain unknown. We were not able to detect PhDEF protein localization in the star and wico flowers so far, therefore we do not know if the PhDEF protein itself might be moving between layers, which would be the simplest mechanistic explanation for the non-autonomous traits that we observe. Indeed, in Antirrhinum petals expressing *DEF* in the L2/L3 layers, the DEF protein was found in small amounts in the epidermis (Perbal et al., 1996). In contrast, Arabidopsis AP3 and PI proteins are unable to move between cell layers (Urbanus et al., 2010). In any case, even if the PhDEF protein moves between layers in our chimeric flowers, it is likely to be in small amounts only, otherwise both flower types would have a wild-type phenotype. Therefore, it is unlikely to be the reason for tube and limb correct development in the star and wico flowers. Alternatively, the non-autonomous effects that we observed might be triggered by mechanical signals transmitted between layers. For instance, in star flowers normal growth of the mesophyll could merely drag along epidermal cells, since cells are connected by their cell walls, which could be sufficient to trigger their expansion and division. More specifically, conical cells are shaped by a circumferential microtubule arrangement

controlled by the microtubule-severing protein KATANIN, and altering this arrangement affects conical cell shape (Ren et al., 2017). Microtubule arrangement responds to mechanical signals (Hamant et al., 2008), which are likely to be transmitted between layers. Therefore, it is possible that the formation of domed cells in the star epidermis is merely triggered by mechanical signals from the growing underlying layer, independent of any petal identity specifier. The molecular or physical nature of the signals involved in communication between layers deserves to be explored in full depth.

Towards the gene regulatory networks of petal development

Our star and wico material granted the opportunity to explore the gene regulatory networks driving petal development in petunia, more specifically by decoupling tube vs. limb development on one hand, and epidermis vs. mesophyll development on the other hand. However, these effects are confounded in our dataset, since mesophyll and tube development are linked in star flowers, whereas epidermis and limb development are linked in wico flowers. Further analyses, like for instance sequencing the transcriptome from star and wico limb and tube tissues separately, would help uncouple these effects. Anyhow, to evaluate the potentiality of our transcriptomic dataset to yield functional results, we focused our analysis on anthocyanin-related genes since we expected them to be downregulated in the white petals of star flowers, and because the anthocyanin biosynthesis and regulatory pathways are very well characterized. Therefore, we examined the presence of anthocyanin-related genes among genes downregulated both in star and *phdef-151* samples, but not deregulated in wico samples. We found a very high number of anthocyanin-related genes in this dataset, suggesting that the initial triggering event for most of the anthocyanin production pathway was missing in star flowers. Most of these genes were downregulated in star samples from stage 8 onwards, which is consistent with the late appearance of pigmentation in the limbs of wild-type petals.

Finally, we investigated the direct link between PhDEF and petal pigmentation and found that, *in vitro*, the PhDEF + PhGLO1 protein complex directly binds to a good predicted binding site in the regulatory region of *AN1*. Specifically, this site lies in the terminator region of *AN1*, which is not incompatible with an activating role in transcription, through DNA looping to the promoter (Jash et al., 2012) or by promoting transcription termination and reinitiation (Wang et al., 2000). Therefore, we hypothesize that PhDEF directly activates *AN1* expression, thereby triggering the petal pigmentation program. Indeed petunia *an1* mutants have completely white petals, consistent with the most upstream position of AN1 in the anthocyanin regulatory pathway (Doodeman et al., 1984; Spelt et al., 2000). If confirmed, the fact that PhDEF regulates the expression of pigmentation

genes would contribute to fill the « missing link » between the identity of a floral organ and its final appearance (Dornelas et al., 2011).

MATERIALS AND METHODS

Plant material, growth conditions and plant phenotyping

The *phdef-151* plants were obtained from the *Petunia x hybrida* W138 line and were grown in a culture room in long day conditions (16h light 22°C; 8h night 18°C; 75-WValoya NS12 LED bars; light intensity: 130 µE). The wico and star flowers were repeatedly obtained from several different *phdef-151* individuals and were maintained by cuttings. Plant and flower pictures were obtained with a CANON EOS 450D camera equipped with objectives SIGMA 18-50mm or SIGMA 50mm. To measure tube length, the flower was cut longitudinally and photographed from the side. To measure limb area, the limbs were flattened as much as possible on a glass slide covered with transparent tape and photographed from the top. The photographs were used to measure D1 and D2 lengths and limb area with ImageJ.

Genotyping

Extraction of genomic DNA from young leaf tissue was performed according to Edwards et al., 1991. The region spanning the *dTph1* insertion site in *PhDEF* was amplified using primers MLY0935/MLY0936 (Table S1). PCR products were separated on a 2% agarose gel, fragments of interest were purified using the NucleoSpin® Gel and PCR Clean-up kit (Macherey-Nagel), and sequenced with Eurofins SupremeRun reactions.

In situ RNA Hybridization

Floral buds from wild-type, 2 wico and 1 star lines were fixated overnight in FAA (3.7% formaldehyde, 5% acetic acid, 50% ethanol), cleared in Histo-clear and embedded in paraffin to perform 8 µm sections. *PhDEF* cDNA was amplified from wild-type petunia inflorescence cDNAs with primers MLY1738/MLY1739 (Table S1), generating a 507 bp fragment excluding the part encoding the highly conserved DNA-binding domain. The digoxigenin-labeled RNA probe was synthesized from the PCR fragment by *in vitro* transcription, using T7 RNA polymerase (Boehringer Mannheim). RNA transcripts were hydrolyzed partially for 42 min by incubation at 60°C in 0.1 M Na_2CO_3/$NaHCO_3$ buffer, pH 10.2. Later steps were performed as described by (Cañas et al., 1994). For imaging, slides were mounted in Entellan (Sigma) and imaged with a Zeiss Axio Imager M2 light microscope equipped with a Zeiss Axio Cam HRc camera.

Scanning Electron Microscopy (SEM)

Scanning electron micrographs were obtained with a HIROX SH-1500 bench top environmental scanning electron miscroscope equipped with a cooling stage. Samples were collected and quickly

imaged to limit dehydration, at -5°C and 5 kV settings. For cell area and length measurements, pictures were taken from 3 petal tubes and 3 petal limbs from different wild-type, star and wico flowers. For each sample, 3 pictures were taken and 5 cells (for the tube) or 10 cells (for the limbs) were measured for each picture. Measures were performed with ImageJ by manually drawing the outline or length of the cells.

RNA-Seq

Petal tissue was collected at 1 pm from several plants steming from a single star line, a single wico line, and several individual wild-type plants (progeny of a single star flower) and *phdef-151* plants (progeny of the same star flower). Tube length was macroscopically measured to compare stages, the corolla was cut open and stamens were removed as much as possible from the corolla by pulling on the filaments fused to the tube. One biological replicate contains total petal tissue from 2 flowers. Tissue was grounded in liquid nitrogen and RNA was extracted with the Spectrum Plant Total RNA Kit (Sigma) including on-column DNase digestion (Sigma). RNA integrity and quantity were determined by a Bioanalyzer RNA 6000 Nano assay (Agilent). Libraries were prepared with poly-A enrichment and single-end 75-bp sequencing was performed on a NextSeq 500 platform (Illumina). 16 to 23 million reads were recovered per library. Reads were checked for quality with FastQC v0.11.4 (https://www.bioinformatics.babraham.ac.uk/projects/fastqc/), adaptors and low-quality ends were trimmed with Cutadapt v 1.16 (Martin, 2011) and custom Perl scripts. The reference genome sequence used for transcriptome analysis is the *Petunia axillaris* v1.6.2 HiC genome published in (Bombarely et al., 2016) and further scaffolded by HiC by DNAzoo (Dudchenko et al., 2017, 2018); gene annotations were transferred from the published assembly to the HiC-scaffolded version using Blat (Kent, 2002), Exonerate (Slater and Birney, 2005) and custom Perl scripts. The complete set of reads was mapped on the reference genome sequence using HISAT2 v2.2.1 (Kim et al., 2015) to identify splicing sites, before performing mapping sample per sample. Reads per gene were counted using FeatureCounts v1.5.1 (Liao et al., 2014). DESeq2 version 3.12 (Love et al., 2014) was used with R version 4.0.3 to perform the Principal Component Analysis and the differential gene expression analysis. Genes having less than 10 reads in the sum of all samples were considered as non-expressed and discarded. Genes were considered to be deregulated if log2FoldChange > 1 or < -1, and p-adjusted value < 0.01. Venn diagrams were built with InteractiVenn (Heberle et al., 2015).

Prediction of MADS-box TF binding sites

Genomic sequences, starting 3 kb upstream the START codon and ending 1 kb downstream the STOP codon, from *PhDEF*, *AN1* and *AN2* were scanned with all MADS-box TF matrices included

in the Jaspar 2020 database (http://jaspar.genereg.net), only removing matrices from AGL42 and AGL55 which are much shorter than the other matrices and therefore yield much higher scores. Relative scores above 0.86 were plotted against their genomic position.

Electrophoretic Gel Shift Assays (EMSAs)

CDS sequences from *PhDEF* and *PhGLO1* were amplified from *Petunia x hybrida* R27 inflorescence cDNAs with primers MLY2382/MLY2383 and MLY2384/2385 respectively (Table S1) and cloned into the *in vitro* translation vector pSPUTK (Stratagene) by NcoI/XbaI restriction. From these vectors, the PhDEF and PhGLO1 proteins were produced with the TnT SP6 High-Yield Wheat Germ Protein Expression System (Promega) according to the manufacturer's instructions. The genomic sequence from *AN1* terminator (0.8 kb) was amplified from *Petunia x hybrida* R27 genomic DNA with primers from Table S1 and cloned into pCR-BluntII-TOPO (ThermoFisher). Binding sites were amplified from these plasmids with primers listed in Table S1, with the forward primer labelled with Cy5 in 5'. The labelled DNA was purified and incubated with the TnT *in vitro* translation mixture as described in (Silva et al., 2015) before loading on a native acrylamide gel.

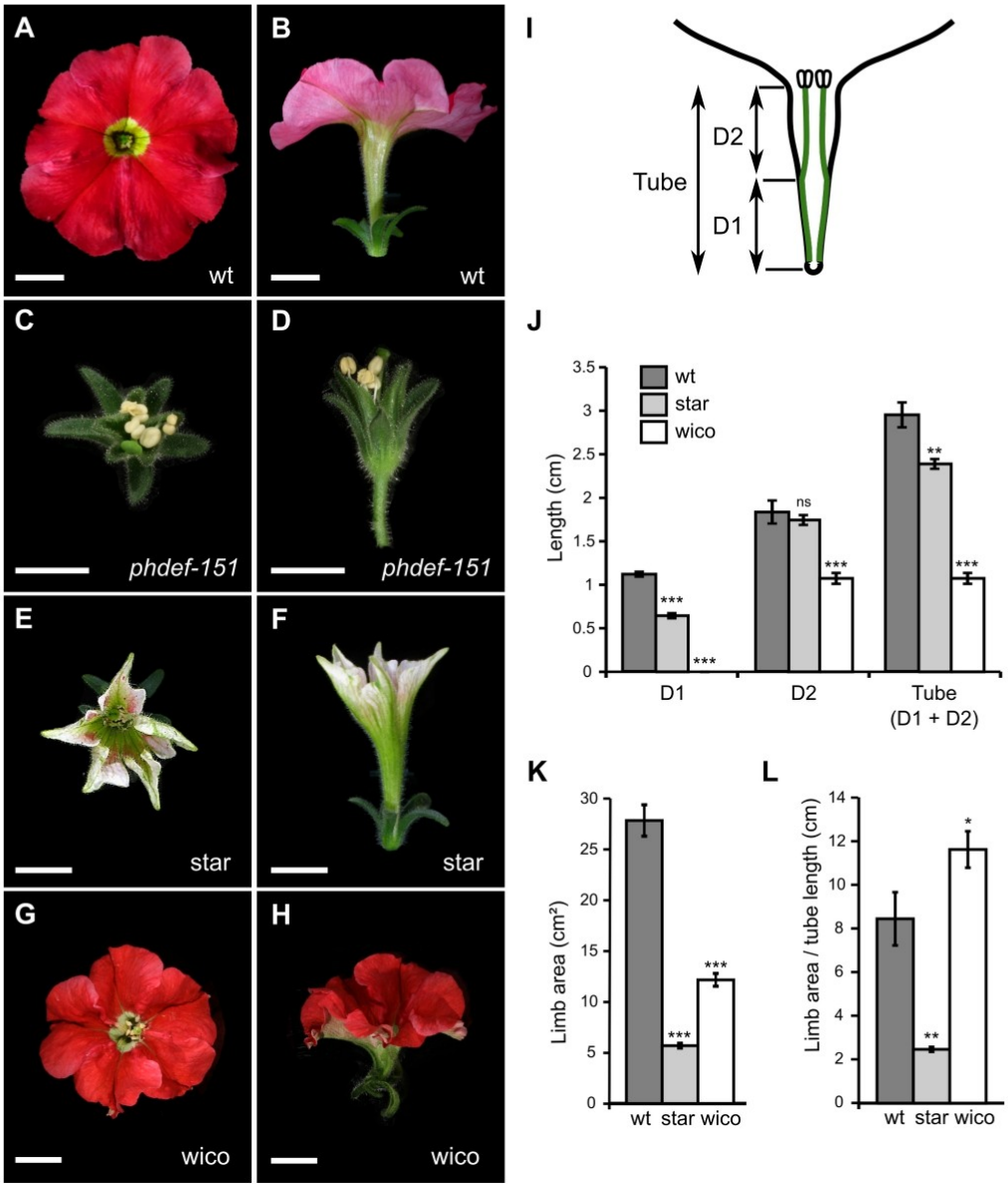

Figure 1. Macroscopic description of the star and wico flowers.

(A-J) Wild type (A, B), *phdef-151* (C, D), star (E, F) and wico wico (G, H) flowers from a top and side view respectively. Scale bar: 1 cm. **(I)** Schematic cross-section of a wild type flower, showing stamens (in green) partially fused to the petal tube. The region of the tube fused to stamens is named D1, and the region of the tube where stamens are free is named D2, as defined in (Stuurman

et al., 2004). **(J)** Average length of regions D1, D2 and total tube length in wt, star and wico flowers. **(K)** Average limb area in wt, star and wico flowers. **(L)** Average ratio between limb area and tube length in wt, star and wico flowers. n = 7 wt flowers, n = 12 star flowers from 4 different branches, n = 18 wico flowers from 5 different branches. Student's t test (* $p < 0.05$, ** $p < 0.01$, *** $p < 0.005$). Error bars represent ± s.e.m.

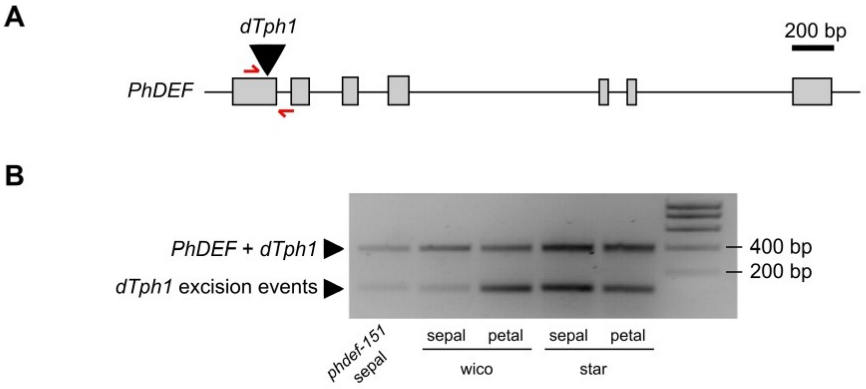

C

Phenotype	Allele	Nucleotidic sequence	Protein Sequence	n
wt	*PhDEF*	CCAGTA------CTGG--------CAAGCTTCAT	DAKVSIIMISS--TG--KLHEFIS	
phdef	*phdef(+8)*	CCAGTA------CTGGCAGTCTGGCAAGCTTCAT	DAKVSIIMISS--TGSLASFMNSL(+22aa)*	1
	phdef(+7)	CCAGTA------CTGGC-GTCTGGCAAGCTTCAT	DAKVSIIMISS--TGVWQAS*	1
star	*PhDEF*	CCAGTA------CTGG--------CAAGCTTCAT	DAKVSIIMISS--TG--KLHEFIS	1
	phdef (+6a)	CCAGTA------CTGG--GTCTGGCAAGCTTCAT	DAKVSIIMISS--TGSGKLHEFIS	7
	phdef (+6b)	CCAGTA------CTGGCA-T-TGGCAAGCTTCAT	DAKVSIIMISS--TGIGKLHEFIS	6
wico	*PhDEF*	CCAGTA------CTGG--------CAAGCTTCAT	DAKVSIIMISS--TG--KLHEFIS	3
	phdef (+6a)	CCAGTA------CTGG--GTCTGGCAAGCTTCAT	DAKVSIIMISS--TGSGKLHEFIS	7
	phdef (+6c)	CCAGTA------CTGGCA--CTGGCAAGCTTCAT	DAKVSIIMISS--TGTGKLHEFIS	3
	phdef (+6d)	CCAGTAGCCAGTCTGG--------CAAGCTTCAT	DAKVSIIMISSSQSG--KLHEFIS	1

Figure 2. Sequencing the *PhDEF* excision alleles in star and wico flowers.

(A) *PhDEF* gene model indicating the position of the *dTph1* insertion in the first exon (black triangle) and the primers used for subsequent amplification and sequencing (in red). **(B)** Amplicons generated with primers spanning the *dTph1* insertion site, on genomic DNA from *phdef-151* second whorl organs and star and wico sepals and petals. The large fragment still contains the *dTph1* transposon inserted (expected size: 407 bp), while small fragments result from different events of *dTph1* excision (expected size: 115 bp) and were subsequently sequenced. **(C)** The small *PhDEF* fragments from (B) were sequenced in the second whorl organs of flowers with a *phdef* (n = 2), star (n = 14) and wico (n = 14) phenotype. The nucleotidic sequence and predicted protein sequence are indicated, with STOP codons represented by a star. Additional nucleotides or amino-acids as compared to the wild-type sequences are indicated in red. n = number of independent reversion events where the same excision footprint was found.

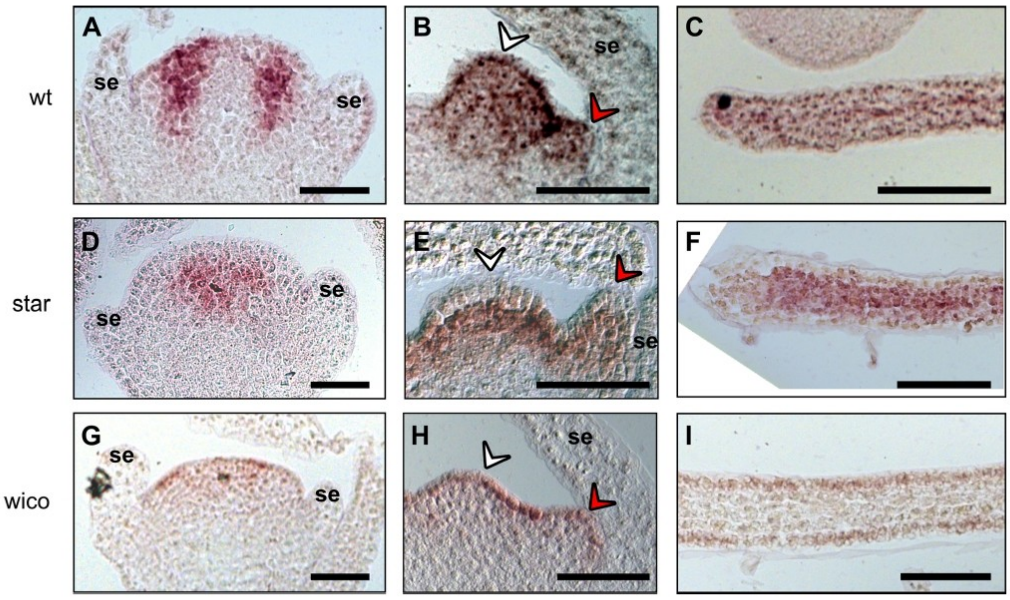

Figure 3. Localization of the *PhDEF* transcript in wild-type, star and wico flowers by *in situ* hybridization.

Longitudinal sections of wild-type (A, B, C), star (D, E, F) and wico (G, H, I) flowers or young petals hybridized with a DIG-labelled *PhDEF* antisense probe. At the earliest stage chosen (A, D, G), sepals are initiating and *PhDEF* is expressed in the future petal / stamen initiation domain. Note that if the section was not performed at the center of the flower, the *PhDEF* signal might artificially appear to be in the middle of the flower (as in D) whereas it is actually on its flanks. At the middle stage chosen (B, E, H), stamens (white arrowhead) and petals (red arrowhead) are initiating, and *PhDEF* is expressed in both primordia. *PhDEF* expression is also detected at the tip of young petal limbs (C, F, I). se: sepals. Scale bar: 50 µm.

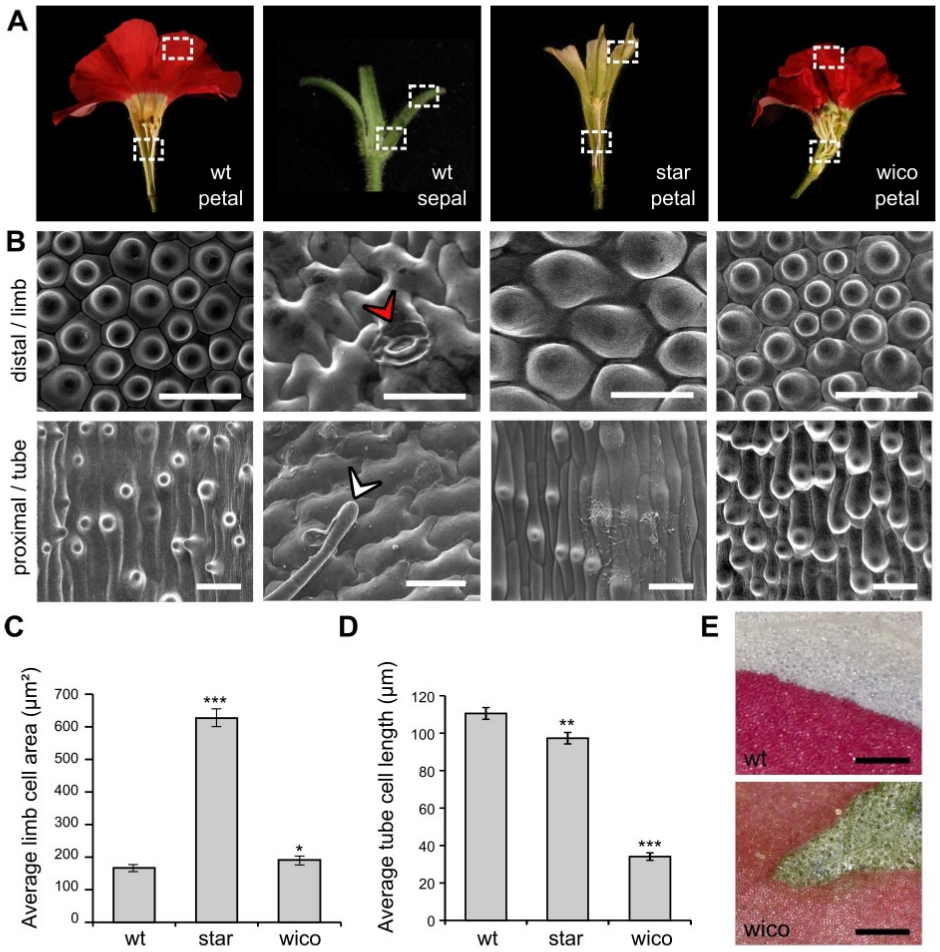

Figure 4. Epidermal cell identities in wt petals and sepals, and star and wico petals.
(A) From left to right: wt petals, wt sepals, star petals and wico petals cut open longitudinally to show areas used for scanning electron microscopy and cross-sections. Petals were subdivided into limb and tube area, and sepals were subdivided into a distal and a proximal part, as shown by the dotted white rectangles. **(B)** Representative scanning electron micrographs from the adaxial side of a wt petal, wt sepal, star petal and wico petal (from left to right). The red arrow points to a stomata and the white arrow points to a trichome. Scale bar: 30 µm. **(C)** Average limb cell area from the adaxial side of wild-type, star and wico petals (n = 30 cells). Student's t test (* $p < 0.05$, ** $p < 0.01$, *** $p < 0.005$). **(D)** Average tube cell length from the adaxial side of wild-type, star and wico petals (n = 45 cells). Wilcoxon rank sum test (* $p < 0.05$, ** $p < 0.01$, *** $p < 0.005$). Error bars represent ± s.e.m. **(E)** Limb area from wild-type (top) and wico (bottom) petals, after their adaxial epidermis

was manually peeled. For wt, the upper half of the picture shows the white underlying mesophyll. For wico, the green triangular area shows the green (chloroplastic) underlying mesophyll.

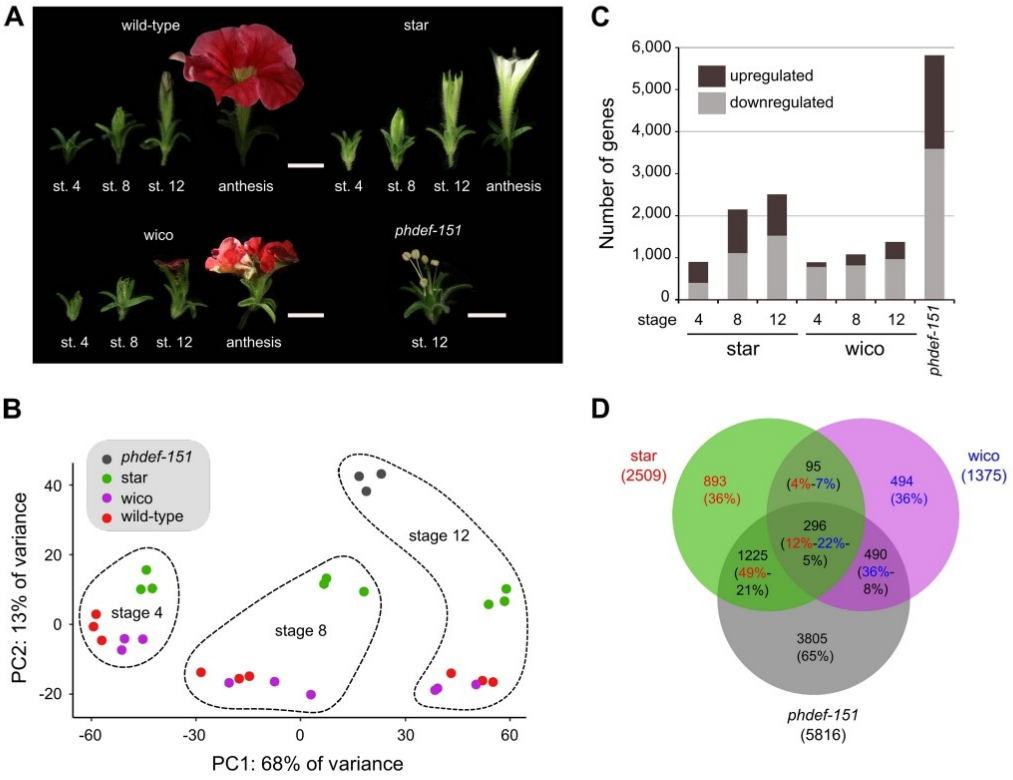

Figure 5. Gene deregulation in star and wico petals.

(A) Flowers from wild-type, star, wico and *phdef-151* at stages 4, 8 and 12 (only stage 12 for *phdef-151*), whose petals or sepals were harvested for transcriptome sequencing. Flowers at anthesis are shown for comparison. Scale bar: 1 cm. **(B)** Principal Component Analysis plot of the samples after analysis of variance with DESeq2, showing that the first principal component corresponds to the developmental stage and the second principal component corresponds to the genotype. **(C)** Number of upregulated and downregulated genes in star, wico and *phdef-151*, as compared to wild-type at the corresponding stages. **(D)** Venn diagram recapitulating the number of deregulated genes in star, wico and *phdef-151* petal samples at stage 12, as compared to wild-type, and their different intersections. Each sector contains the number of deregulated genes, and between parenthesis is the percentage of genes that it represents from the total number of deregulated genes in the corresponding sample, with a colour code (red = percentage of deregulated genes from star samples / blue = from wico samples / black = from *phdef-151* samples).

		Phenotype of the progeny (% of the total)		
		phdef	wild-type	pink wild-type
Parent flower	wico-1	15 (94%)		1 (6%)
	wico-2	14 (88%)	1 (6%)	1 (6%)
	wico-3	16 (100%)		
	wico-4	15 (94%)		1 (6%)
	wico-5	16 (100%)		
	wico-6	12 (100%)		
	wico-7	12 (100%)		
	star-1	11 (46%)	4 (17%)	9 (38%)
	star-2	4 (25%)	4 (25%)	8 (50%)
	star-3	7 (29%)	5 (21%)	12 (50%)
	star-4	3 (19%)	3 (19%)	10 (63%)

Table 1. Progeny of the star and wico flowers after selfing.

7 wico flowers and 4 star flowers have been selfed and their progeny has been phenotyped and classified into *phdef*, wild-type or pink wild-type phenotype. Summing the star progeny for the 4 parents gives 25 *phdef*, 16 wild-type and 39 pink wild-type plants, which is not significantly different to a 1:1:2 ratio (chi-square test, $p = 0.22$). Note that for wico, we found 4 plants with wild-type or pink wild-type flowers in the progeny, and all of them were linked to the presence of a *de novo* transposon excision from the *PhDEF* locus, restoring either a *PhDEF+6* (in the case of pink wild-type progeny) or a wild-type *PhDEF* (in the case of the wild-type progeny) allele.

Acknowledgments

We thank Patrice Bolland, Justin Berger and Alexis Lacroix for plant care assistance, the PLATIM platform (SFR BioSciences Lyon, UAR3444/CNRS, US8/Inserm, ENS de Lyon, UCBL) for electron microscopy technical support, Benjamin Gillet and Sandrine Hugues from the sequencing platform of the Institut de Génomique Fonctionnelle de Lyon for library preparation and sequencing of the transcriptomes of this study, and Rémy Belois for assistance for *in situ* hybridization experiments. This work was supported by grants to M.M. from the Agence Nationale de la Recherche (grant ANR-19-CE13-0019, FLOWER LAYER) and from IDEXLYON (Université de Lyon, grant ELAN-ERC), by a PhD fellowship to M.C. from the French Ministry of Higher Education and Research, and by a grant to V.H. and C.Z. from the Agence Nationale de la Recherche (grant ANR-16-CE92-0023, FLOPINET).

Author Contribution

M.M. and M.V conceived and designed the experiments. M.C., Q.C.S, P.M., P.C., V.H. and S.R.B. performed the experiments. M.C., Q.C.S., J.J., M.V. and M.M. analyzed the data. M.C., C.Z., M.V. and M.M. wrote the article.

Supporting Information

Figure S1. Additional pictures of star and wico flowers.
Figure S2. Stamens are unfused to the tube in wico flowers.
Figure S3. Wild-type and pink wild-type flowers descendant from a star parent.
Figure S4. Additional pictures of *PhDEF* transcript *in situ* hybridization in wild-type, star and wico flowers.
Figure S5. Epidermal revertant sectors on star petals.
Figure S6. Autonomous and non-autonomous effects in star and wico petals.
Figure S7. Prediction of MADS-box DNA binding sites in the genomic sequence of *AN2.*

Table S1. List of primers used in this study.
Table S2. Genotyping results of the progeny of a star flower.
Table S3. Differential gene expression calculated by DESeq2.
Table S4. List of the 504 genes downregulated in star and *phdef-151* samples.

References

Albert, N.W., Lewis, D.H., Zhang, H., Schwinn, K.E., Jameson, P.E., and Davies, K.M. (2011). Members of an R2R3-MYB transcription factor family in Petunia are developmentally and environmentally regulated to control complex floral and vegetative pigmentation patterning. Plant J **65**: 771–784.

Angenent, G.C., Busscher, M., Franken, J., Mol, J.N., and van Tunen, A.J. (1992). Differential expression of two MADS box genes in wild-type and mutant petunia flowers. Plant Cell **4**: 983–993.

Bissell, E.K. and Diggle, P.K. (2008). Floral Morphology in Nicotiana: Architectural and Temporal Effects on Phenotypic Integration. International Journal of Plant Sciences **169**: 225–240.

Bombarely, A. et al. (2016). Insight into the evolution of the Solanaceae from the parental genomes of Petunia hybrida. Nat Plants **2**: 16074.

Bouhidel, K. and Irish, V.F. (1996). Cellular Interactions Mediated by the HomeoticPISTILLATAGene Determine Cell Fate in theArabidopsisFlower. Developmental Biology **174**: 22–31.

Brandoli, C., Petri, C., Egea-Cortines, M., and Weiss, J. (2020). The clock gene Gigantea 1 from Petunia hybrida coordinates vegetative growth and inflorescence architecture. Sci Rep **10**: 275.

Cañas, L.A., Busscher, M., Angenent, G.C., Beltrán, J.-P., and Tunen, A.J.V. (1994). Nuclear localization of the petunia MADS box protein FBP1. The Plant Journal **6**: 597–604.

Cartolano, M., Castillo, R., Efremova, N., Kuckenberg, M., Zethof, J., Gerats, T., Schwarz-Sommer, Z., and Vandenbussche, M. (2007). A conserved microRNA module exerts homeotic control over Petunia hybrida and Antirrhinum majus floral organ identity. Nat Genet **39**: 901–905.

Coen, E.S. and Meyerowitz, E.M. (1991). The war of the whorls: genetic interactions controlling flower development. Nature **353**: 31–37.

De Keukeleire, P., Maes, T., Sauer, M., Zethof, J., Van Montagu, M., and Gerats, T. (2001). Analysis by Transposon Display of the behavior of the dTph1 element family during ontogeny and inbreeding of Petunia hybrida. Mol Genet Genomics **265**: 72–81.

Doodeman, M., Boersma, E.A., Koomen, W., and Bianchi, F. (1984). Genetic analysis of instability in Petunia hybrida: 1. A highly unstable mutation induced by a transposable element inserted at the An1 locus for flower colour. Theor Appl Genet **67**: 345–355.

Dornelas, M.C., Patreze, C.M., Angenent, G.C., and Immink, R.G.H. (2011). MADS: the missing link between identity and growth? Trends Plant Sci **16**: 89–97.

Dudchenko, O. et al. (2018). The Juicebox Assembly Tools module facilitates de novo assembly of mammalian genomes with chromosome-length scaffolds for under $1000. bioRxiv: 254797.

Dudchenko, O., Batra, S.S., Omer, A.D., Nyquist, S.K., Hoeger, M., Durand, N.C., Shamim, M.S., Machol, I., Lander, E.S., Aiden, A.P., and Aiden, E.L. (2017). De novo assembly of the Aedes aegypti genome using Hi-C yields chromosome-length scaffolds. Science **356**: 92–95.

Efremova, N., Perbal, M.-C., Yephremov, A., Hofmann, W.A., Saedler, H., and Schwarz-Sommer, Z. (2001). Epidermal control of floral organ identity by class B homeotic genes in Antirrhinum and Arabidopsis. Development **128**: 2661–2671.

Fornes, O. et al. (2020). JASPAR 2020: update of the open-access database of transcription factor binding profiles. Nucleic Acids Res **48**: D87–D92.

Frank, M.H. and Chitwood, D.H. (2016). Plant chimeras: The good, the bad, and the “Bizzaria.” Dev. Biol. **419**: 41–53.

Galliot, C., Stuurman, J., and Kuhlemeier, C. (2006). The genetic dissection of floral pollination syndromes. Curr Opin Plant Biol **9**: 78–82.

Gerats, A.G., Huits, H., Vrijlandt, E., Marana, C., Souer, E., and Beld, M. (1990). Molecular characterization of a nonautonomous transposable element (dTph1) of petunia. Plant Cell **2**: 1121–1128.

Hamant, O., Heisler, M.G., Jönsson, H., Krupinski, P., Uyttewaal, M., Bokov, P., Corson, F., Sahlin, P., Boudaoud, A., Meyerowitz, E.M., Couder, Y., and Traas, J. (2008). Developmental patterning by mechanical signals in Arabidopsis. Science **322**: 1650–1655.
Heberle, H., Meirelles, G.V., da Silva, F.R., Telles, G.P., and Minghim, R. (2015). InteractiVenn: a web-based tool for the analysis of sets through Venn diagrams. BMC Bioinformatics **16**: 169.
Heijmans, K., Ament, K., Rijpkema, A.S., Zethof, J., Wolters-Arts, M., Gerats, T., and Vandenbussche, M. (2012). Redefining C and D in the petunia ABC. Plant Cell **24**: 2305–2317.
Hill, T.A., Day, C.D., Zondlo, S.C., Thackeray, A.G., and Irish, V.F. (1998). Discrete spatial and temporal cis-acting elements regulate transcription of the Arabidopsis floral homeotic gene APETALA3. Development **125**: 1711–1721.
Hoballah, M.E., Gubitz, T., Stuurman, J., Broger, L., Barone, M., Mandel, T., Dell'Olivo, A., Arnold, M., and Kuhlemeier, C. (2007). Single gene-mediated shift in pollinator attraction in Petunia. Plant Cell **19**: 779–790.
van Houwelingen, A., Souer, E., Mol, J., and Koes, R. (1999). Epigenetic interactions among three dTph1 transposons in two homologous chromosomes activate a new excision-repair mechanism in petunia. Plant Cell **11**: 1319–1336.
Jash, A., Yun, K., Sahoo, A., So, J.-S., and Im, S.-H. (2012). Looping mediated interaction between the promoter and 3' UTR regulates type II collagen expression in chondrocytes. PLoS One **7**: e40828.
Jenik, P.D. and Irish, V.F. (2000). Regulation of cell proliferation patterns by homeotic genes during Arabidopsis floral development. Development **127**: 1267–1276.
Jenik, P.D. and Irish, V.F. (2001). The Arabidopsis floral homeotic gene APETALA3 differentially regulates intercellular signaling required for petal and stamen development. Development **128**: 13–23.
Kent, W.J. (2002). BLAT—The BLAST-Like Alignment Tool. Genome Res. **12**: 656–664.
Kim, D., Langmead, B., and Salzberg, S.L. (2015). HISAT: a fast spliced aligner with low memory requirements. Nat Methods **12**: 357–360.
Koes, R., Verweij, W., and Quattrocchio, F. (2005). Flavonoids: a colorful model for the regulation and evolution of biochemical pathways. Trends Plant Sci **10**: 236–242.
Kostyun, J.L., Gibson, M.J.S., King, C.M., and Moyle, L.C. (2019). A simple genetic architecture and low constraint allow rapid floral evolution in a diverse and recently radiating plant genus. New Phytol **223**: 1009–1022.
van der Krol, A.R., Brunelle, A., Tsuchimoto, S., and Chua, N.H. (1993). Functional analysis of petunia floral homeotic MADS box gene pMADS1. Genes Dev **7**: 1214–1228.
Kutschera, U., Bergfeld, R., and Schopfer, P. (1987). Cooperation of epidermis and inner tissues in auxin-mediated growth of maize coleoptiles. Planta **170**: 168–180.
Kutschera, U. and Niklas, K.J. (2007). The epidermal-growth-control theory of stem elongation: an old and a new perspective. J. Plant Physiol. **164**: 1395–1409.
Liao, Y., Smyth, G.K., and Shi, W. (2014). featureCounts: an efficient general purpose program for assigning sequence reads to genomic features. Bioinformatics **30**: 923–930.
Love, M.I., Huber, W., and Anders, S. (2014). Moderated estimation of fold change and dispersion for RNA-seq data with DESeq2. Genome Biol **15**: 550.
Martin, M. (2011). Cutadapt removes adapter sequences from high-throughput sequencing reads. EMBnet.journal **17**: 10–12.
Meyerowitz, E.M. (1997). Genetic control of cell division patterns in developing plants. Cell **88**: 299–308.
Morel, P., Chambrier, P., Boltz, V., Chamot, S., Rozier, F., Rodrigues Bento, S., Trehin, C., Monniaux, M., Zethof, J., and Vandenbussche, M. (2019). Divergent Functional Diversification Patterns in the SEP/AGL6/AP1 MADS-Box Transcription Factor Superclade. Plant Cell **31**: 3033–3056.

Moyroud, E. and Glover, B.J. (2017). The Evolution of Diverse Floral Morphologies. Curr. Biol. **27**: R941–R951.
Perbal, M.C., Haughn, G., Saedler, H., and Schwarz-Sommer, Z. (1996). Non-cell-autonomous function of the Antirrhinum floral homeotic proteins DEFICIENS and GLOBOSA is exerted by their polar cell-to-cell trafficking. Development **122**: 3433–3441.
Purugganan, M.D., Rounsley, S.D., Schmidt, R.J., and Yanofsky, M.F. (1995). Molecular evolution of flower development: diversification of the plant MADS-box regulatory gene family. Genetics **140**: 345–356.
Quattrocchio, F., Verweij, W., Kroon, A., Spelt, C., Mol, J., and Koes, R. (2006). PH4 of Petunia is an R2R3 MYB protein that activates vacuolar acidification through interactions with basic-helix-loop-helix transcription factors of the anthocyanin pathway. Plant Cell **18**: 1274–1291.
Quattrocchio, F., Wing, J., van der Woude, K., Souer, E., de Vetten, N., Mol, J., and Koes, R. (1999). Molecular analysis of the anthocyanin2 gene of petunia and its role in the evolution of flower color. Plant Cell **11**: 1433–1444.
Reale, L., Porceddu, A., Lanfaloni, L., Moretti, C., Zenoni, S., Pezzotti, M., Romano, B., and Ferranti, F. (2002). Patterns of cell division and expansion in developing petals of Petunia hybrida. Sex Plant Reprod **15**: 123–132.
Reck-Kortmann, M., Silva-Arias, G.A., Segatto, A.L.A., Mader, G., Bonatto, S.L., and de Freitas, L.B. (2014). Multilocus phylogeny reconstruction: new insights into the evolutionary history of the genus Petunia. Mol Phylogenet Evol **81**: 19–28.
Ren, H., Dang, X., Cai, X., Yu, P., Li, Y., Zhang, S., Liu, M., Chen, B., and Lin, D. (2017). Spatio-temporal orientation of microtubules controls conical cell shape in Arabidopsis thaliana petals. PLOS Genetics **13**: e1006851.
Riechmann, J.L., Krizek, B.A., and Meyerowitz, E.M. (1996a). Dimerization specificity of Arabidopsis MADS domain homeotic proteins APETALA1, APETALA3, PISTILLATA, and AGAMOUS. Proc Natl Acad Sci U S A **93**: 4793–4798.
Riechmann, J.L., Wang, M., and Meyerowitz, E.M. (1996b). DNA-binding properties of Arabidopsis MADS domain homeotic proteins APETALA1, APETALA3, PISTILLATA and AGAMOUS. Nucleic Acids Res **24**: 3134–3141.
Rijpkema, A.S., Royaert, S., Zethof, J., Weerden, G. van der, Gerats, T., and Vandenbussche, M. (2006). Analysis of the Petunia TM6 MADS Box Gene Reveals Functional Divergence within the DEF/AP3 Lineage. The Plant Cell **18**: 1819–1832.
Sandelin, A., Alkema, W., Engström, P., Wasserman, W.W., and Lenhard, B. (2004). JASPAR: an open-access database for eukaryotic transcription factor binding profiles. Nucleic Acids Res **32**: D91-94.
Satina, S. and Blakeslee, A.F. (1941). Periclinal Chimeras in Datura Stramonium in Relation to Development of Leaf and Flower. American Journal of Botany **28**: 862–871.
Satina, S., Blakeslee, A.F., and Avery, A.G. (1940). Demonstration of the Three Germ Layers in the Shoot Apex of Datura by Means of Induced Polyploidy in Periclinal Chimeras. American Journal of Botany **27**: 895–905.
Savaldi-Goldstein, S. and Chory, J. (2008). Growth coordination and the shoot epidermis. Curr. Opin. Plant Biol. **11**: 42–48.
Savaldi-Goldstein, S., Peto, C., and Chory, J. (2007). The epidermis both drives and restricts plant shoot growth. Nature **446**: 199–202.
Scheres, B. (2001). Plant cell identity. The role of position and lineage. Plant Physiol **125**: 112–114.
Schwarz-Sommer, Z., Huijser, P., Nacken, W., Saedler, H., and Sommer, H. (1990). Genetic Control of Flower Development by Homeotic Genes in Antirrhinum majus. Science **250**: 931–936.
Silva, C.S., Puranik, S., Round, A., Brennich, M., Jourdain, A., Parcy, F., Hugouvieux, V., and Zubieta, C. (2015). Evolution of the Plant Reproduction Master Regulators LFY and the MADS

Transcription Factors: The Role of Protein Structure in the Evolutionary Development of the Flower. Front Plant Sci **6**: 1193.
Slater, G.S.C. and Birney, E. (2005). Automated generation of heuristics for biological sequence comparison. BMC Bioinformatics **6**: 31.
Spelt, C., Quattrocchio, F., Mol, J.N.M., and Koes, R. (2000). anthocyanin1 of Petunia Encodes a Basic Helix-Loop-Helix Protein That Directly Activates Transcription of Structural Anthocyanin Genes. The Plant Cell **12**: 1619–1631.
Stewart, R.N. and Burk, L.G. (1970). Independence of Tissues Derived from Apical Layers in Ontogeny of the Tobacco Leaf and Ovary. American Journal of Botany **57**: 1010–1016.
Stormo, G.D. (2013). Modeling the specificity of protein-DNA interactions. Quant Biol **1**: 115–130.
Stuurman, J., Hoballah, M.E., Broger, L., Moore, J., Basten, C., and Kuhlemeier, C. (2004). Dissection of floral pollination syndromes in Petunia. Genetics **168**: 1585–1599.
Terry, M.I., Pérez-Sanz, F., Díaz-Galián, M.V., Pérez de Los Cobos, F., Navarro, P.J., Egea-Cortines, M., and Weiss, J. (2019). The Petunia CHANEL Gene is a ZEITLUPE Ortholog Coordinating Growth and Scent Profiles. Cells **8**.
Theißen, G., Kim, J.T., and Saedler, H. (1996). Classification and phylogeny of the MADS-box multigene family suggest defined roles of MADS-box gene subfamilies in the morphological evolution of eukaryotes. J Mol Evol **43**: 484–516.
Tornielli, G., Koes, R., and Quattrocchio, F. (2009). The Genetics of Flower Color. In Petunia: Evolutionary, Developmental and Physiological Genetics, T. Gerats and J. Strommer, eds (Springer: New York, NY), pp. 269–299.
Tröbner, W., Ramirez, L., Motte, P., Hue, I., Huijser, P., Lönnig, W.E., Saedler, H., Sommer, H., and Schwarz-Sommer, Z. (1992). GLOBOSA: a homeotic gene which interacts with DEFICIENS in the control of Antirrhinum floral organogenesis. EMBO J **11**: 4693–4704.
Urbanus, S.L., Dinh, Q.D.P., Angenent, G.C., and Immink, R.G.H. (2010). Investigation of MADS domain transcription factor dynamics in the floral meristem. Plant Signal Behav **5**: 1260–1262.
Vandenbussche, M., Horstman, A., Zethof, J., Koes, R., Rijpkema, A.S., and Gerats, T. (2009). Differential recruitment of WOX transcription factors for lateral development and organ fusion in Petunia and Arabidopsis. Plant Cell **21**: 2269–2283.
Vandenbussche, M., Janssen, A., Zethof, J., van Orsouw, N., Peters, J., van Eijk, M.J.T., Rijpkema, A.S., Schneiders, H., Santhanam, P., de Been, M., van Tunen, A., and Gerats, T. (2008). Generation of a 3D indexed Petunia insertion database for reverse genetics. Plant J **54**: 1105–1114.
Vandenbussche, M., Zethof, J., Royaert, S., Weterings, K., and Gerats, T. (2004). The duplicated B-class heterodimer model: whorl-specific effects and complex genetic interactions in Petunia hybrida flower development. Plant Cell **16**: 741–754.
Venail, J., Dell'olivo, A., and Kuhlemeier, C. (2010). Speciation genes in the genus Petunia. Philos Trans R Soc Lond B Biol Sci **365**: 461–468.
Vincent, C.A., Carpenter, R., and Coen, E.S. (2003). Interactions between gene activity and cell layers during floral development. The Plant Journal **33**: 765–774.
de Vlaming, P., Gerats, A.G.M., Wiering, H., Wijsman, H.J.W., Cornu, A., Farcy, E., and Maizonnier, D. (1984). Petunia hybrida: A short description of the action of 91 genes, their origin and their map location. Plant Mol Biol Rep **2**: 21–42.
Wang, Z., Bai, L., Hsieh, Y.-J., and Roeder, R.G. (2000). Nuclear factor 1 (NF1) affects accurate termination and multiple-round transcription by human RNA polymerase III. The EMBO Journal **19**: 6823–6832.

Wuest, S.E., O'Maoileidigh, D.S., Rae, L., Kwasniewska, K., Raganelli, A., Hanczaryk, K., Lohan, A.J., Loftus, B., Graciet, E., and Wellmer, F. (2012). Molecular basis for the specification of floral organs by APETALA3 and PISTILLATA. Proc. Natl. Acad. Sci. U.S.A. **109**: 13452–13457.
Yadav, R.K., Tavakkoli, M., Xie, M., Girke, T., and Reddy, G.V. (2014). A high-resolution gene expression map of the Arabidopsis shoot meristem stem cell niche. Development **141**: 2735–2744.
Zenoni, S., Reale, L., Tornielli, G.B., Lanfaloni, L., Porceddu, A., Ferrarini, A., Moretti, C., Zamboni, A., Speghini, A., Ferranti, F., and Pezzotti, M. (2004). Downregulation of the Petunia hybrida alpha-expansin gene PhEXP1 reduces the amount of crystalline cellulose in cell walls and leads to phenotypic changes in petal limbs. Plant Cell **16**: 295–308.
Zhong, J. and Preston, J.C. (2015). Bridging the gaps: evolution and development of perianth fusion. New Phytol. **208**: 330–335.

Résumé

La première fleur, apparue il y a environ 250 millions d'années, est vue comme une innovation de l'évolution. En effet, cette structure reproductrice est particulièrement efficace, en particulier grâce à sa capacité à attirer des pollinisateurs, ce qui assure une fécondation croisée et un brassage génétique crucial au maitien des espèces. La fleur est à la fois une structure robuste à l'échelle intra-spécifique, puisque son organisation ne varie pas au sein d'une espèce, et une structure plastique à l'échelle inter-spécifique, puisque une grande variété de morphologies florales sont observables chez les plantes à fleurs. La fleur montre donc une grande évolvabilité, ce qui a fasciné Darwin en son temps, qui a qualifié l'apparition et la diversification rapide des plantes à fleurs d'« abominable mystère ». Au cours de ma carrière de recherche, je me suis intéressée à l'évolution de la fleur sous des angles moléculaires, génétiques et développementaux, en utilisant différentes approches et différentes espèces modèles. Pendant ma thèse, j'ai étudié l'évolution biochimique de LEAFY, un régulateur clé de la formation de la fleur, pourtant aussi présent dans le reste des plantes terrestres qui ne forment pas de fleurs. Au cours de mon post-doc, je me suis intéressée à la base génétique et développementale de la robustesse du patron floral, en étudiant la perte variable de pétales chez la Cardamine. Enfin, je m'intéresse actuellement aux processus du développement du pétale chez Petunia, et en particulier à la contribution des différentes couches cellulaires du pétale à sa morphologie finale. Ces différentes étapes de mon parcours m'ont permis d'avoir un regard large sur les processus évolutifs et développementaux des plantes.

Summary

The first flower, that appeared around 250 million years ago, is generally seen as a key evolutionary innovation. Indeed, this reproductive structure is particularly efficient, in particular because it attracts pollinators, which ensures cross-pollination and the maintenance of genetic diversity important for species survival. The flower is, on the one hand, a robust structure at the intra-specific scale, since its organization does not vary within a single species, and on the other hand, a plastic structure at the inter-specific scale, since a very large diversity of floral morphologies can be found in flowering plants. The flower is highly evolvable, which fascinated Darwin who qualified the emergence and rapid radiation of flowering plants as an "abominable mystery". Throughout my research career, I have studied flower evolution under its molecular, genetic and developmental aspects, using a wide range of approaches in different model species. During my PhD, I investigated the biochemical evolution of LEAFY, a key regulator of flower formation, but still present in other land plants that do not form flowers. During my post-doc, I got interested in the genetic and developmental basis for floral bauplan robutness, through the study of variable petal loss in Cardamine. Now, I am investigating the process of petal development in Petunia, and in particular the role of cell layers in petal final morphology. These different steps of my research career have given me a large vision on plant evolutionary and developmental processes.